



**University of
Nottingham**

UK | CHINA | MALAYSIA

Characterization of Novel Glycosyl Hydrolases with Application in the Food Industry

Lidia Delgado Calvo-Flores

Supervisors:

Prof. Francesca Paradisi

Prof. Ian Fisk

A thesis submitted to the University of Nottingham for the degree
of Doctor of Philosophy in Sustainable Chemistry

January 2021

Contents

Abstract.....	vii
Abbreviations.....	ix
Chapter 1: General introduction.....	11
1.1 Biocatalysis	12
1.2 Enzymes in the food industry.....	15
1.3 Glycosyl Hydrolases	18
1.4 Extremophiles.....	22
1.5 Wine	24
1.5.1 History of wine-making	24
1.5.2 The wine business.....	25
1.5.3 The wine-making process.....	28
1.5.4 Enzymes in winemaking	31
1.6 Vanilla	37
1.6.1 Processing of vanilla pods	37
1.6.2 Chemistry of green and cured vanilla beans	38
1.6.3 Economics of the vanilla crop	39
1.6.4 World trade.....	43

1.7	Soybean	45
1.7.1	Introduction.....	45
1.7.2	World trade.....	45
1.7.3	Chemical composition and properties	47
1.8	Bibliography.....	49
Chapter 2 Aims and objectives.....		57
Chapter 3 Materials and methods.....		60
3.1	Reagents.....	61
3.2	General instrumentation.....	61
3.3	Cell cultures and manipulation.....	63
3.3.1	Bacterial strains.....	63
3.3.2	Culture medium.....	63
3.3.3	Preparation of chemically competent cells.....	64
3.3.4	Preparation of electrocompetent cells.....	65
3.3.5	Transformation of competent E. coli cells.....	65
3.4	General procedures.....	66
3.4.1	Gene cloning.....	66
3.4.2	Agarose gel electrophoresis.....	66
3.4.3	Protein overexpression and purification.....	67
3.4.4	Protein quantification.....	68

3.4.5	SDS-PAGE:	69
3.4.6	Size exclusion chromatography.....	70
3.4.7	Crystallisation.....	71
3.4.8	Enzymatic activity assay.....	76
3.4.9	Kinetic characterisation.....	76
3.4.10	pH effect on enzyme activity and stability.....	76
3.4.11	Temperature effect on enzyme activity and stability.....	77
3.4.12	Wine analysis.....	77
3.4.13	Vanillin analysis.....	80
3.4.14	Isoflavones analysis.....	82
3.5	Bibliography.....	85
Chapter 4 Selection of candidates.....		87
4.1	Introduction.....	88
4.2	<i>Halothermothrix orenii</i>	88
4.2.1	Activity assays.....	90
4.2.2	Stability assays.....	94
4.3	Gene selection of new candidates	98
4.4	Characterisation of the new candidates: AacGH1, AheGH1 and PanGH1.	105
4.4.1	Cloning, expression, purification and kinetics	105

4.4.2	Size-exclusion chromatography.....	110
4.4.3	Crystallisation	111
4.4.4	Activity assays.....	121
4.4.5	Stability assays.....	125
4.5	Bibliography.....	133

Chapter 5 Hydrolytic capacity of *HorGH1*, *AheGH1* and *AacGH1* towards two wine glucosides.....136

5.1	Introduction.....	137
5.2	Enzyme expression, purification and lyophilisation	139
5.3	Assessment of the enzymatic performance in model wines and juices ..	140
5.3.1	Composition of the matrices	140
5.3.2	Enzymatic stability	141
5.3.3	Release of volatiles from glucosides in model systems.....	143
5.4	Assessment of the enzymatic performance in real wines and juices	150
5.4.1	Composition of the matrices	150
5.4.2	Enzymatic stability	151
5.4.3	Release of volatiles from glucosides in real wines and juice	152
5.5	Detailed pH stability assay in MW1, MW2 and MJ	154
5.6	Conclusions.....	156

5.7	Bibliography.....	157
Chapter 6 Hydrolytic capacity of <i>HorGH1</i>, <i>AheGH1</i> and <i>AacGH1</i> towards glucovanillin and soybean isoflavones.....160		
6.1	Introduction.....	161
6.2	Assessment of the enzymatic performance towards glucovanillin	163
6.2.1	Enzymatic hydrolysis over synthetic vanillin.....	163
6.2.2	Enzymatic hydrolysis over real vanilla extract.....	164
6.3	Assessment of the enzymatic performance towards synthetic isoflavone glucosides	168
6.4	Enzymatic performance over soybean flour	169
6.5	Bibliography.....	175
Chapter 7 Conclusions and final remarks.....176		
Aknowledgements.....180		

Abstract

In industrial processes, enzymes are considered as a green alternative to traditional chemical catalysis as they are biodegradable, reusable and they do not produce waste products in excess.

Enzymes have been applied to food products since early times of civilization, for instance in the production of bread, wine or milk curd. More recently, glycosidases, a family of enzymes catalysing the hydrolysis of glycosidic bonds in complex sugars, are becoming key tools within the food industry because of their ability to hydrolyse very stable glycosidic bonds in a clean and efficient way.

However, many glycolytic processes in the food industry involve the use of harsh conditions (low pH, high concentrations of ethanol, high temperatures) that can lead to enzyme inactivation. A very promising approach to address this issue is the substitution of mesophilic organisms by extremophilic organisms as source of enzymes; as they thrive in extreme environments, their enzymes are generally performing better than their mesophilic counterparts.

In this sense, two novel extemo-adapted β -glycosidases (family 1) have been selected and characterized, and their performance tested under different environmental conditions (glucose, fructose, organic co-solvents and arrange of pHs and temperatures) that could be generally found in food industrial processes (Chapter 4). In a second stage, the hydrolytic capacity of these enzymes towards 2 wine glucosides (Chapter 5) and towards

glucovanillin and soybean isoflavones (Chapter 6) have been assessed with excellent prospects for their application in those food processes.

Abbreviations

AacGH1	<i>Alicyclobacillus acidiphilus</i> β Glycosidase
AheGH1	<i>Alicyclobacillus herbarius</i> β Glycosidase
ACN	Acetonitrile
<i>A. niger</i>	<i>Aspergillus niger</i>
DMSO	Dimethyl Sulfoxide
DNA	Deoxyribonucleic acid
<i>E. coli</i>	<i>Escherichia coli</i>
EDA	Ethylenediamine
EDTA	Ethylenediaminetetraacetic acid
etOH	Ethanol
GH	Glycosyl Hydrolase
GH-1	Glycosyl Hydrolase family 1
HCl	Hydrochloric acid
<i>Hor</i>	<i>Halothermothrix orenii</i> β Glycosidase
IPTG	Isopropyl β -D-1-thiogalactopyranoside
iPrOH	Isopropanol
K_{cat}	Turnover number
K_M	Substrate concentration at which the rate is half V_{max}
LB	Luria-Bertani
MW	Molecular Weight
MeOH	Methanol
NaCl	Sodium Chloride
NaOH	Sodium Hydroxide
NCBI	National Centre of Biotechnology Information
NEB	New England Biolabs
OD	Optical density
O/N	Overnight
pNP-Glc	Para-nitrophenyl-glucoopyranoside
PEI	Polyethyleneimine
<i>S. cerevisiae</i>	<i>Saccharomyces cerevisiae</i>
SDS PAGE	Sodium Dodecyl Sulphate Polyacrylamide Gel Electrophoresis
SOC	Super Optimal Broth with Catabolite repression
TB	Terrific Broth
THF	Tetrahydrofuran
TEMED	Tetramethylethylenediamine
US \$	American dollar
UV	Ultra Violet
V_{max}	Maximum rate of the enzymatic reaction

Amino acids

A	Ala
C	Cys
D	Asp
E	Glu
F	Phe

G	Gly
H	His
I	Ile
K	Lys
L	Leu
M	Met
N	Asn
P	Pro
Q	Gln
R	Arg
S	Ser
T	Thr
V	Val
W	Trp
Y	Tyr

DNA and RNA nucleotides

A	Adenine
C	Cytosine
T	Thymine
G	Guanine
U	Uracil

Units of measure

bp	Base Pair
g	Gram
mol	Mole
Da	Dalton
kDa	Kilo Dalton
L	Litre
h	Hour
s	Second
mg	Milligram
mhL	Million of hectolitres
mL	Millilitre
min	Minute
M	Molarity
rpm	Rotation per minute
v	Volts
Ve	Elution Volume
Ve/Vo	Elution Volume/ Void Volume
v/v	Volume/ volume
w/v	Weight/ volume

Chapter 1: General introduction

1.1 Biocatalysis

Catalysts are molecules capable of diminishing the energy barriers of a reaction, speeding up the transformation of substrates into products, and remaining unaltered.

Enzymes are protein-based catalysts presenting important advantages compared to chemical catalysts:¹

- a) Greater regio-, stereo- and chemoselectivity than the chemically-catalyzed reactions
- b) Catalysis of reactions under physiological conditions (pH and temperature)
- c) Greener catalysts because they are biocompatible, biodegradable, can be reused, produce less by-products and are less toxic
- d) Enzymes can be produced in unlimited quantities

At industrial level, the success of a catalyst depends ultimately on its economics but also its environmental metrics. In the 1980s, there was growing concern in the chemical industry regarding the abundant amounts of waste being generated. A pressing shift from traditional concepts of reaction efficiency and selectivity, focus on chemical yield, to the valorisation of raw materials utilization, elimination of waste, and avoidance of toxic and/or hazardous substances was urgently needed.^{2,3} This led to the emergence of the term “Green Chemistry”, which basically means pollution prevention better than waste remediation.

Nowadays the success of a catalyst at an industrial level depends on its sustainability metrics at the three levels; economy, society and ecology.

Enzymes processes have become competitive and have been introduced in industry where they accomplish these sustainability goals better than alternative processes. Due to the advantages mentioned earlier, biocatalytic processes have demonstrated to be more environmentally attractive, more cost-effective, and therefore more sustainable. In fact, biocatalysis complies with 10 of the 12 principles of green chemistry defined by Anastas and Warner in 1998⁴ (Table 1.1).

Table 1.1. Green Chemistry and Biocatalysis⁵

	Principle of green chemistry	Biocatalysis
1	Waste prevention instead of remediation	significantly reduced waste
2	Atom efficiency	more atom- and step-economical
3	Less hazardous materials	generally low toxicity
4	Safer products by design	not relevant (product not process)
5	Innocuous solvents and auxiliaries	usually performed in water
6	Energy efficient by design	mild conditions/energy-efficient
7	Preferably renewable feedstocks	enzymes are renewable
8	Shorter synthesis (avoid derivatization)	avoids protection/deprotection steps
9	Catalytic rather than stoichiometric reagents	enzymes are catalysts
10	Design products for degradation	not relevant (product not process)
11	Real-time analysis	applicability to biocatalytic processes
12	Inherently safer processes	mild and safe conditions

While biocatalysis has steadily replaced traditional chemical processes in industry in the last decades, enzymes still show some undesirable features.

Due to their natural origin, enzymes can present low stability under industrial conditions (high temperatures, extreme pH values, aggressive solvents, etc), and some enzymes can still be expensive to produce, especially if require purification steps, or co-substrates. In addition, as enzymes are proteins, they constitute potential allergens when inhaled or ingested.¹

Luckily these drawbacks are being addressed by the development of new tools in biochemistry, bioinformatics, and micro- and molecular biology like rational protein design and in vitro evolution in combination with high-throughput screening tools.^{6,7}

1.2 Enzymes in the food industry

Enzymes have been used since the early times of civilization in food related products. Some examples are the use of yeast in baking bread already known by ancient Egyptians, the fermentation of grapes to wine, the conversion of milk to curds in containers made of animal stomachs, meat tenderization with papain or use of moulds to make some oriental fermented foods.⁸ More recently, enzymatic preparations have been used since the beginning of the 20th century for the stabilization of beers as well as the stabilization and clarification of wines and fruit juices. While the first generation of enzymatic preparations was unspecific due to the limited understanding of complex science, manufacturers have been continuously trying to improve the specificity of technical enzymes (Table 1.2).

Table 1.2. Enzymes usage in food applications.⁹ Reproduced from reference [9].

Enzyme	Source	Action in food	Application
α -Amylase	<i>Aspergillus spp.</i> <i>Bacillus spp.</i> <i>Microbacterium imperiale</i>	Wheat starch hydrolysis	Amylase dough softening, increased bread volume, aid in the production of sugars for yeast fermentation
α -acetolactate	<i>Bacillus subtilis</i>	Converts acetolactate to acetoin	Reduction of wine maturation time by circumventing need of decarboxylase for secondary fermentation of diacetyl to acetoin
Amyloglucosidase	<i>Aspergillus niger</i> <i>Rhizopus spp.</i>	Hydrolyzes starch dextrins to glucose (saccharification)	One stage of high fructose corn syrup production; production of "lite" beers
Aminopeptidase	<i>Lactococcus lactis</i> <i>Aspergillus spp.</i> <i>Rhizopus oryzae</i>	Releases free amino acids from N-terminus of proteins and peptides	Debittering protein hydrolyzates accelerating cheese maturation
Catalase	<i>Aspergillus niger</i> <i>Micrococcus luteus</i>	Breaks down hydrogen peroxide to water and oxygen	Oxygen removal technology, combined with glucose oxidase
Cellulase	<i>Aspergillus niger</i> <i>Trichoderma spp.</i>	Hydrolases cellulose	Fruit liquefaction in juice production
Chymosin	<i>Aspergillus awamori</i> <i>Kluyveromyces lactis</i>	Hydrolases κ -casein	Coagulation of milk for cheese making

Cyclodextrin glucanotransferase	<i>Bacillus spp.</i>	Synthesize cyclodextrins from liquefied starch	Cyclodextrins are food grade microencapsulants for colours, flavours and vitamins
β -Galactosidase (lactase)	<i>Aspergillus spp.</i> <i>Kluyveromyces spp.</i>	Hydrolyses milk lactose to glucose and galactose	Sweetening milk and whey; products for lactose-intolerant individuals; reduction of crystallisation in ice cream containing whey; improving functionality of whey protein concentrates; manufacture of lactulose
β -Glucanase	<i>Aspergillus spp.</i> <i>Bacillus subtilis</i>	Hydrolyses β -glucans in beer mashes	Filtration aids, haze prevention in beer production
Glucose isomerase	<i>Actinoplanes missouriensis</i> <i>Bacillus coagulans</i> <i>Streptomyces lividans</i> <i>Streptomyces rubiginosus</i>	Converts glucose to fructose	Production of high fructose corn syrup
Glucose oxidase	<i>Aspergillus niger</i> <i>Penicillium chrysogenum</i>	Oxidises glucose to gluconic acid	Oxygen removal from food packaging; removal of glucose from egg white to prevent browning
Hemicellulase and xylanase	<i>Aspergillus spp.</i> <i>Bacillus subtilis</i> <i>Trichoderma reesei</i>	Hydrolyses hemicelluloses	Bread improvement through improved crumb structure
Lipase and esterase	<i>Aspergillus spp.</i> <i>Candida spp.</i> <i>Rhizomucor miehei</i> <i>Penicillium roqueforti</i> <i>Rhizopus spp.</i> <i>Bacillus subtilis</i>	Hydrolyses triglycerides to fatty acids and glycerol; hydrolases alkyl esters to fatty acids and alcohol	Flavour enhancement in cheese products; fat function modification by interesterification; synthesis of flavour esters
Pectinase (polygalactouronase)	<i>Aspergillus spp.</i> <i>Penicillium funiculosum</i>	Hydrolyses pectine	Clarification of fruit juices by depectinization
Pectinesterase	<i>Aspergillus spp.</i>	Removes methyl groups from galactose units in pectin	With pectinase in depectinization technology
Pentosanase	<i>Humicola insolens</i> <i>Trichoderma reesei</i>	Hydrolyzes pentosans (soluble non-starch polysaccharides in wheat flours)	Part of bread dough improvement technology
Pullulanase	<i>Bacillus spp.</i> <i>Klebsiella spp.</i>	Hydrolyzes 1–6 bonds that form branches in starch structure	Starch saccharification (improves efficiency)
Protease (proteinase)	<i>Aspergillus spp.</i> <i>Rhizomucor miehei</i> <i>Cryphonectria parasitica</i> <i>Penicillium citrinum</i> <i>Rhizopus niveus</i> <i>Bacillus spp.</i>	Hydrolysis of κ -casein; hydrolysis of animal and vegetable food proteins; hydrolysis of wheat glutens	Milk coagulation for cheese making; hydrolyzate production for soups and savoury foods; bread dough improvement

Current use of enzymes in the food industry mainly applies to ingredient production and texture modification with applications in beverage clarification, brewing, baking, meat tenderization or production of low-lactose milk and high-fructose corn syrup.

Industrial food enzymes fall into three principal groups: hydrolases, oxidoreductases, and isomerases, and their bulk production is carried out using mainly two microbial genera: *Bacillus* and *Aspergillus*.¹⁰

and the formation of a covalent glycosyl–enzyme intermediate. In the second step, the carboxylate deprotonates a water molecule which attacks the anomeric carbon yielding a sugar with the same anomeric configuration of the substrate (Fig. 1.2).¹³

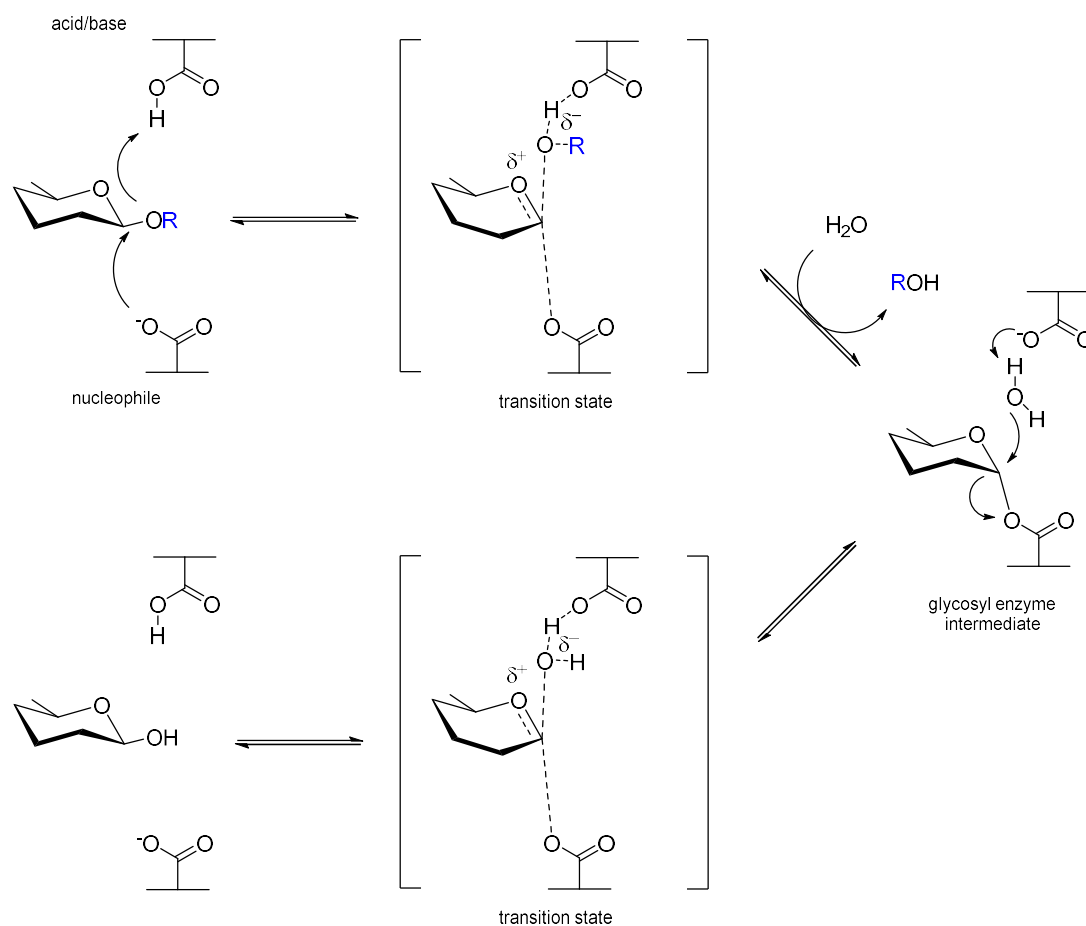


Figure 1.2. Retaining mechanism for a β -Glycosidase proceeding through a oxocarbenium ion-like transition state.¹²

Hydrolysis of monoglucosides requires only one β -glycosidase, while the hydrolysis of disaccharide glycosides is achieved in two sequential steps (Fig. 1.3).^{14–17}

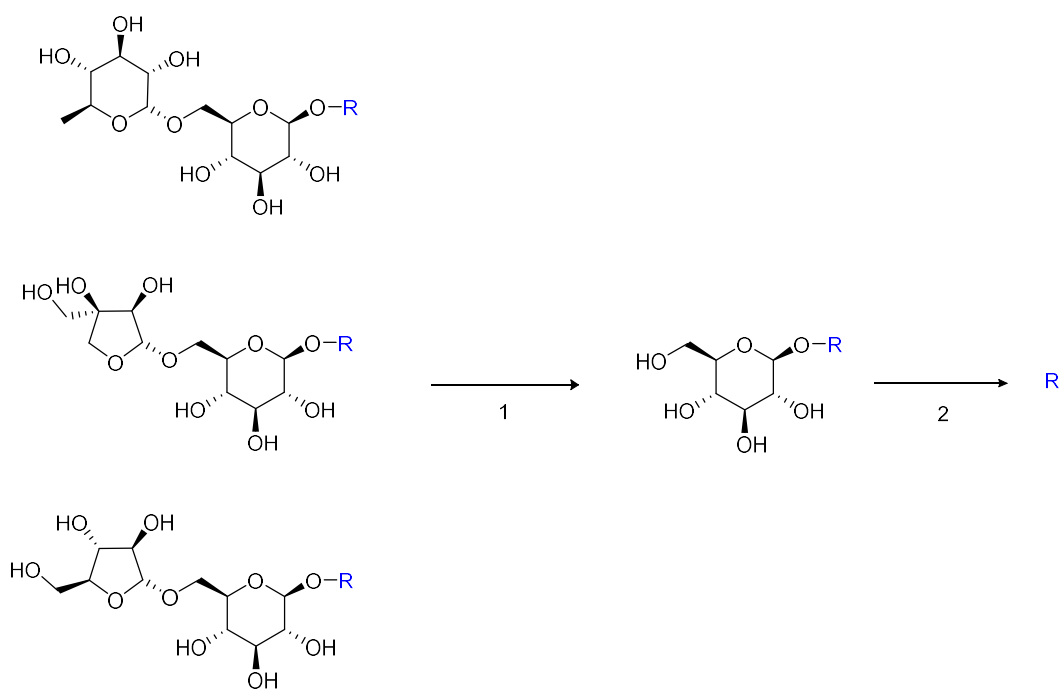


Figure 1.3. Sequential enzymatic hydrolysis of disaccharidic aroma precursors. A α -rhamnosidase, a α -arabinosidase, or a β -apiosidase releases the aroma glucopyranoside (step 1). A β -glucosidase splits the glucose aglycone bond, releasing the volatile aroma (step 2).

Glycosidases are gaining momentum due to the broad range of industrial applications they catalyse, including the degradation of plant materials¹⁸ (e.g. cellulases to degrade cellulose to glucose, which can be used for ethanol production), in the paper and pulp industry¹⁹ (e.g. xylanases to remove hemicelluloses from paper pulp), pharmaceutical industry²⁰ (e.g. degradation of microbial biofilms) but especially in the food industry⁶ (e.g. invertases to manufacture glucose and fructose from sucrose, amylases for the production of maltodextrins) where they are becoming key tools to hydrolyse very stable glycosidic bonds in a clean and efficient way.

However, many glycolytic processes in the food industry involve the use of harsh conditions (low pH, high concentrations of ethanol, high temperatures²¹) that can lead to enzyme inactivation. A very promising approach to address

this issue is the substitution of mesophilic organisms by extremophilic organisms as source of enzymes; as they thrive in extreme environments, their enzymes are generally performing better than their mesophilic counterparts.²²

1.4 Extremophiles

Extremophiles are organisms well adapted to extreme environmental conditions which can be unbearably hostile or even lethal for other forms of life. They have been found in depths of 6.7 km inside the Earth's crust, 11 km deep inside the ocean; from extreme acidic (pH 0) to extreme basic conditions (pH 12.8); and from hydrothermal vents at 122 °C to frozen sea water, at -20 °C.²³ Some have adapted to grow in toxic waste, organic solvents, and heavy metals.

Some examples of extremophiles are thermophiles, organisms that grow at elevated temperatures, acidophiles, that are able of withstanding a pH as low as 3 and below, halophiles, that can tolerate high salt concentrations or psychrophiles, with preferred growth temperatures below 0 °C.²⁴

Halothermothrix orenii is a thermohalophilic Gram-negative anaerobic bacterium isolated from a Tunisian salt lake. It grows optimally at 60 °C (max. 70 °C) with 10 % NaCl (growth range between 4 and 20 %) and optimal pH range of 6.5 - 7.0 (growth within pH range of 5.5–8.2).²⁵ Genome analysis performed by Mavromatis *et al.*²⁶ revealed that the genome consists of one circular chromosome of 2578146 bps encoding 2451 predicted genes. Protein sequence analyses and metabolic reconstruction discovered a unique combination of strategies for thermophilic and halophilic adaptation, hence *H. orenii* can serve as a model organism for the study of the adaptation under thermohalophilic conditions and the development of biotechnological

applications under conditions which may benefit from high temperatures and high salt concentrations.

According to Bhattacharya et al.²⁵ the *H. orenii* genome contains two β -glucosidase enzyme coding genes: Hore_19810 with a nucleotide sequence of 2220 bp encoding a 739 amino acid polypeptide with a molecular weight of 81.86 kDa and Hore_04820, with a nucleotide sequence of 1299 bp, encoding for a 432 amino acid containing polypeptide with a molecular weight of 50.44 kDa. The β -glucosidase coding gene Hore_04820 has been cloned, over-expressed in *E. coli* and purified using metal-ion affinity chromatography described by Kori et al.²⁷ The recombinant protein appeared as 53 kDa polypeptide unit as monitored by SDS- PAGE under reducing and denaturing conditions. The enzyme was found to be active at high temperatures, however, no other biochemical characterization was performed.

This β -glucosidase from *H. orenii* (*HorGH1*) has been used as a template to select the other 2 β -glucosidases (*AheGH1* and *AacGH1*) presented in this thesis work, from the acidophilic organisms *Alicyclobacillus herbarius* and *Alicyclobacillus acidiphilus*.

1.5 Wine

1.5.1 History of wine-making

The origins of wine are dated around the 4th millennium B.C.²⁸ in the area of Russia, between the Baltic and the Caspian seas. About 7000 years ago, the establishment of agricultural practices resulted in the “Cradle of Civilization” of Egypt and Mesopotamia leading to the domestication of wild vines.²⁹

From these areas, vines and wine-making practices spread to the region of the Mediterranean, and after the decay of these civilizations, wine production in Europe was not (re)established until the late medieval times.

Later, with European colonization, grapevine cultivation was expanded into most of the temperate regions of the globe. The expansion of vines and wine was also closely related with social and cultural aspects of societies.

Wine began to adopt its modern expression during the 17th century. The use of sulphur treatments in the barrel became quite common in Western Europe. This practice remarkably increased the possibility of producing wines of better quality and also of extending wine’s durability.

In the 1860s, the scientific achievements of Louis Pasteur on microbiological processes involved in wine-making (the role of yeasts in fermentation, the role of some lactic acid bacteria (LAB) in wine decay) formed the bases of the modern wine industry.^{30,31}

During the 1870s, most of the wine grapes vineyards in Europe were devastated by *Phylloxera*, a root pest accidentally imported from North

America, crashing the wine industry. By the same time, it was found that Native American vines were immune to the pest, and the practice of splicing European grapevines into American rootstocks to protect vineyards from the insect was established, a practice which continues to these days. In the late 19th century, wine production was completely established in France.

Nowadays, Italy, Spain and France are still the three main producers of wine, however, non-traditional producing regions such as Australia, New Zealand, South Africa, United States, Argentina and Chile are rapidly gaining importance in the wine market.

1.5.2 The wine business

Since the 1970s, the wine market has become considerably more competitive. Throughout the 21st century wine consumption has decreased in the traditional “Old World” wine producing countries, whereas new competitors have emerged from nations such as United States, Australia, South Africa and Chile.³²

Growth in global demand is principally motivated by a change in consumers’ predilections and lifestyles in some traditional consumer markets, such as United States and United Kingdom, or by new consumers in emerging markets, such as Brazil, China, India, or Russia.³³

The following statistics about vineyard surface area, grape production and wine production and consumption have been taken and adapted from the OIV 2019 Statistical Report on World Vitiviniculture³⁴ and the State of the World Vitivinicultural Sector in 2019.³⁵

World wine production in 2019 was estimated at 260 million of hectolitres (Fig. 1.4), from which, 156 mhL corresponded to EU production. Italy (47.5 mhL), France (42.1 mhL) and Spain (33.5 mhL) accounted for 48% of world wine production in 2019.

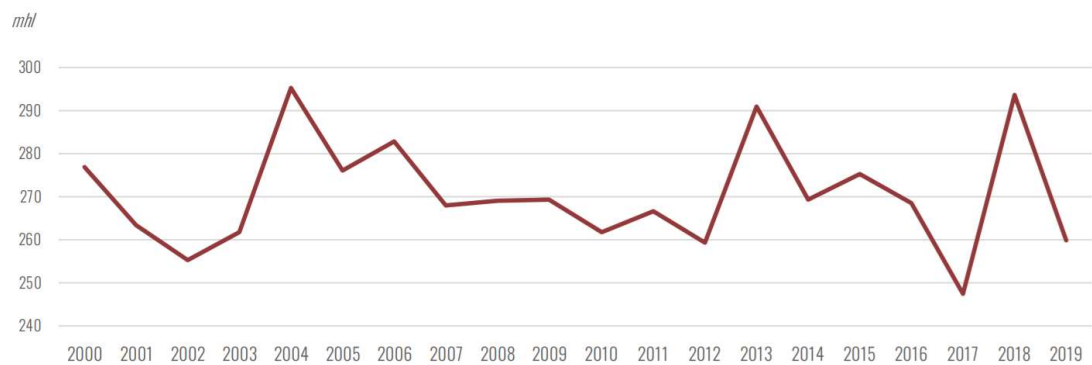


Figure 1.4. Evolution of world wine production (juices and musts excluded).³⁵

World wine consumption was estimated at 244 mhL in 2019 (Fig. 1.5). EU consumed an estimate volume of wine of about 128 mhL, accounting for 53% of the world consumption. The USA, with 33 mhL, confirmed their position as the world's largest wine consumption country. China and Japan were, respectively, the first and second highest consumers in Asia with 17.8 mhL and 3.5 mhL.

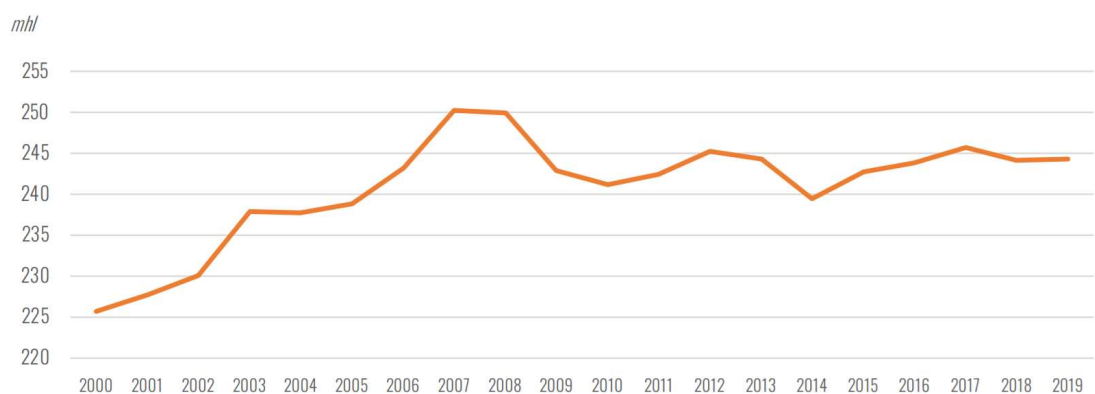


Figure 1.5. Evolution of world wine consumption in 2019.³⁵

With respect to the international trade of wine, the world wine export market had expanded in 2019 with respect to 2018 both in volume (Fig. 1.6), estimated at 105.8 mhl (+1.7%), and in value (Fig. 1.7), with 31.8 bn EUR (+0.9%).

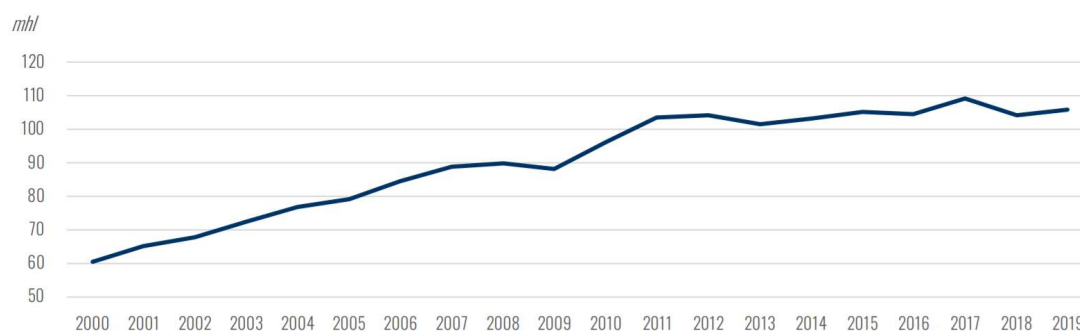


Figure 1.6. Evolution of international trade of wine by volume.

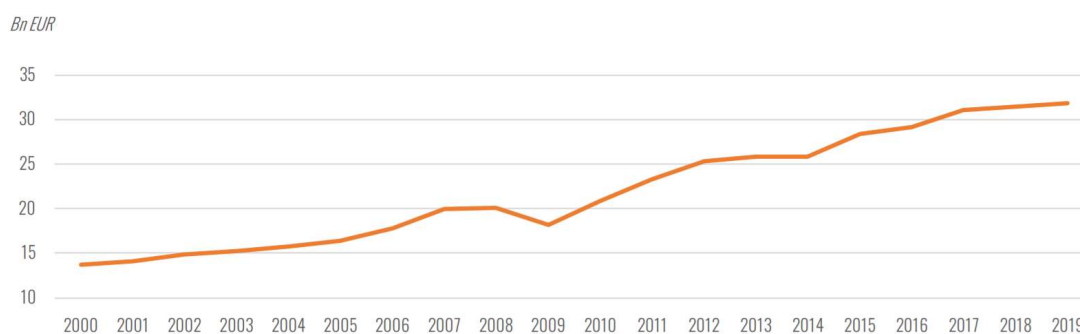


Figure 1.7. Evolution of international trade of wine by value.

In terms of volume, Italy was the largest exporter accounting for 20.5% of the global market. Together with Spain and France, they are responsible for 54% of the world market. In terms of value, France, Italy and Spain also secured the top positions, with France being the most important exporter (9.8 bn EUR).

1.5.3 The wine-making process

A scheme of the wine-making process is represented in Figure 1.8.

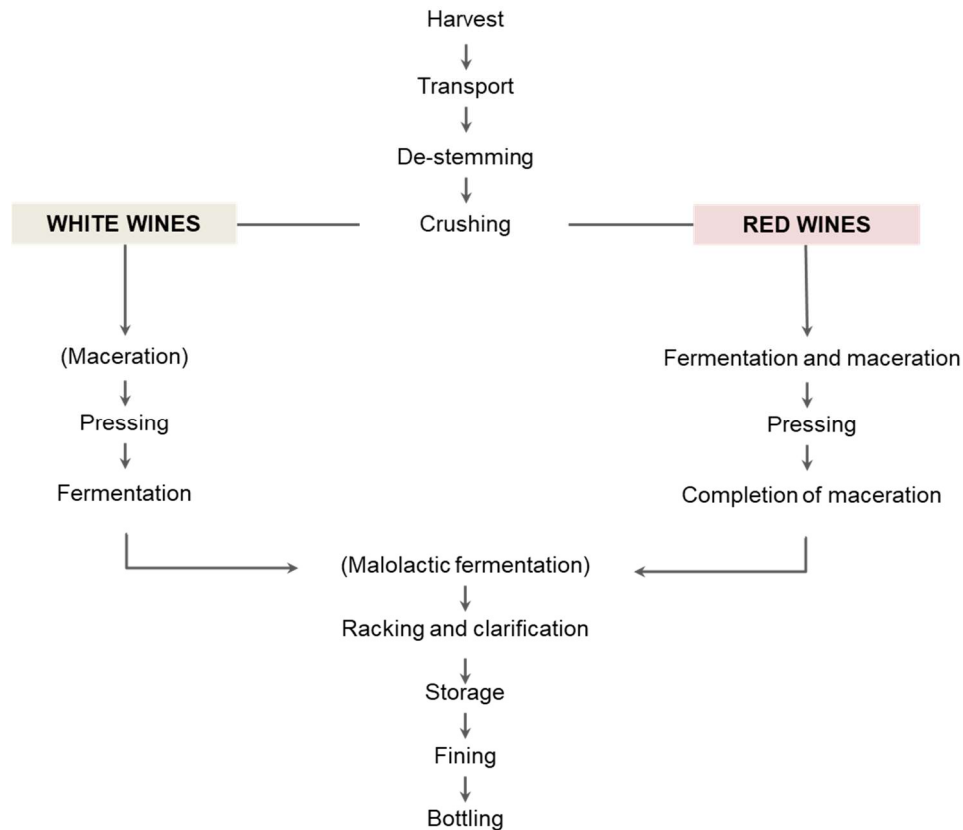


Figure 1.8. Vinification process for white and red wines.

Firstly, in the wine-making process, it is necessary to find and harvest high quality grapes in their optimum condition, determined by their acid and sugar content. This relation will influence the wine aroma, a key parameter affecting the quality of a wine.

Immediately after de-stemming, the fruit is crushed as softly as possible, since an excess of pressure might damage the seeds, which would lead to an extra of phenolic compounds imparting bitterness and astringency to the wine. By

crushing, grape juice is released, facilitating the access of yeasts to the sugar content.

Maceration is an important step in the process as it facilitates the extraction of nutrients, flavours and colourants from the pulp, skin and seeds. For red wines, maceration is prolonged and occurs at the same time as alcoholic fermentation. For white wines, maceration is avoided or kept to a minimum, lasting no more than a few hours.

The following stage is fermentation, considered the most important phase in the elaboration of a wine. During fermentation, the fermentable sugars (glucose and fructose) contained in the must are converted by yeasts into ethanol and carbon dioxide with the generation of heat, the excess of which has to be removed. The process runs for 2 or 3 weeks at a temperature around 20-27°C (no more than 30°C). During fermentation, yeasts not only transform sugars into alcohol, but also generate important bouquet and flavour attributes that will define the wine.

A second fermentation can occur in this process. This time, lactic acid bacteria converts the bitter-tasting malic acid into lactic acid, with a softer taste, producing at the same time a small amount of CO₂ and raising the pH value. Malolactic fermentation is particularly valuable in wines with high acidity, as it improves the taste characteristics, but not desirable in wines already high in pH or low in acidity. Almost all red wines benefit from malolactic fermentation. By contrast, white wines, with more delicate fragrances, are more susceptible to suffer undesirable flavour changes induced by this second fermentation.

Newly fermented wines are stored and protected from environmental oxygen to limit microbial spoilage. After several weeks, the wine is racked. This process involves drawing off the wine from the barrel to just above the level of the sediments (lees) that have settled during spontaneous (or induced) clarification, and transferring it to clean barrels. Oxygenation due to racking is a fundamental point in the development of the colour and flavour of red wines. In these wines with higher phenol content, oxygen is used in complex chemical reactions leading to their softening.

The last stages of winemaking are maturation and aging. Maturation is commonly used for red wines and less extended for white wines. Wines can be stored and matured in stainless steel tanks, although the formation of aromas is different from those wines matured in oak barrels. The main reason for using oak is to allow the extraction of aromatic compounds from the wood into the wine.

Clarification happens spontaneously in most wines during storage, with the sediments removed during maturation and previously to bottling. Also, before bottling, several treatments can be applied to the wine to assure its stability. The practice of fining consists of the precipitation of some compounds (dissolved proteins, excess of tannins) which could affect the long-term stability and wine's flavour. Many fining agents have been used by wine-makers for a long time and they are considered as traditional wine-making aids, for example egg white, casein, gelatine, bentonite or activated carbon. All the fining agents are removed before bottling.

Many white wines and the majority of red wines do not require aging and are sold straight away. Nevertheless, some wines are expected to mature in the bottle before being released to the market.

1.5.4 *Enzymes in winemaking*

In the case of wine, enzymes play a key role; actually, wine can be considered the final product of the enzymatic transformation of grape juice. There are at least 10 enzymes³⁶ involved in this process and most of them are endogenous to the grape itself or to the microorganisms present in the winery environment.

In traditional winemaking, fermentation takes place spontaneously. The yeasts present in the grape and in the winery's environment make it possible. Apart from *Saccharomyces* sp., *Debaryomyces*, *Hanseniaspora*, *Brettanomyces*, *Candida*, *Metschnikowia*, *Pichia* and *Zygosaccharomyces*³⁷ species are also found. Although all these yeasts are present in the first stages of the fermentation, *Saccharomyces* progressively takes over as it adapts better to more extreme conditions (anaerobic environment, low pH, high levels of ethanol, addition of sulphur dioxide as antioxidant).

Throughout the process, these yeasts synthesize enzymes that influence the fermentation positively or negatively, depending on the conditions of the medium and the nature of the enzyme. In addition to yeasts, LAB convert malic acid to lactic acid and CO₂ via malate decarboxylase. Despite this conversion being the main enzymatic activity, LAB are also being investigated for the wide range of secondary metabolic reactions that they catalyse. These modifications influence the taste, flavour and stability of wine and include

glucosidases, esterases, proteases and enzymes related with the citrate metabolism.^{15,38} Some of the endogenous enzymes are mentioned, along with their function in table 1.3.

Table 1.3. Enzymes derived from grapes and wine associated microorganisms. Reproduced from reference [39].

Enzyme	Function
Grapes (<i>Vitis vinifera</i>)	
Glycosidases	Hydrolyse sugar conjugates of tertiary alcohols, it is inhibited by glucose, optimum pH 5-6.
Protopectinases	Produce water soluble, highly polymerized pectin substances from protopectins
Pectin methylesterases	Split methyl ester groups of polygalacturonic acids, release methanol, convert pectin to pectate; thermostable: optimum pH 7-8
Polygalactouronases	Hydrolyse α -D-1,4-glycosidic bonds adjacent to free carboxyl groups in low methylated pectins and pectate; optimum pH 4-5
Pectin lyases	Depolymerise highly esterified pectins
Proteases	Hydrolyses peptide bonds between amino acid residues of proteins; inhibited by ethanol; thermostable; optimum pH 2.
Peroxidases	Oxidation metabolism of phenolic compounds during grape maturation; activity limited by peroxide deficiency and SO ₂ in must.
Yeast (<i>S. cerevisiae</i>)	
β -Glucosidases	Some yeasts produce β -Glucosidases not repressed by glucose
β -Glucanases	Extra cellular, cell wall bound and intracellular, accelerate the autolysis process and release mannoproteins
Proteases	Acidic endoprotease A accelerates the autolysis process
Pectinases	Some yeasts degrade pectic substances to a limited extent; inhibited by glucose levels <2%
Bacteria (LAB)	
Malolactic enzymes	Convert malic acid to lactic acid
Esterases	Involved in ester formation
Lipolytic enzymes	Degrade lipids
Fungi (<i>Botrytis cinerea</i>)	
Glycosidases	Degrade all aromatic potential or fungal infected grapes
Laccases	Broad specificity to phenolic compounds, cause oxidation and browning
Pectinases	Saponifying and depolymerising enzymes; cause degradation of plant cells walls and grape rotting.
Cellulases	Multi-component complexes: endo-, exoglucanases and cellobiases; synergistic working, degrade plant cell walls.
Phospholipases	Degrade phospholipids in cell membranes
Esterases	Involved in ester formation
Proteases	Aspartic proteases occur early in fungal infection, determine the rate and extent of rotting caused by pectinases; soluble; thermostable.

Over the last two decades commercial enzymatic preparations have become very popular in the wine industry,³⁹ giving the winemakers many advantages such as:

- Speeding up settling and clarification processes
- Increased juice yield
- Improved diffusion of phenolic compounds and aroma precursors
- Improved colour stability
- Softening of the wine structure
- Increased of the content of aromatic components
- Improved wine filterability

Enzymes are now exploited in winemaking to improve the efficiency of processes but also to improve wine's quality attributes such as aroma, mouthfeel and structure. The most common commercial preparations in winemaking are pectinases, cellulases, hemicellulases, glucanases and glycosidases.²¹

1.5.4.1 The aroma of wine

The chemistry involved in the flavour of wine has been the focus of extensive research due to the complexity of the volatile aromas contributing to wine's flavour and their variations due to grape varieties, growing regions and vintage years.

Up until the beginning of the 20th century, the attention of wine flavour research was principally on the core components contributing to taste and aroma

(ethanol, organic acids and sugars), the compounds associated with the protection of wine's quality, and the ones related with defects or undesirable aromas such as acetic acid.

In the 1900s, as wine-making technology improved and the incidence of defects decreased, flavour chemistry research focused on understanding the chemical components that contribute to particular sensory attributes associated with different grapes and wines.⁴⁰

The development of wine's aroma is complex, as it is the result of the interaction of many factors such as harvesting, grape variety, viticultural practices, yeast and bacterial metabolism during fermentation, winemaking techniques, type of ageing, etc.^{31,41}

Generally, the constituents of wine contributing to its taste are non-volatile compounds soluble in water or water/alcohol mixtures, while compounds responsible for the aroma and flavour are volatile. While over 800 aromatic compounds have been identified in wines, only a small amount make a substantial contribution to its aroma.⁴² Most of these compounds have pleasant fruity and floral aromas, and low perception thresholds.⁴³

Wine aromatic compounds can be classified based on their origin into three groups.⁴⁴

1. Primary aromas: Originated in the grape
2. Secondary aromas: Arising from the vinification process
3. Tertiary aromas: Generated during maturation or ageing processes

However, this classification is not very accurate as all the aromas arise from the grape and they evolve with the process of wine-making and aging.⁴⁵

In grapes, a considerable part of these compounds are entrapped in form of flavourless, odourless, non-volatile glycosides.⁴⁶ In fact, glycosylated compounds in young wines are two to eight times more abundant than those in the free form.^{47,48}

The aglycone moieties are usually terpenols, but linalool oxides and terpene diols and triols can be found as well (Fig. 1.9). Other type of aroma precursors such as C₆ compounds, fusel alcohols, C₁₃ norisoprenoids, phenolic acids and volatile phenols may also occur.⁴⁹⁻⁵¹

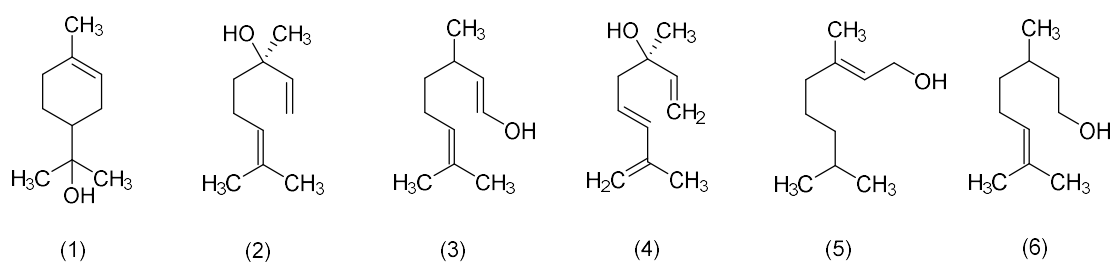


Figure 1.9. Main terpenols of grapes and wines. (1) α -terpineol, (2) linalool, (3) nerol, (4) ho-trienol, (5) geraniol, (6) citronellol.

Upon hydrolysis of the glycosides, the behaviour of the aromatic compounds differs. Usually, monoterpene glycosides will directly produce a volatile aroma compound, while norisoprenoid glycosides may produce odourless products which require additional chemistry to become aromatic volatiles.⁵²

The sugar moiety can be a monosaccharide glycoside, in which the sugar is a β -D-glucose unit, or a disaccharide, in which the glucose is further substituted

with a second sugar unit, typically α -L-arabinofuranoside, α -L-rhamnopyranoside, or β -D-apiofuranoside (Fig. 1.10).⁵³

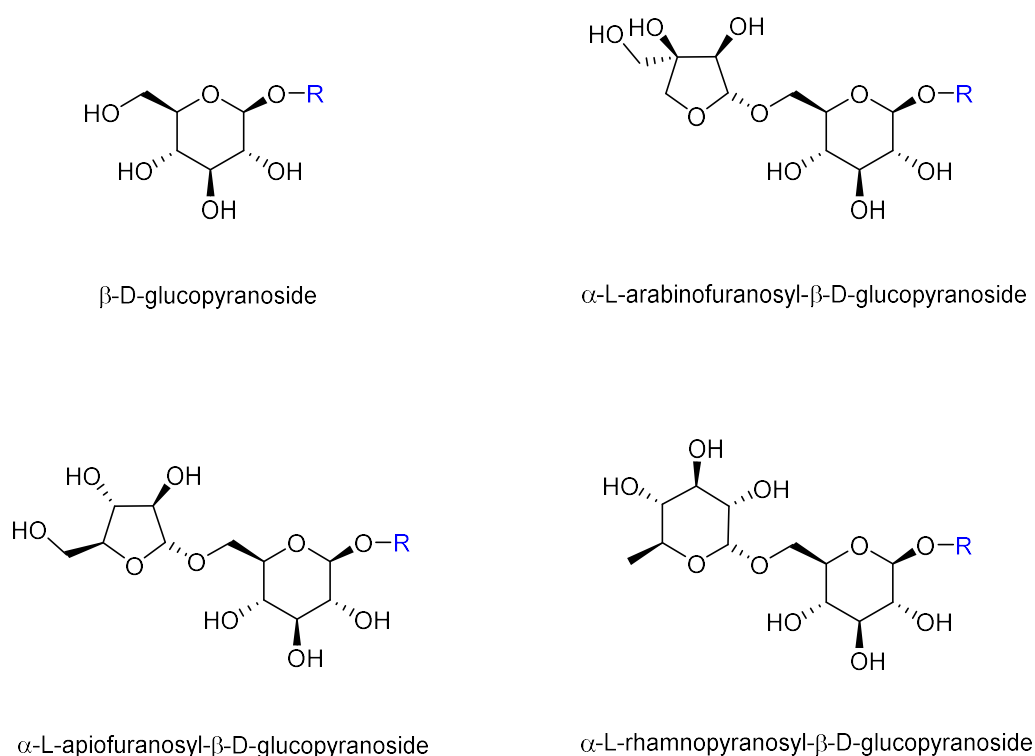


Figure 1.10. Sugar moieties of glycosylated aroma precursors.

The hydrolysis of the glycosides can occur through acid hydrolysis, which is spontaneous during pre-fermentation and fermentation stages,⁵⁴ or can be mediated by endogenous glycosidases (with a very limited effect).⁵⁵ Exogenous glycosidases to improve wine aroma are therefore highly relevant as they do not damage wine structure and quality like other treatments such as heating, acid hydrolysis or application of crude enzyme preparations.⁴⁹

1.6 Vanilla

Vanilla is a tropical orchid, from the family *Orchidaceae*,⁵⁶ originated in Mexico, and in some Central American countries as Costa Rica and Honduras. From about 110 species identified, only 3 are important in terms of cultivation and commerce, *V. planifolia* Jacks. ex Andrews is the only one of economic importance for its flavour qualities, as it is the primary source of the vanilla aroma.⁵⁷

1.6.1 Processing of vanilla pods

Traditionally vanilla curing process comprises of four major stages including killing, sweating, drying and conditioning, with an overall duration of 150-180 days.⁵⁷ The curing process varies depending on the regions, but normally the killing stage involves the submersion of the beans in hot water for 1-2 minutes, the aim is the disruption of the plant cells so the endogenous enzymes can get in contact with their substrates. The sweating step takes approximately 1-2 weeks, during this time the beans are spread under the sun until they get hot and then, at night, they are wrapped up in sheets and left overnight in a hermetic container to “sweat”. During this period enzymatic reactions occur (glucosidases and oxidases) and the vanilla pods get the distinguishing brown colour. After that, the beans need to get dry, this process is performed indoors, normally using fans to create air currents, and last for 2-4 weeks. The last and more time-consuming step is the conditioning, process that can last up to 6 months. During this stage, beans are stored in a conditioned room to allow several biochemical reactions to take place.⁵⁸

During such a long process, a series of biochemical and enzymatic changes generate about 200 compounds which give the characteristic flavour and aroma of vanilla.⁵⁹

1.6.2 *Chemistry of green and cured vanilla beans*

Green vanilla pods do not have the characteristic scent of vanilla, because vanillin is principally present in the glycosylated non-volatile form of glucovanillin.

The distribution of glucovanillin in the bean increases from the basal to the apical part, with the core central part containing the highest concentration. In contrast, plant endogenous β -glucosidases are found in the outer part of the bean, consequently, in order for the hydrolysis to take place, glucovanillin needs to diffuse to the outside region of the bean during the first days of curing to get in contact with the enzymes.⁶⁰ However, it has been reported that glycosidases are not very resistant to heat, and after scalding, most of their activity is lost.⁶¹ It is known though, that the main contribution to the vanilla aroma comes from vanillin⁶² and by the end of the curing process, almost all of the glucoside has been converted into vanillin,⁵⁸ contributing to 1–2% (w/w) of the cured pod.⁶³ Then, if β -glucosidases are really inhibited by the scalding procedure, that would mean that a significant part of vanilla formation must be owed to nonenzymatic, possibly spontaneous, hydrolytic reactions.

Apart from vanillin, other additional compounds also contribute to the complexity and roundedness that distinguishes vanilla from synthetic vanillin: non-volatile compounds include tannins, polyphenols, free amino acids and

resins, but the volatile constituents such as aromatic acids, aromatic alcohols, aromatic esters, phenols, carbonyls, aliphatic alcohols, lactones, terpenoids, aromatic and aliphatic hydrocarbons, heterocyclics, etc are clearly more relevant.⁶⁴

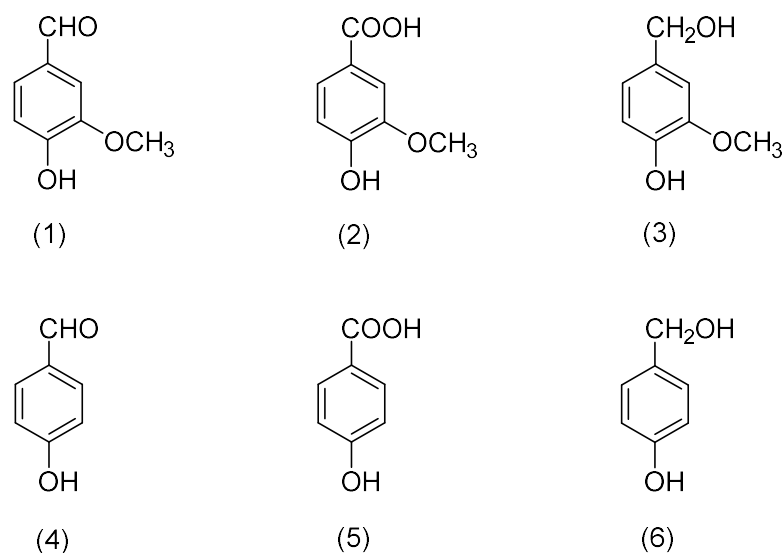


Figure 1.11. Chemical structures of principal vanilla flavour compounds: (1) Vanillin, (2) Vanillic acid, (3) Vanillyl alcohol, (4) p-hydroxybenzaldehyde, (5) p-hydroxybenzoic acid, (6) p-hydroxybenzyl alcohol.

1.6.3 Economics of the vanilla crop

Vanilla is the third most popular spice in the world after saffron and cardamom.⁶⁵ Vanilla aroma is widely used in the food, medicine, pharmaceutical, cosmetic, and perfume industries, among others.

The length, labour-intensity, high sensitivity to the conditions during growth and processing cause high and fluctuant prices of natural vanilla (non-synthetic vanilla extract costing up to 200 times that of synthetic vanillin substitute).⁶⁶ In addition, non-synthetic vanilla production is incapable of meeting the global demand for vanilla flavour (global demand for cured vanilla

substitution of synthetic vanillin for non-synthetic vanillin produced by environmentally friendly processes.

Several biotechnological approaches involving microorganisms have been developed for the production of vanillin, being lignin, isoeugenol, eugenol and ferulic acid the main substrates; all of these precursors are chemically close to the vanillin molecule, cheap and easily available.⁶⁸ It is important to highlight that products obtained through biotechnological procedures from natural substrates are considered as natural and hence vanillin produced using microorganisms is a natural form of vanillin. Some examples of native and engineered microorganisms that have been used to produce vanillin from various substrates can be seen in Table 1.4.

Table 1.4. Various biotechnological approaches used for the synthesis of vanillin.⁷⁰

Substrate	Microorganisms employed	Yield (g/L)
Eugenol	<i>Pseudomonas</i> sp. HR199	2.6
	Recombinant <i>E. coli</i> XL1-Blue(pSKvaomPcalAmcalB) and <i>E. coli</i> (pSKechE/Hfcs)	0.3
	<i>Pseudomonas</i> sp. HR199	0.3
	<i>Amycolatopsis</i> sp. HR167(pRLE6SKvaom)	–
	<i>Amycolatopsis</i> sp. HR167; <i>Rhodococcus opacus</i> PD630	Trace amounts
	<i>Aspergillus niger</i>	–
	<i>P. resinovorans</i> SPR1	0.24
	Isoeugenol	<i>Bacillus subtilis</i>
	<i>Pseudomonas putida</i> I58	Trace amounts
	<i>Arthrobacter</i> sp. TA13	Trace amounts
	<i>Bacillus fusiformis</i> SW-B9	32.5
	<i>Bacillus subtilis</i> HS8	1.36
	<i>Bacillus fusiformis</i> CGMCC1347	8.1
	<i>Pseudomonas chlororaphis</i> CDAE5	1.2
	<i>Bacillus pumilus</i> S-1	3.8
	<i>Pseudomonas putida</i> IE27	16.1
	Recombinant <i>E. coli</i> BL21(DE3)	28.3

	<i>Pseudomonas nitroreducens</i> Jin 1	–
	<i>Candida galli</i>	0.58
	<i>Psychrobacter</i> sp. Strain CSW4	1.28
Ferulic acid	<i>Streptomyces setonii</i> ATCC 39116	>10
	Mutant <i>Pseudomonas putida</i>	2.247
	<i>P. cinnabarinus</i> MUCL39533	0.16
	<i>P. cinnabarinus</i> MUCL39533	0.584
	<i>Pseudomonas</i> sp.	0.0085
	<i>Pseudomonas putida</i>	>10
	<i>Streptomyces halstedii</i> GE107678	0.10–0.15
	<i>E. coli</i> strain JM109/pBB1	0.006
	<i>Pseudomonas fluorescens</i> AN103	–
	Recombinant <i>E. coli</i>	1.1
	<i>A. niger</i> CGMCC0774, <i>Pycnoporus cinnabarinus</i> CGMCC1115	5
	Lactic acid bacteria	Trace amounts
	<i>Amycolatopsis</i> sp. HR167	>10
	<i>Streptomyces</i> sp. V-1	19.2
	<i>E. coli</i> JM109 (pBB1)	2.52
	Recombinant <i>E. coli</i>	5.14
	<i>Pseudomonas fluorescens</i> BF13	–
	Recombinant <i>E. coli</i>	6.6 kg/kg biomass
	<i>Staphylococcus aureus</i>	0.045
	<i>Pycnoporus cinnabarinus</i>	0.126
Glucose	<i>E. coli</i> KL7/ pKL5.97A (ATCC98859) and <i>Neurospora crassa</i>	Trace amounts
	Recombinant <i>Schizosaccharomyces pombe</i>	0.065
	Recombinant <i>S. cerevisiae</i>	0.045
	Recombinant <i>S. cerevisiae</i>	0.500
Vanillic acid	<i>Zygorhynchus moelleri</i>	0.05
	<i>Micromucor isabellinus</i>	1.96
	<i>Aspergillus fumigatus</i>	1.09
	<i>P. cinnabarinus</i> MUCL39533	0.767
Solid-state fermentation using green coconut husk	<i>Phanerochaete chrysosporium</i>	52.5 µg/g

However, biotechnological production of vanillin is not intended to replace natural vanilla extract but synthetic vanillin, at an affordable price and with a

non-synthetic flavour.⁷¹ The natural vanilla extract from pods is instead reserved for high quality products.⁶⁶

1.6.4 World trade

The main vanilla producing countries in 2018 were Madagascar, Indonesia, Mexico, Papua New Guinea, China, and then others, which supply most of the vanilla consumed in the world (Fig. 1.13).

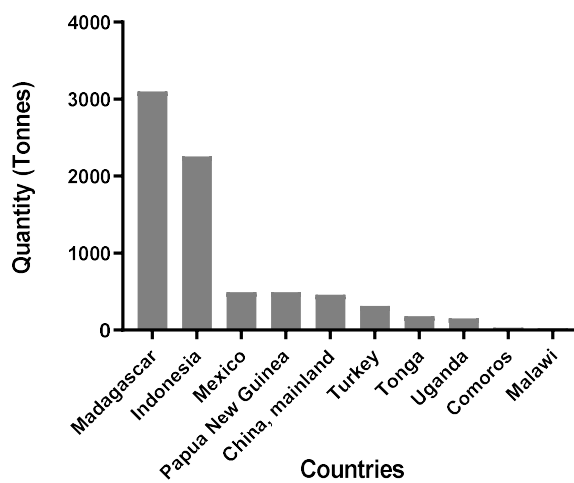


Figure 1.13. Top 10 country, Production of vanilla in 2018.⁷²

Vanilla production in Madagascar represents 40% from the total world production, with an annual volume of 2146 tonnes in 2017, meaning 700 million US \$ (Fig. 1.14).

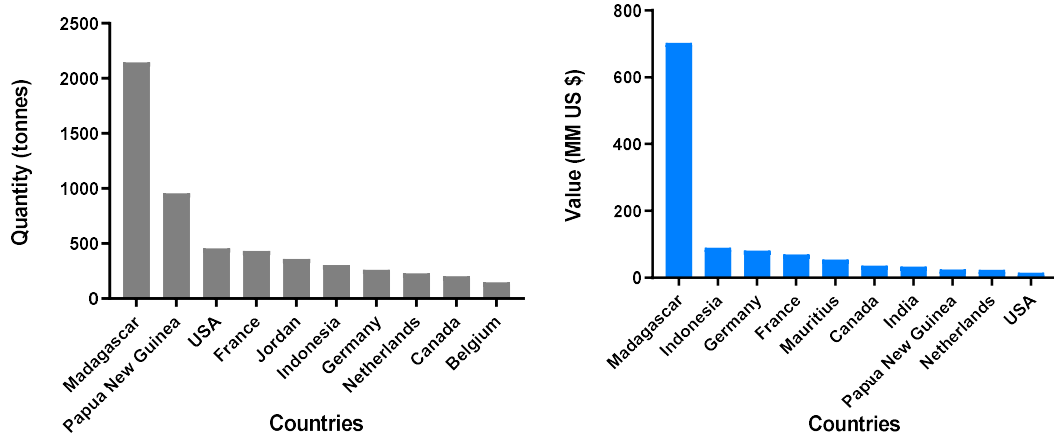


Figure 1.14. Top 10 Country, Export of vanilla in 2017. Left: Quantity; Right: Value.⁷²

The top vanilla importer country with a massive gap from the rest in 2017 was the United States of America, with 16,300 tonnes, followed by France and Canada (Fig. 1.15). To have an exhaustive overview, it is also important to mention those countries that cure vanilla and re-export the finished product making significant profit without running the risks related with the primary production. The leading European re-exporters in 2017 were France, the Netherlands and Germany.

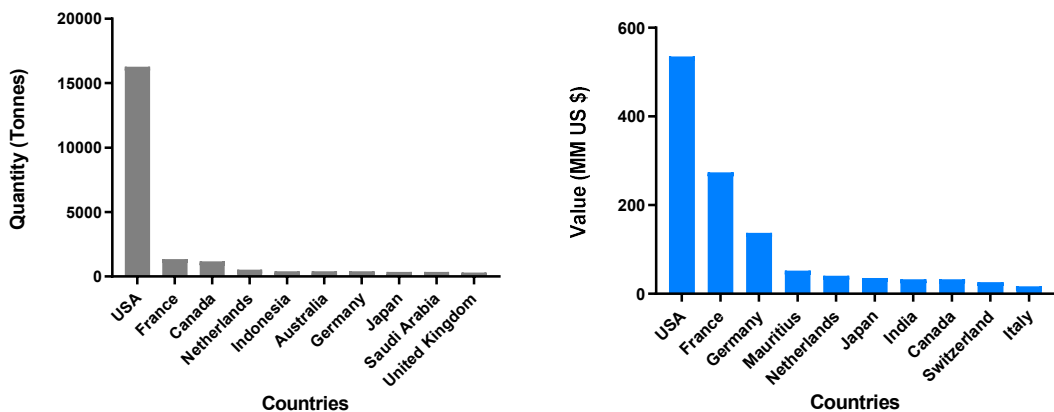


Figure 1.15. Top 10 Country, Import of vanilla in 2017. Left: Quantity; Right: Value.⁷²

1.7 Soybean

1.7.1 Introduction

Soybean (*Glycine max*) originated in China and it constitutes one of the largest sources of vegetable oil in the world with the highest protein content among all others food crops,⁷³ providing more than 25% of the total world protein for food and animal feed.⁷⁴ It is among the 16 main crops cultivated worldwide (barley, cassava, groundnut, maize, millet, potato, oil palm, rapeseed, rice, rye, sorghum, soybean, sugar beet, sugarcane, sunflower, and wheat).⁷⁵

1.7.2 World trade

The demand for soybean is gradually increasing as soybean is becoming one of the most important leguminous seed crops.⁷⁶ The global production of soybean increased around 13-fold from 1961 to 2017.⁷⁷

Until the 1980s, the United States of America was the country producing more than 50% of soybean worldwide, however nowadays, Brazil and Argentina follow the USA as top world soybean producing nations. These three countries, together with China and India account for more than 92% of the world's soybean production (Fig. 1.16).⁷⁸

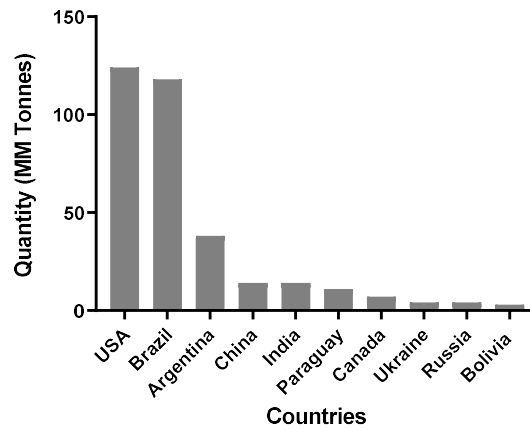


Figure 1.16. Top 10 country, Production of soybeans in 2018.⁷²

With regard to exports, Brazil, USA, Argentina, Paraguay and Canada are the main 5 exporters (Fig. 1.17). Since 1990, Brazil has been exporting a third of the world's total soybean, and USA, a quarter.⁷⁹ In terms of import, China accounts for more than 75% of the global soybean imports (Fig. 1.18).

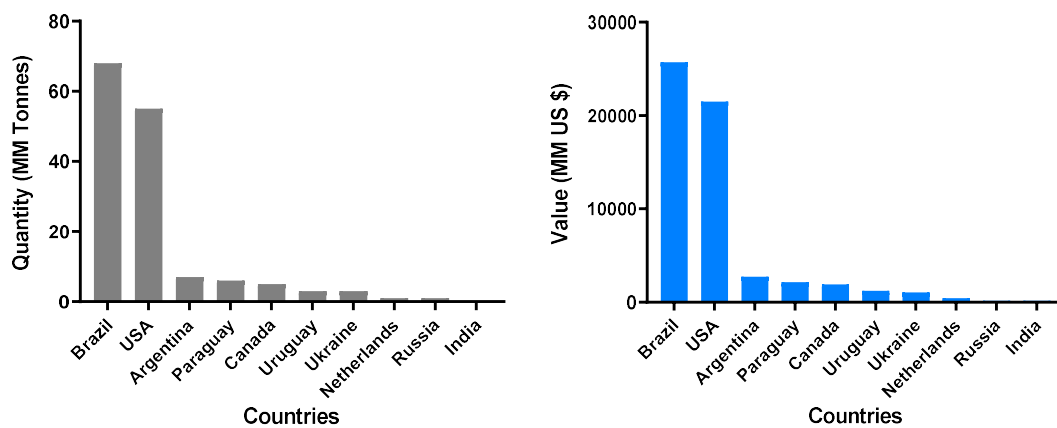


Figure 1.17. Top 10 Country, Export of soybean in 2017. Left: Quantity; Right: Value.⁷²

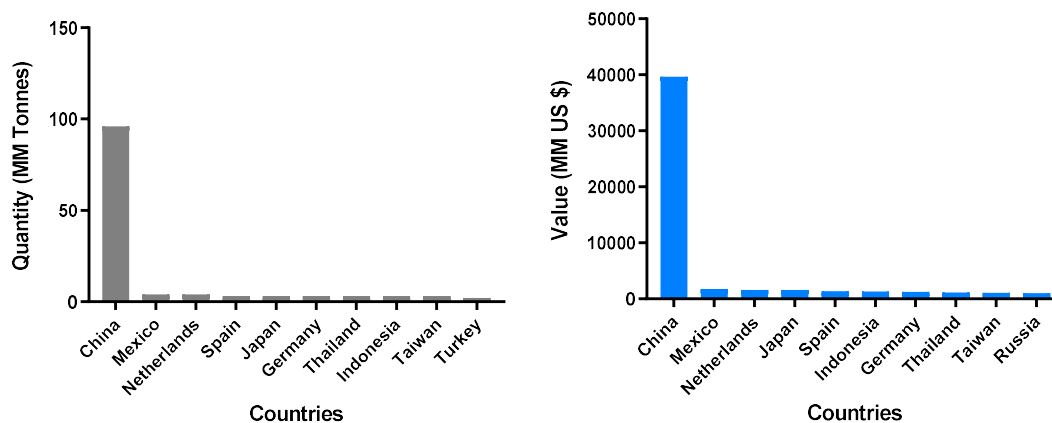


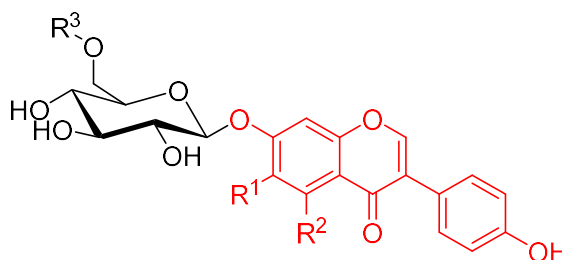
Figure 1.18. Top 10 Country, Import of soybean in 2017. Left: Quantity; Right: Value.⁷²

1.7.3 Chemical composition and properties

Its consumption has become more and more popular in recent years because it is an excellent protein source for the human diet. In addition, soybean contains several compounds, such as isoflavones, considered important food supplements due to their health benefits. They have been reported to have many physiological properties such as anticancer, anti-menopausal, aid in combating osteoporosis, heart disease, diabetes, Kawasaki disease as well as displaying anti-aging effects.^{80,81} The mechanism through which isoflavones achieve the above-mentioned functions is based on their estrogenic properties, their roles as protein tyrosine kinase inhibitors, regulators of gene transcription, modulators of transcription factors and as antioxidants.⁸²

Soybeans contain mainly three types of isoflavones (daidzein, genistein, and glycitein), which may be found in four different forms: as aglycons, 7-O- β -D-

glucosides, 7-O-(6"-O-acetyl) glucosides, or 7-O-(6"-O-malonyl) glucosides (Fig. 1.19).⁸³



glycitin: $R^1 = \text{OMe}$, $R^2 = \text{H}$

genistin: $R^1 = \text{H}$, $R^2 = \text{OH}$

daidzin: $R^1 = R^2 = \text{H}$

$R^3 = \text{H}$, acetyl, or malonyl

Figure 1.19. Structure of the main isoflavone glucosides (glycitin, genistin, and daidzin) found in soybean. The isoflavone moiety (glycitein, genistein, and daidzein) is highlighted in red. The sugar may be further acetylated or malonylated.

Recently, commercial preparations of isoflavones have become very popular as a result of the health benefits reported, however, when the biological activities of these compounds are considered, the bioavailability of the aglycone has been suggested to be higher than that of the glycoside; however, it is a minor constituent of unfermented soy products.⁸⁴

β -glucosidases can be used to hydrolyse isoflavones glucosides to their aglycons. The industrial processing for extracting isoflavones from soybeans includes the use of organic solvents (mostly ethanol) to solubilise the isoflavones.⁸⁵ Accordingly, resistance to organic solvents is one of the essential features that a β -glucosidase applied to this process would have to present. However, the fact is that many β -glucosidases from mesophilic organisms are inhibited by both organic solvents⁸⁶ and glucose.^{87,88}

1.8 Bibliography

- 1 K. Buchholz, V. Kasche and U. T. Bornscheuer, *Biocatalysts and Enzyme Technology*, 2nd Ed., 2012.
- 2 R. A. Sheldon, *Chem. Soc. Rev.*, 2012, **41**, 1437–1451.
- 3 R. A. Sheldon, *ACS Sustain. Chem. Eng.*, 2018, **6**, 32–48.
- 4 J. C. Anastas, P.; Warner, *Green Chemistry: Theory and Practice*, Oxford University Press: Oxford, U.K., 1998.
- 5 R. A. Sheldon and J. M. Woodley, *Chem. Rev.*, 2018, **118**, 801–838.
- 6 N. A. Ackaah-Gyasi, P. Patel, Y. Zhang and B. K. Simpson, *Current and future uses of enzymes in food processing*, Elsevier Ltd., 2015.
- 7 S. Temple, 2001, *Nature*, **414**, 112–117.
- 8 S. L. Neidleman, *Food Technol.*, 1991, **45**, 88.
- 9 R. J. Whitehurst and a M. Van Oort, *Enzymes in Food Technology Second edition Edited by*, 2010.
- 10 J. James and B. K. Simpson, *Crit. Rev. Food Sci. Nutr.*, 1996, **36**, 437–463.
- 11 S. Martínez Cuesta, S. A. Rahman, N. Furnham and J. M. Thornton, *Biophys. J.*, 2015, **109**, 1082–1086.
- 12 D. J. Vocadlo and G. J. Davies, *Curr. Opin. Chem. Biol.*, 2008, **12**, 539–555.
- 13 B. Di Lauro, A. Strazzulli, G. Perugino, F. La Cara, E. Bedini, M. M. Corsaro, M. Rossi and M. Moracci, *Biochim. Biophys. Acta - Proteins*

- Proteomics*, 2008, **1784**, 292–301.
- 14 C. Caldini, F. Bonomi, P. G. Pifferi, G. Lanzarini and Y. M. Galante, *Enzyme Microb. Technol.*, 1994, **16**, 286–291.
- 15 M. S. Cappello, G. Zapparoli, A. Logrieco and E. J. Bartowsky, *Int. J. Food Microbiol.*, 2017, **243**, 16–27
- 16 C. Bayonove, *Carbohydr. Res.*, 1988, **184**, 139–149.
- 17 J. Krisch, M. Takó, T. Papp and C. Vágvölgyi, *Curr. Res. Technol. Educ. Top. Appl. Microbiol. Microb. Biotechnol.*, 2010, 891–896.
- 18 R. N. Maeda, C. A. Barcelos, L. M. M. S. Anna and N. Pereira, *J. Biotechnol.*, 2013, **163**, 38–44.
- 19 F. I. Qeshmi, A. Homaei, P. Fernandes, R. Hemmati, B. W. Dijkstra and K. Khajeh, *Biochim. Biophys. Acta - Proteins Proteomics*, 2020, **1868**, 140312.
- 20 A. K. Nagraj and D. Gokhale, *Adv. Microbiol.*, 2018, **08**, 687–698.
- 21 K. D. Mojsov, D. Andronikov, A. Janevski, S. Jordeva and S. Zezova, *Adv. Technol.*, 2015, **4**, 94–100.
- 22 S. Elleuche, C. Schröder, K. Sahm and G. Antranikian, *Curr. Opin. Biotechnol.*, 2014, **29**, 116–123.
- 23 P. H. Rampelotto, *Life (Basel, Switzerland)*, 2013, **3**, 482–5.
- 24 A. Krüger, C. Schäfers, C. Schröder and G. Antranikian, *N. Biotechnol.*, 2018, **40**, 144–153.
- 25 A. Bhattacharya and B. I. Pletschke, *Enzyme Microb. Technol.*, 2014, **55**, 159–169.

- 26 K. Mavromatis, N. Ivanova, I. Anderson, A. Lykidis, S. D. Hooper, H. Sun, V. Kunin, A. Lapidus, P. Hugenholtz, B. Patel and N. C. Kyrpides, *PLoS One*, 2009, **4**, 1.
- 27 L. D. Kori, A. Hofmann and B. K. C. Patel, *Acta Crystallogr. Sect. F Struct. Biol. Cryst. Commun.*, 2011, **67**, 111–113.
- 28 P. McGovern, S. J. Fleming and S. H. Katz, *The origins and ancient history of wine*, Routledge, 1995.
- 29 R. S. Jackson, *Chapter 13 – Innovations in Winemaking*, Elsevier Inc., 2017.
- 30 R. S. Jackson, *Wine Science Principles and Applications*, 3rd Ed., Elsevier Inc., 2008.
- 31 B. Jokie and R. J. Clarke, *Wine Flavour Chemistry*, West Sussex, 2nd Ed., John Wiley & Sons, 2012.
- 32 L. F. Bisson, A. L. Waterhouse, S. E. Ebeler, M. A. Walker and J. T. Lapsley, *Nature*, 2002, **418**, 696–699.
- 33 A. Gilinsky, S. K. Newton and R. F. Vega, *Agric. Agric. Sci. Procedia*, 2016, **8**, 37–49.
- 34 OIV and International Organisation of Vine and Wine, *2019 Stat. Rep. World Vitiviniculture*, 2019, 23.
- 35 OIV and International Organisation of Vine and Wine, *State of the World Vitivinicultural Sector in 2019*, 2019.
- 36 P. Van Rensburg and I. S. Pretorius, *South African J. Enol. Vitic.*, 2000, **21**, 52–73.

- 37 M. A. Villena, J. F. Ú. Iranzo and A. I. B. Pérez, *Enzyme Microb. Technol.*, 2007, **40**, 420–425
- 38 M. Iorizzo, B. Testa, S. J. Lombardi, A. García-Ruiz, C. Muñoz-González, B. Bartolomé and M. V. Moreno-Arribas, *LWT - Food Sci. Technol.*, 2016, **73**, 557–566.
- 39 K. Mojsov, *IJMT*, 2013, **3**, 112–127.
- 40 P. Polásková, J. Herszage and S. E. Ebeler, *Chem. Soc. Rev.*, 2008, **37**, 2478–2489.
- 41 E. J. Bartowsky and A. R. Borneman, *Appl. Microbiol. Biotechnol.*, 2011, **92**, 441–447.
- 42 N. Loscos, P. Hernández-Orte, J. Cacho and V. Ferreira, *J. Agric. Food Chem.*, 2009, **57**, 2468–2480.
- 43 D. M. Martin, A. Chiang, S. T. Lund and J. Bohlmann, *Planta*, 2012, **236**, 919–929.
- 44 E. Sánchez Palomo, M. C. Díaz-Maroto Hidalgo, M. Á. González-Viñas and M. S. Pérez-Coello, *Food Chem.*, 2005, **92**, 627–635.
- 45 T. Ilc, D. Werck-Reichhart and N. Navrot, *Front. Plant Sci.*, 2016, **7**, 1472.
- 46 G. K. Skouroumounis, R. Massy-Westropp, M. A. Sefton and P. J. Williams, *J. Agric. Food Chem.*, 1995, **43**, 974–980.
- 47 M. Dziadas and H. H. Jeleń, *Anal. Chim. Acta*, 2010, **677**, 43–49.
- 48 M. Ghaste, L. Narduzzi, S. Carlin, U. Vrhovsek, V. Shulaev and F. Mattivi, *Food Chem.*, 2015, **188**, 309–319.
- 49 A. Grimaldi, E. Bartowsky and V. Jiranek, *Int. J. Food Microbiol.*, 2005,

- 105**, 233–244.
- 50 V. Cheynier, R. Schneider, J. Salmon and H. Fulcrand, *Compr. Nat. Prod. II*, 2010, 1119–1172.
- 51 J. J. Mateo and M. Jiménez, *J. Chromatogr. A*, 2000, **881**, 557–567.
- 52 A. K. Hjelmeland and S. E. Ebeler, *Am. J. Enol. Vitic.*, 2015, **66**, 1–11.
- 53 M. Ugliano, E. J. Bartowsky, J. McCarthy, L. Moio and P. A. Henschke, *J. Agric. Food Chem.*, 2006, **54**, 6322–6331.
- 54 T. Cabaroglu, S. Selli, A. Canbas, J. P. Lepoutre and Z. Günata, *Enzyme Microb. Technol.*, 2003, **33**, 581–587.
- 55 A. Sabel, S. Martens, A. Petri, H. König and H. Claus, *Ann. Microbiol.*, 2014, **64**, 483–491.
- 56 E. Childers, N. F., Cibes, H. R. and Hernandez-Medina, in *The Orchids, a Scientific Survey*, Wither, C., 1959, pp. 477–508.
- 57 K. Anuradha, B. N. Shyamala and M. M. Naidu, *Crit. Rev. Food Sci. Nutr.*, 2013, **53**, 1250–1276.
- 58 M. J. W. Dignum, J. Kerler and R. Verpoorte, *Food Rev. Int.*, 2001, **17**, 119–120.
- 59 I. Baqueiro-Peña and J. Á. Guerrero-Beltrán, *J. Appl. Res. Med. Aromat. Plants*, 2017, **6**, 1–9.
- 60 F. E. Arana, *Food Res.*, 1943, **8**, 343–351.
- 61 C. Ranadive, A.S.; Szkutnica, K.; Guerrero, J.G.; Frenkel, Singapore, 1983, p. 147.

- 62 D. Klimes, I Lamparsky, *Int Flavours Food Addit.*, 1976, 272–291.
- 63 A. K. Sinha, U. K. Sharma and N. Sharma, *Int. J. Food Sci. Nutr.*, 2008, **59**, 299–326.
- 64 S. Ramachandra Rao and G. Ravishankar, *J. Sci. Food Agric.*, 2000, **80**, 289–304.
- 65 S. Azeez, in *Chemistry of Spices*, CABI Publishing, Wallingford, Kerala, India, 2008.
- 66 H. Khoyratty, Shahnoo, Kodja and R. Verpoorte, *Ind. Crops Prod.*, 2018, **125**, 433–442.
- 67 V. T. Pardío, A. Flores, K. M. López, D. I. Martínez, O. Márquez and K. N. Waliszewski, *J. Food Sci. Technol.*, 2018, **55**, 2059–2067.
- 68 A. Converti, B. Aliakbarian, J. M. Domínguez, G. B. Vázquez and P. Perego, *Brazilian J. Microbiol.*, 2010, **41**, 519–530.
- 69 N. J. Gallage and B. L. Møller, *Mol. Plant*, 2015, **8**, 40–57.
- 70 B. Kaur and D. Chakraborty, *Appl. Biochem. Biotechnol.*, 2013, **169**, 1353–1372.
- 71 I. Labuda, in *Handbook of Vanilla Science and Technology*, ed. F. C. Havkin-Frenkel, D., Belanger, Wiley-Blackwell, Oxford, 2011, pp. 301–327.
- 72 Food and Agriculture Organization of the United Nations. FAOSTAT Statistical Database. Rome, FAO, 1997.
- 73 M. C. Pagano and M. Miransari, *The importance of soybean production worldwide*, Elsevier Inc., 2016.

- 74 P. H. Graham and C. P. Vance, *Plant Physiol.*, 2003, **131**, 872–877.
- 75 J. A. Foley, N. Ramankutty, K. A. Brauman, E. S. Cassidy, J. S. Gerber, M. Johnston, N. D. Mueller, C. O’Connell, D. K. Ray, P. C. West, C. Balzer, E. M. Bennett, S. R. Carpenter, J. Hill, C. Monfreda, S. Polasky, J. Rockström, J. Sheehan, S. Siebert, D. Tilman and D. P. M. Zaks, *Nature*, 2011, **478**, 337–342.
- 76 D. K. Ray, N. D. Mueller, P. C. West and J. A. Foley, *PLoS One*, 2013, **8**, 6.
- 77 S. Liu, M. Zhang, F. Feng and Z. Tian, *Mol. Plant*, 2020, **13**, 688–697.
- 78 D. N. Rodríguez-Navarro, I. M. Oliver, M. A. Contreras and J. E. Ruiz-Sainz, *Agron. Sustain. Dev.*, 2011, **31**, 173–190.
- 79 P. Cremaq, The miracle of cerrado. *The economist*, 28th August 2010. <https://www.economist.com/briefing/2010/08/26/the-miracle-of-the-cerrado>
- 80 Q. Wang, X. Ge, X. Tian, Y. Zhang, J. Zhang and P. Zhang, *Biomed. Reports*, 2013, **1**, 697–701.
- 81 C. Cui, R. L. Birru, B. E. Snitz, M. Ihara, C. Kakuta, B. J. Lopresti, H. J. Aizenstein, O. L. Lopez, C. A. Mathis, Y. Miyamoto, L. H. Kuller and A. Sekikawa, *Nutr. Rev.*, 2020, **78**, 134–144.
- 82 M. Q. Ren, G. Kuhn, J. Wegner and J. Chen, *Eur. J. Nutr.*, 2001, **40**, 135–146.
- 83 S. Kudou, Y. Fleury, D. Welti, D. Magnolato, T. Uchida, K. Kitamura and K. Okubo, *Agric. Biol. Chem.*, 1991, **55**, 2227–2233.

- 84 D. C. Vitale, C. Piazza, B. Melilli, F. Drago and S. Salomone, *Eur. J. Drug Metab. Pharmacokinet.*, 2013, **38**, 15–25.
- 85 P. A. Murphy, K. Barua and C. C. Hauck, *J. Chromatogr. B Anal. Technol. Biomed. Life Sci.*, 2002, **777**, 129–138.
- 86 J. Batra and S. Mishra, *J. Mol. Catal. B Enzym.*, 2013, **96**, 61–66.
- 87 P. O. De Giuseppe, T. D. A. C. B. Souza, F. H. M. Souza, L. M. Zanphorlin, C. B. Machado, R. J. Ward, J. A. Jorge, R. D. P. M. Furriel and M. T. Murakami, *Acta Crystallogr. Sect. D Biol. Crystallogr.*, 2014, **70**, 1631–1639.
- 88 C. S. Chan, L. L. Sin, K.-G. Chan, M. S. Shamsir, F. A. Manan, R. K. Sani and K. M. Goh, *Biotechnol. Biofuels*, 2016, **9**, 174.

Chapter 2 Aims and objectives

The principal aim of this research project is the characterisation of novel β -glycosidases with the ability to overcome some of the physico-chemical problems that usually characterise food industrial processes.

Within this context, the substitution of mesophilic organisms from extremophilic organisms as source of these industrial enzymes is a potential solution. Extremophiles are organisms very well adapted to extreme environmental conditions, hence extremozymes are thought to better withstand the harsh conditions (pH, temperature, organic solvents, sugars), of some food processes like, for instance, wine-making.

This PhD thesis focusses on the characterisation of 2 novel β -glucosidases and testing their suitability in 3 different processes typical of the food industry: wine-making, isolation of soy isoflavones and isolation of vanillin. To that end, the following steps will be taken:

- ✓ Identification of novel β -glucosidases through the screening of different extremophile's genomes based on their homology with HorGH1, the enzyme used as a template, and the ability of the candidates to thrive in acidic environments.

- ✓ Performance of enzyme kinetics and initial characterisation of both enzymes including activity and stability assays in the presence of different extreme conditions as organic solvents, sugars and a broad range of temperatures and pHs with the aim of pre-testing the enzymes' suitability to be applied in some food industrial processes.

- ✓ Application of the enzymes in 3 food processes mimicking the conditions of the real industrial process.

Chapter 3 Materials and methods

All the work presented in this chapter is my own contribution unless stated otherwise.

3.1 Reagents

Commercially available reagents and cell growing media were purchased from ACROS Organics, Sigma Aldrich, Thermo Fisher Scientific or Merck. Organic solvents were purchased from Sigma-Aldrich. Synthetic genes, Plasmid DNA purification kit, PCR product purification, CloneJET PCR cloning kit and DNA purification were purchased from Qiagen, Thermo or Macherey-Nagel. DNA ladder, protein marker, restriction enzymes and Q5 High Fidelity DNA polymerase were purchased from New England Biolabs. QuickChange lighting multi-site directed mutagenesis kit was purchased from Agilent-Technologies. Transparent 96-well plates and 1 mL cuvettes were purchased from Corning and Sigma Aldrich respectively.

3.2 General instrumentation

DNA amplification and temperature stability assays were performed in a PCR thermal Cycler SensoQuest® Labcycler 48 and Applied Biosystem® Verti®.

DNA electrophoresis and Protein SDS-PAGE were carried out using a power supply EPS 301 from Amershan Bioscience.

Plasmid purification was performed using the NucleoSpin Plasmid purification kit from Macherey-Nagel®, PCR product purification was performed with the QIAquick PCR purification kit from Qiagen® and agarose gel DNA extraction was performed using the QIAquick Gel Extraction kit from Qiagen®.

Solid medium plates and liquid cultures were incubated in a static incubator Thermo Scientific MaxQ6000 with temperature control from 4 to 60 °C or New

Brunswick Scientific Model C24 for temperatures from 30 to 37 °C.

Cell debris were removed from cell lysate suspension using a centrifuge Thermo® Heraeus Multifuge with Thermo Fiberlite F15 for volumes larger than 2mL, at 4 °C.

General centrifuge cycles were performed using Thermo® Microcentrifuge Accuspin Micro 17R, with controlled temperature for volumes of 2 mL or less.

Cells were lysed by sonication using a Fisher brand Ultrasonic Liquid processor FB120 with timer and pulser from Fisher brand.

Protein purifications were performed with a chromatography system AKTAPrime® Start from GE Healthcare using HisTrap FF 1 mL, HisTrap FF 5mL (GE Healthchare) or Ni-NTA Superflow Cartridges (Qiagen).

Size exclusion chromatography was performed using an AKTAPure® using a Superdex 200 Increase 10/300 GL (GE Healthcare) column.

SPME-GC-MS analysis were performed on an an Agilent 6890A gas chromatograph and an Agilent 5973 mass selective detector (Agilent Technologies, Forest Hill, Australia) fitted with a Gerstel autosampler (MPS).

HPLC analysis were performed on an Agilent Technologies HPLC 1200 or a Thermo Scientific Dionex Ultimate 3000 Series HPLC coupled with a Waters X-Bridge C18 (3.5µm, 2.1 x 100 mm).

Absorbance reading and scanning, as well as enzymatic tests, were performed on an EPOCH2 microplate and cuvette reader from BioTeck®.

General pipetting was done with Micropipettes P5000, P1000, P200, P20,

P10 and P2.5 from StarLab® and Eppendorf® Multipipette E2.

pH-meter Orion Star A111, calibrated regularly with standard solutions (pH 4, pH 7 and pH 10 from Sigma-Aldrich).

Chemicals were weighted using balances model PS5602, model CSC2000 or an analytical series PAS214C, all from Thermo Scientific®.

Other common instruments used during the experiments: Lab-Line® Multi-Block Heater, Benchtop Shaker Carl Stuart Limited IKA®, Vortex mixer Wizard from FisherBrand® and microwave cooker from Daewoo®.

3.3 Cell cultures and manipulation

3.3.1 Bacterial strains

The following bacterial strains were used:

- *E. coli* XL10-Gold for construct replication and extraction. Genotype: endA1 glnV44 recA1 thi-1 gyrA96 relA1 lac Hte Δ(mcrA)183 Δ(mcrCB-hsdSMR-mrr)173 tetRF'[proAB lacIqZΔM15 Tn10(TetR Amy CmR)]
- *E. coli* BL21 (DE3) as a standard protein expression strain. Genotype: *E. coli* str. B F⁻ ompT gal dcm lon hsdSB(rB-mB-) λ (DE3 [lacI lacUV5-T7p07 ind1sam7 nin5]) [malB+] K-12(λ s)

3.3.2 Culture medium

- LB medium: N-Z amine (10g), yeast extract (5g), NaCl (10g) and distilled H₂O (1 L).
- LB agar plates: N-Z amine (10g), yeast extract (5g), NaCl (10g), agar (15g) and distilled H₂O (1 L).

- SOB medium: N-Z amine (5g), yeast extract (1.25g), NaCl (0.25g), KCl (0.05g), MgCl₂ 6H₂O (0.5g), MgSO₄ 6H₂O (0.6g) and distilled H₂O (250 mL).
- TB medium: N-Z amine (12g), yeast extract (24g), glycerol (5g), K₂HPO₄ (2.2g) and KH₂PO₄ (9.4g) and distilled H₂O (1L).
- ZYP-5052 auto-induction media: N-Z-Amine (3 g), yeast extract (1.5 g), 1M K₂HPO₄ (15 mL), 1M KH₂PO₄ (15 mL), 1M (NH₄)₂SO₄ (7.5 mL) 1000x trace element solution (0,6 mL) consists of: FeCl₂ (50 mM), CaCl₂ (20 mM), MnCl₂ (10 mM), ZnSO₄ (10 mM), CoCl₂ (2 mM), CuCl₂ (2 mM), NiCl₂ (2 mM), HCl (60 mM), Na₂MoO₄ (2 mM), Na₂SeO₄ (2 mM) and H₃BO₃ (2 mM) (sterilized by filtration); 50x 5052 solution (6 mL) consists of: glycerol (25 g), glucose (2,5 g), α-lactose monohydrate (10 g) and dH₂O (to 100 mL) in dH₂O (to 300 mL).

3.3.3 Preparation of chemically competent cells

A single colony of *E. coli* of the desired strain was inoculated into LB medium (50 mL) and grown at 37 °C, 150 rpm to an OD₆₀₀ of approximately 0.4. The culture was then placed on ice for 20 minutes and subsequently harvested by centrifugation at 3000g for 15 minutes at 4 °C. The cells were resuspended in 10 mL of an ice-cold 100 mM magnesium chloride solution and harvested again in the same conditions as before. The pellet was resuspended in 20 mL of an ice-cold solution of 100 mM calcium chloride and incubated in ice for 30 minutes. After the last harvesting by centrifugation (3000g, 10 minutes, 4 °C), resuspended in 0.5 mL of the previous solution and aliquoted in 40 µL in 1.5 mL microcentrifuge tubes and frozen at -80 °C.

3.3.4 Preparation of electrocompetent cells

A single colony of *E. coli* of the desired strain was inoculated into LB medium (50 mL) and grown at 37 °C, 150 rpm to an OD₆₀₀ of approximately 0.4. The cells were chilled in ice for 20 minutes and then harvested by centrifugation at 3000 rpm, 15 minutes at 4 °C. The pellet was then carefully resuspended in ice-cold sterilized water followed by centrifugation at the same conditions as before. The wash step was repeated with 25 mL of water and then 15 mL of water/glycerol 10%. The pellet was finally resuspended in 0.5 mL of water/glycerol 10% and aliquoted (50 µL) in 1.5 mL microcentrifuge tubes which were flash frozen and stored at -80 °C.

3.3.5 Transformation of competent *E. coli* cells

Under sterile conditions, 0.2-2 µL (100 ng) of plasmid DNA harbouring the gene of interest was transferred to a tube containing chemically competent *E. coli* BL21(DE3) cells (40 µL aliquot). The contents of the tube were mixed gently, incubated on ice for 30 min, heat-shocked at 42 °C for 70 s and transferred back to ice for 5 min. LB medium (250 µL) was added to the tube and incubated at 37°C, 150 rpm for 1 h. The culture was then plated onto LB agar plates supplemented with the appropriate antibiotic. Plates were incubated overnight at 37 °C and stored at 4 °C.

For the electroporation, 1 µL of plasmid DNA was added to 50 µL of electrocompetent cells and then transferred into an ice-cold electroporation cuvette. Cells were electroporated at 1.8 kV for approximately 5 ms, followed by the addition of 500 µL of SOB medium immediately after. Cells were left to grow for 1 hour at 37 °C and 180 rpm before spreading onto LB-agar plates

containing the appropriate antibiotic where they were grown overnight at 37 °C.

3.4 General procedures

3.4.1 Gene cloning

AheGH1 and *AacGH1* were subcloned from the commercially ordered construction from Thermo Fisher Scientific® containing the enzyme sequence of *Alicyclobacillus herbarius* and *Alicyclobacillus acidiphilus* β -glycosidase respectively optimized for expression in *Escherichia coli*.

When using PCR, the reaction was performed using Q5® High-Fidelity DNA polymerase from New England Biolabs. The primers, ordered from Thermo Fisher Scientific, were designed to amplify the desired gene and incorporate restriction sites on both ends. After PCR, the product was purified using the PCR purification kit, and both the gene and the desired vector were digested with the appropriate restriction enzymes. Ligation was performed overnight at 16 °C using T4-DNA ligase from New England Biolabs. After ligation, electro competent cells were used for the transformation. The correct assembly of the final construction was confirmed by sequencing.

3.4.2 Agarose gel electrophoresis

DNA assay gel electrophoresis was performed using an agarose concentration of 0.8% (w/v). The solution was made by dissolving agarose powder (0.32 g) in 40 mL of TAE buffer by heating it in a standard microwave oven until the solution was completely clear. When the temperature was low enough without leaving it solidify, 4 μ L of SYBR safe DNA staining were added. The solution was then loaded into the mold and left to solidify.

Samples were prepared appropriately mixing them with the Gel Loading Dye Purple (6x) from New England Biolabs. The electrophoresis was conducted routinely at 75V and 150 mA for 45 minutes.

3.4.3 *Protein overexpression and purification*

Protein overexpression was performed after competent cells were transformed with the expression vector harbouring the desired protein.

When using autoinduction media, one single colony was inoculated directly in the flask with either 50 mL or 300 mL of ZYP- 5052 media supplemented with ampicillin. For proteins expressed with LB medium, an overnight pre-inoculum of at least 10 mL was prepared the day before and grown at 37 °C and 1/100 of the final volume added to 300 mL of the corresponding media supplemented with ampicillin (0.1 mg/mL). When the OD₆₀₀ was between 0.6-0.8, IPTG (1mM) was added as inductor for the overexpression of the enzyme and the culture left at 30 °C O/N.

After the chosen time, cell cultures were harvested at 4000 g for 20 minutes at 4°C in the appropriate centrifuge tubes and the cells separated from the medium. The supernatant was carefully removed, and the cells resuspended in a minimum of 3 mL of loading buffer/g of pellet. The cell lysis was performed in ice using the sonicator in pulse mode (6 min cycle, 5s on, 5s off, 50% amplitude, ¼ inch probe, Fisherbrand™ Model 120 Sonic Dismembrator). The lysate was then centrifuged at 14500 rpm, for 1 h at 4°C. The collected supernatant was filtered with 0.45 µm Millex PVDF filters before loading onto the Ni²⁺ preloaded column.

The affinity chromatography was performed using an AKTA Start system with

the appropriate column. The filtered crude extract was loaded and left washing until the non-specific proteins were completely eluted. After that, an isocratic wash step with 10% of elution buffer was performed to elute the remaining non-specific proteins bounded onto the column. Finally, 100% of elution buffer was passed through the column and protein elution monitored by UV. Fractions were collected and those containing the desired protein pooled and placed into dialysis tubing. The protein samples were dialyzed at least for 20 hours replacing the buffer at least 2 times at room temperature. The pure proteins were stored at room temperature. The composition of the different buffers used in the purification are detailed in Table 3.1.

Table 3.1. Loading, elution and dialysis buffers.

Loading buffer	HEPES (50 mM), NaCl (150 mM), imidazole (10 mM), pH 7.5
Elution buffer	HEPES (50 mM), NaCl (150 mM), imidazole (300 mM), pH 7.5
Dialysis buffer	HEPES (50 mM), NaCl (150 mM), pH 7.5

3.4.4 Protein quantification

3.4.4.1 By BioTek Take3 Microplate reader

Determination of protein concentration was performed by measuring absorbance at 280 nm based on the absorbance of UV light by the aromatic amino acids tryptophan and tyrosine and disulphide bonded cysteine residues in protein solutions. The protein concentration was then calculated using the Beer-Lambert law. Molar extinction coefficients for each protein were estimated by ProtPram (Table 3.2). All absorbance readings were carried out using a BioTek Take3 Microplate reader.

Table 3.2. Extinction coefficient and molecular masses used for the calculation of protein concentration using a Take3 plate in combination with EPOCH2.

Protein	Extinction Coefficient ($M^{-1} \text{ cm}^{-1}$)	Molecular mass (kDa)
<i>HorGH1</i>	106230	52.1
<i>AheGH1</i>	108415	54.8
<i>AacGH1</i>	115865	54.6
<i>PanGH1</i>	105770	55.9

3.4.4.2 *By Bradford*

During my placement at the AWRI, determination of protein concentration was performed by measuring spectroscopically the change in the colour of Coomassie Blue from red to blue upon binding proteins. In the absence of protein, when the dye is red, Bradford reagent has an absorbance maximum (A_{max}) of 470 nm. In the presence of protein, the change to the anionic blue form of the dye shifts the A_{max} to 595 nm.

Since the amount of the blue anionic form is proportional to the amount of protein in the sample, the quantity of protein in a sample can be calculated directly by measuring the absorption at 595 nm.

3.4.5 *SDS-PAGE:*

SDS-PAGE assay was performed following the original procedure.¹ The running gel (12%: 1.95 mL of Tris HCl 1.5M pH8.8, 2.25 mL acrylamide 40%, 3.125 mL of dH₂O, 75 μ L SDS 10%, 75 μ L ammonium persulfate 10% (w/v) and 7.5 μ L TEMED) was prepared and loaded in between the two glass pieces, adding a few drops of isopropanol on top to avoid the formation of a

meniscus. After the gel was polymerized, the stacking gel was prepared and loaded (0.25 mL 1M Tris pH 6.8, 0.33 mL acrylamide 40%, 1.4 mL dH₂O, 20 μ L SDS 10%, 20 μ L ammonium persulfate 10% (w/v) and 3 μ L TEMED). Before loading, the samples were heated at 90°C for at least 10 minutes after mixed with an equal volume of the 2x loading buffer (0.18 M Tris-HCl buffer pH6, 3.8 mM β - mercaptoethanol, 7.2% (w/v) SDS, 36% (w/v) glycerol and 0.36 (w/v) bromophenol blue). The assay was run at 30 mA, 300 V for 70 minutes. The protein marker, Unstained Protein Standard broad range (10-200 KDa) was loaded as a comparison. The gel was then removed from the mold and either stained with Coomassie blue staining solution (2% Coomassie brilliant blue R-250 in aqueous solution 50% methanol and 10% acetic acid) for 15-30 minutes following destaining with the destaining solution (aqueous solution 7.5% methanol and 10% acetic acid) overnight or with Instant Blue (Expedeon®) solution overnight.

3.4.6 Size exclusion chromatography

The molecular mass of the native proteins was determined by size exclusion chromatography on a Superdex 200 Increase 10/300 GL column with a total bed column of 24 mL from GE Healthcare. The column was equilibrated with 20 mM sodium phosphate buffer pH 8 with 150 mM NaCl. 750 μ L of the purified enzymes (1 mg/mL final concentration) were then injected and the experiment run at a flow of 0.8 mL/min. Fractions were collected and those corresponding to the eluted peak were assayed for concentration and activity to confirm the protein was still active and therefore, correctly folded. A calibration curve was prepared using the Sigma Aldrich Gel Filtration Markers Kit for Protein Molecular Weights 12,000–200,000 Da (MWGF200): β -amylase (200 kDa),

yeast alcohol dehydrogenase (150 kDa), bovine serum albumin (66 kDa) and the void volume indicated by blue dextran (2000 kDa).

3.4.7 Crystallisation

Crystallisation was performed by the Structural Biology group led by Dr. Louise Gourlay at the University of Milan.

3.4.7.1 Crystallisation of *AheGH1*

AheGH1 crystals were grown using the sitting drop vapour diffusion technique, using an Orxy4 crystallisation robot (Douglas Instruments). Briefly, 400 nL drops comprising 10 mg/ml *AheGH1*, in 10 mM HEPES pH 7.5, 100 mM NaCl. Drops were set up in 3-drop, round CrystalQuick 96-well plates (Greiner Bio-One). Each reservoir contained 100 μ L of 96 different crystallisation conditions from the PACT Premier screen (Molecular Dimensions). *AheGH1* crystals grew after 5 days in condition F2 (0.2 M NaBr, 20% (w/v) PEG 3350, 0.1 M Bis Tris Propane pH 6.5, at room temperature. Crystals were cryoprotected 0.1 M Bis Tris Propane pH 6.5, 30% (w/v) PEG 3350 and 30% ethylene glycol cryocooled in liquid nitrogen.

3.4.7.2 Data collection and 3D structure determination of *AheGH1*

X-ray diffraction data were collected on the I04 beamline at the Diamond Light Source (DLS Didcot, UK). Diffraction data were reduced using XDS² and anisotropically truncated and scaled with STARANISO.³ Data collection statistics are reported in Table 3.3.

Table 3.3. Data collection and refinement statistics. Data collection and refinement statistics for X-ray diffraction data collected on a single crystal of AheGH1. Values in parenthesis correspond to the high-resolution shell. For cross-validation, 5% experimental reflections were randomly selected to calculate the R_{free} .

AHE (PDB code 6YN7)	
Crystal	
Space group	P 1 2 ₁ 1
Unit cell dimensions a, b, c (Å); β (°)	100.45 93.35 106.38; 98.70
Data collection	
Beamline	DLS I04
Wavelength (Å)	0.979
Resolution (Å)	105.16-1.98 (2.27-1.98)
Total reflections	401061 (16134)
Unique reflections	58817 (2941)
R_{merge}	0.17 (1.05)
$\#R_{\text{meas}}$	0.18 (1.15)
$I/\sigma(I)$	7.0 (1.5)
$^+CC_{1/2}$	0.996 (0.693)
Completeness (%) <small>ellipsoidal</small>	93.5 (66.5)
Redundancy	6.8 (5.5)
Wilson B-factor (Å)	22.70
Refinement	
Resolution (Å)	1.98
No. reflections	58600
$R_{\text{work}} / R_{\text{free}}$	24.7/29.8
No. atoms	
Protein	14243
Water	273
B factors	
Protein	26.7
Water	20.8
R.m.s. deviations	
Bond lengths (Å)	0.002
Bond angles (°)	0.456
Clash scores	5.44
Ramachandran	
Favored (%)	96.1
Allowed (%)	3.9

† Redundancy-independent merging R factor R_{meas} estimated by multiplying the conventional R_{merge} value by the factor $[N/(N-1)]^{1/2}$, where N is the data multiplicity.

+ $CC_{1/2}$ is the correlation coefficient of the mean intensities between two random half-sets of data.

The structure was solved by molecular replacement using MOLREP⁴ from the CCP4 suite using the crystal structure of a thermostable β -glucosidase from

Halothermothrix orenii as a search model (PDB entry 4PTV).⁵ The model was further built using Coot⁶ and refined using phenix.refine⁷ and BUSTER.⁸ Water molecules were added using ARP/wARP suite⁹ and manually inspected in Coot. The final model was inspected and validated with MolProbity.¹⁰ Coordinates and structure factors of *AheGH1* have been deposited in the Protein Data Bank (www.rcsb.org) with accession code 6YN7.

3.4.7.3 Crystallisation of *AacGH1*

AacGH1 (10 mg/ml; 10 mM HEPES pH 7.5, 100mM NaCl) was crystallized in 0.8 µl microseeded sitting drops prepared using the Orxy 4 crystallisation robot (Douglas Instruments) and flat-bottomed, Greiner CrystalQuick 96 well sitting drop plates (Greiner Bio-one), incubated at 20 °C. Microseeds were prepared by crushing *AacGH1* microcrystals that grew over 1 week in a 0.5 µl drops containing 50% protein mixed with condition H3 (0.1 M Bis-Tris pH 5.5 and 25% (w/v) PEG3350) from the JCSG screen (Molecular Dimensions), using the Seed Bead Kit (Hampton Research). Seeded drops contained 0.10 µl seed stock, 0.4 µl protein (10 mg/ml) and 0.30 µl reservoir solution and were suspended over 100 µl reservoir solution: H3 condition (0.2M sodium iodide, 0.1 M Bis-Tris Propane pH 8.5 and 20% (w/v) PEG3350) from the PACT screen (Molecular Dimensions). Crystals were cryoprotected in 0.1 M Bis-Tris Propane pH 8.5 and 40% (w/v) PEG3350. X-ray diffraction data were collected on crystals that grew over two weeks.

3.4.7.4 Data collection and 3D structure determination of *AacGH1*.

X-ray diffraction data were collected on a single *AacGH1* crystal at 1.55 Å resolution on the XDR2 beamline at the ELETTRA synchrotron facility (Trieste, Italy). The space group was initially determined as a P2, however, data

analysis using XTRIAGE available under the Phenix suite revealed evidence of twinning. It was not possible to solve the structure in this space group, therefore the structure was solved in the triclinic (P1) space group with the following unit cell parameters: $a = 62.7 \text{ \AA}$, $b = 91.6 \text{ \AA}$, $c = 159.3 \text{ \AA}$, $\alpha = 88.4^\circ$, $\beta = 89.6^\circ$, $\gamma = 90.0^\circ$ (Table 3.4). Eight *AacGH1* chains (Chains A to H) were present in the P1 asymmetric unit, with an estimated Matthew's coefficient of $2.86 \text{ \AA}^3/\text{Da}$ (57.0 % solvent content). Data reduction was carried out using XDS² and STARANISO.³ Search model identification and molecular replacement was carried out using BALBES using the amino acid sequence as the input.¹¹ Structure completion was carried out manually and refined at 1.95 \AA to convergence using COOT and REFMAC5, and structure geometry was validated by Molprobit in the PHENIX platform (Table 3.4).^{7,12,13} Atomic coordinates and structure factors were deposited in the RCSB Protein Data Bank (www.rcsb.org) under the accession code 6ZIV.

Table 3.4. Data collection statistics and refinement parameters for AacGH1. X-ray diffraction data were collected on AacGH1 at 1.55 Å on a single crystal. Parentheses indicate parameters related to the high-resolution cell 1.55-1.64 Å. Data were refined to 1.95 Å. $aR_{\text{merge}} = R_{\text{merge}} = \sum |I - \langle I \rangle| / \sum I \times 100$, where I is the intensity of a reflection and $\langle I \rangle$ is the average intensity. $bR_{\text{factor}} = \sum |F_o - F_c| / \sum F_o \times 100$; cR_{free} for cross-validation, 10% experimental reflections were randomly selected to calculate the R_{free} .

	<i>AacGH1</i> (PDB code 6ZIV)
Data collection	
Space group	P1
Cell dimensions	
<i>a</i> , <i>b</i> , <i>c</i> (Å)	62.6 91.6 159.2
α , β , γ (°)	88.4 89.6 90.0
Resolution (Å)	(46.0 - 1.55)
No. unique reflections	367007 (18439)
^a R_{merge}	0.561 (0.098)
$I / \sigma I$	9 (2.2)
Completeness (%) _{ellipsoidal}	91.1 (84.9)
Redundancy	3.3 (3.2)
Refinement	
Resolution (Å)	1.95-50.0
^b R_{factor} / ^c R_{free}	26.2/29.6
No. atoms	
Protein	28596
Bis Tris Propane	152
Ethylene glycol	28
Sodium ion	8
Iodide ion	1
Water	1889
<i>B</i> -factors (Å ²)	
Protein	11.6
Bis Tris Propane	10.4
Ethylene glycol	19.1
Sodium ion	18.6
Iodide ion	189.5
Water	17.6
RMSD:	
Bond lengths (Å)	1.31
Bond angles (°)	0.0072
Ramachandran Plot (%)	
Favored Regions	97.4
Allowed Regions	99.7

3.4.8 Enzymatic activity assay

The standard activity test was performed by adding 10 μL of the suitable enzyme dilution to a 96-well plate per triplicate. Immediately before the assay, 0.29 mL of the reaction solution HEPES (50 mM), pNPG (10 mM), pH 7.4 were added and the *p*-nitrophenol ($\epsilon = 8.64 \text{ mM}^{-1} \text{ cm}^{-1}$) formation was followed at 420 nm for 10 minutes. The specific activity (U/mg) was expressed as μmol of product formed per minute per mg of protein.

3.4.9 Kinetic characterisation

To measure the kinetic properties of the studied enzymes, the concentration of the substrate was varied, and the enzymatic activity measured using the same method as in the standard activity assay. Data was then plotted and fitted to the standard Michaelis-Menten curve using GraphPad™.

3.4.10 pH effect on enzyme activity and stability

Experiments to investigate the optimum pH for enzyme activity were performed using the spectrophotometric assay outlined above with some modifications. In this case, a universal buffer (25 mM citric acid, 25 mM KH_2PO_4 , 25 mM Tris, 12.5 mM $\text{Na}_2\text{B}_4\text{O}_7$, and 25 mM KCl) was used instead of HEPES buffer to cover a broad range of pH values (from pH 1-12). Similarly, pH stability experiments were performed in universal buffer. The purified enzyme was first diluted in universal buffer at the desired pH and stored at 25 °C for different incubation times. After the incubation period, the residual enzyme activity was measured using the spectrophotometric assay described above.

3.4.11 *Temperature effect on enzyme activity and stability*

Experiments to investigate the optimum temperature for enzyme activity were performed using the spectrophotometric assay outlined above across a range of temperatures (from 4 °C to 60 °C). For the stability experiment, the enzyme was stored in HEPES buffer and incubated at the desired temperature for different incubation periods. After the incubation period, the residual enzyme activity was measured using the spectrophotometric assay described above.

3.4.12 *Wine analysis*

3.4.12.1 *Model wines and juices*

Two different model wines were selected as representatives of a completely sugar dry wine and a table wine with sugar concentrations typical for Australian commercial wines.¹⁴ Model wine 1 (MW1) consisted of saturated potassium hydrogen tartrate with 10 % (v/v) ethanol, pH 3.5. Model wine 2 (MW2) consisted of saturated potassium hydrogen tartrate with 10% (v/v) ethanol, 6 g/L glucose, 6 g/L fructose, pH 3.5.

Model juice (MJ) was prepared using water, 100 g/L glucose, 100 g/L fructose, 0.2 g/L citric acid, 3 g/L malic acid, 2.5 g/L tartaric acid, pH 3.7. pH was adjusted with tartaric acid 1M in all cases.

3.4.12.2 *Real wines and juices*

Two commercially available wines, one white (WW) and one red (RW), and a Chardonnay grape juice (WJ) produced in-house were used. A 2017 Chardonnay from Riverina, Australia with an alcohol content of 12.2% v/v, 4.9 g/L glucose and fructose, titratable acid 6.4 g/L and pH 3.35, a 2016 Shiraz

from South Eastern Australia with an alcohol content of 13.9% v/v, 5.8 g/L glucose and fructose, titratable acid 6.2 g/L and pH 3.66 and a Chardonnay juice with total soluble solids 22.6 °Brix (~20 % total sugar content), 52 mg/L SO₂ and pH 3.5. Chardonnay and Shiraz grape varieties were chosen due to their low monoterpene content.

3.4.12.3 *Enzymatic treatment*

In separate 20 mL SPME vials, 3 mL of MW1, MW2, MJ, WW, RW and WJ were spiked with 5 µg of geranyl glucoside and 5 µg of guaiacyl glucoside. Different amounts of Rapidase[®], *HorGH1*, *AheGH1* or *AacGH1* were added. The samples were left shaking at 22 °C over different incubation periods to allow enzymatic hydrolysis. The reaction was stopped by adding 2 mL of saturated CaCl₂. Internal standards, d₇-geraniol and d₃-guaiacol, were added (2 µg) and the liberated aglycones were analysed using SPME-GCMS. All experiments were carried out in triplicate.

Geraniol and guaiacol calibration curves with a linear range between 0.02-5 µg were performed for each matrix.

3.4.12.4 *SPME-GC-MS analysis*

A Gerstel autosampler (MPS) (Lasersan Australasia Pty Ltd, Robina, Queensland, Australia) was fitted with a 2 cm DVB/CAR/PDMS fibre assembly (Supelco, Bellefonte, PA) to sample the headspace above the stirred sample for 20 min at 35 °C, immediately prior to instrumental analysis. Analyses were carried out with an Agilent 6890A gas chromatograph and an Agilent 5973 mass selective detector (Agilent Technologies, Forest Hill, Australia) fitted with a Gerstel autosampler (MPS). Injection was done in pulsed splitless mode.

The splitter, at 58:1, was opened after 60 s. The injection liner was a Supelco injection sleeve made of 0.75 mm i.d. deactivated borosilicate glass. The gas chromatograph was fitted with a 30 m x 0.25 mm Agilent J&W DB-35ms Ultra Inert column, 0.25 µm film thickness. The carrier gas was helium, linear velocity was 36 cm/s, and flow rate was 1 mL/min. The oven temperature, was held at 40 °C for 1 min, increased to 240 °C at a 5 °C/min rate, and held at this temperature for 2 min. The injector temperature was 220 °C, and the transfer line was held at 240 °C. Positive electron ionisation mass spectra at eV were recorded in SIM mode with m/z 69, 81, 93, 99, 109, 121, 123, 124, 127, 128, 136, 154, and 161 with dwell 25 ms.

Mass Hunter software (version B.09.00 Agilent) was used for the quantitative analysis.

The hydrolysis percentages were calculated using the following equations:

$$\% \text{ geraniol release} = \left(\frac{\text{amount of free geraniol detected}}{\text{amount of geranyl glucoside added}} \right) \frac{316}{154} \times 100$$

$$\% \text{ guaiacol release} = \left(\frac{\text{amount of free guaiacol detected}}{\text{amount of guaiacyl glucoside added}} \right) \frac{286}{124} \times 100$$

3.4.12.5 Data analysis

For the experiments in model wines (MW1, MW2) and model juice (MJ) two-way analyses of variance (ANOVA) (GraphPad Prism 8, San Diego, California, USA) were carried out to assess the effects of enzyme and incubation period on the hydrolysis of glycosides. For the experiments in real wines (WW, RW) and real juice (WJ) a paired t-test was run to assess the effect of the enzyme. Significant difference values were calculated in all cases (****p ≤ 0.0001; ***p ≤ 0.001; **p ≤ 0.01, *p < 0.05).

3.4.13 Vanillin analysis

3.4.13.1 Synthetic vanillin

3.4.13.1.1 Stock solution

Vanillin 4-O- β -D-glucoside standard stock solution was prepared in water with a concentration of 10 mM. Calibration solutions were prepared by diluting the main stock solution.

3.4.13.1.2 Enzymatic hydrolysis

Prior to the testing of the enzyme in the real matrix, a solution containing 5 mM synthetic vanillin 4-O- β -D-glucoside was prepared. 9 replicates of 100 μ L volume containing the synthetic vanillin glucoside (4.5 mM final concentration) and the enzyme (0.1 mg/mL final concentration) were left in agitation at 30 °C. After 10, 20 and 30 minutes, 3 replicates were taken to analyse the progression of the hydrolysis. 450 μ L of ACN and 450 μ L of 0.2% HCL were added to stop the enzymatic reaction and top up the sample until 1 mL total volume. The samples were then analysed by HPLC.

3.4.13.2 Vanillin extraction from vanilla pods

3.4.13.2.1 Cured vanilla pods

1 g of cured vanilla pod was cut into 5 mm pieces. 8 mL of pure ethanol were added, and the solution was left macerating with shaking for 30 min at 30 °C. After this time, 12 mL of distilled water were added to achieve a final ethanol concentration in the sample of 40 % (v/v). The sample was then sonicated for 20 min (5 s on, 5 s off, 60 % amplitude), centrifugated for 30 min at 10000 g and filtered using a 0.45 μ m filter.

3.4.13.2.2 Green vanilla pods

For the green vanilla pod, the same extraction protocol as with the cured vanilla was followed, but in order to be consistent, 2.7 g of fresh vanilla pod were used instead of 1 g as the fresh pod was 2.7 times heavier than a cured one of similar length. 4 mL of ethanol were used for the maceration step and topped up with 16 mL of distilled water, giving a final ethanol concentration of 20% (v/v).

3.4.13.3 Green vanilla pod treatment

After the extraction, 0.5 mg/mL of enzyme were added to a tube containing 2 mL of the cured and green vanilla extraction in each triplicate, and the samples were left under shaking at 30 °C. To follow the progress of the biotransformation, 100 µL aliquots were taken from the 2 mL sample after 15 min, 30 min, 1 h, 3 h, 24 h and 48 h and transferred to sample vials. 450 µL of ACN and 450 µL of 0.2 % HCL were added to the mix, the samples were filtered (0.45 µm) and analysed by HPLC.

3.4.13.4 Reverse-phase HPLC analysis of biotransformations

Samples were analysed using a ThermoFisher Ultimate 3000 Reverse-phase HPLC (diode array detector) on a Waters XBridge C18 column (3.5 µm, 2.1 x 150 mm) with the following method: A: 0.1% TFA in water, B: 0.1% TFA in acetonitrile. Gradient: 0 min 95% A 5% B; 1 min 95% A 5% B; 5 min 5% A 95% B; 5.10 min 0% A 100% B; 6.60 min 0% A 100% B; 7 min 95% A 5% B; 10 min 95% A 5% B. Injection volume 2 µL, at 45 °C with a flow rate of 0.8 mL/min.

Table 3.5. Retention times of the different compounds used.

Compound	Retention time (min)
Vanillin	3.05
Vanillin 4-O- β -D-Glucoside	1.53
4-hydroxybenzoic acid	1.65
Vanillic acid	2.46
4-hydroxybenzaldehyde	2.47

Conversions were calculated from a calibration curve of authentic standards. Peak areas were integrated manually (280 nm), and the correlation coefficients were obtained using the Microsoft Excel® linear regression model application.

3.4.14 Isoflavones analysis

3.4.14.1 Synthetic isoflavones standards

3.4.14.1.1 Stock solutions

Stock solutions for the β -glucoside isoflavones (daidzin, glycitin and genistin) and for the aglycon isoflavones (daidzein, glycitein and genistein) were prepared from authentic samples (1 mg/mL in ethanol for daidzin, daidzein and genistein and 1 mg/mL in DMSO for genistin, glycitin and glycitein). Calibration solutions were prepared by dilution of the main stock solutions.

3.4.14.1.2 Enzymatic reaction

Prior to the testing of the enzymes in the real matrix, a solution containing the 3 main isoflavone glucosides present in soybeans (daidzin, genistin and glycitin) were prepared in triplicate. 100 μ L sample containing the 3

isoflavones glucosides (150 µg/mL final concentration) and the enzyme (0.05 mg/mL final concentration) were left in agitation at 30 °C for 15 minutes. After that time, 450 µL of ACN were added to stop the enzymatic reaction and 450 µL of distilled water were added to top up until 1 mL total volume. The samples were then analysed by HPLC.

3.4.14.2 *Isoflavone extraction from soybean flour*

1 g of soybean flour was weighed out and suspended in 4 mL of ethanol and 16 mL of distilled water. The sample was then sonicated for 20 min (5 s on, 5 s off, 60 % amplitude) centrifuged for 30 min at 4500 g and filtered using a 0.45 µm filter.

3.4.14.2.1 Enzymatic biotransformation

After the extraction, 0.5 mg/mL of the enzyme were added to a tube containing 3 mL of soybean extraction, in triplicate, and the samples were left in shaking at 30 °C. To follow the progress of the biotransformation, 100 µL aliquots were taken from the sample after 15 m, 30 m, 1 h, 3 h, 24 h and 48 h and transferred to HPLC vials. 450 µL of ACN and 450 µL of distilled water were added to stop the enzymatic reaction. The samples were then filtered (0.45 µm) and analysed by HPLC, using the same method described in section 1.4.13.3 of this chapter.

Conversions were calculated from a calibration curve of authentic standards. Peak areas were manually integrated, and the correlation coefficients were obtained using the Microsoft Excel® linear regression model application.

Table 3.6. Retention times of the different compounds used.

Compound	Retention time (min)
Daidzin	3.18
Daidzein	3.76
Genistin	3.40
Malonyl-Daidzin	3.44
Malonyl-Genistin	3.62
Genistein	4.04
Glycitin	3.22
Glycitein	3.82

3.5 Bibliography

- 1 U. K. Laemmli, *Nature*, 1970, **227**, 680–685.
- 2 W. Kabsch, *Acta Crystallogr. Sect. D Biol. Crystallogr.*, 2010, **66**, 125–132.
- 3 I.J. Tickle, C. Flensburg, P. Keller, W. Paciorek, A. Sharff, C. Vonrhein, G. Bricogne, 2018, STARANISO. Cambridge, United Kingdom: Global Phasing Ltd.A.
- 4 A. Vagin and A. Teplyakov, *J. Appl. Crystallogr.*, 1997, **30**, 1022–1025.
- 5 N. Hassan, T.-H. Nguyen, M. Intanon, L. D. Kori, B. K. C. Patel, D. Haltrich, C. Divne and T. C. Tan, *Appl. Microbiol. Biotechnol.*, 2015, **99**, 1731–1744.
- 6 P. Emsley and K. Cowtan, *Acta Crystallogr. Sect. D Biol. Crystallogr.*, 2004, **60**, 2126–2132.
- 7 P. D. Adams, P. V. Afonine, G. Bunkóczi, V. B. Chen, I. W. Davis, N. Echols, J. J. Headd, L. W. Hung, G. J. Kapral, R. W. Grosse-Kunstleve, A. J. McCoy, N. W. Moriarty, R. Oeffner, R. J. Read, D. C. Richardson, J. S. Richardson, T. C. Terwilliger and P. H. Zwart, *Acta Crystallogr. Sect. D Biol. Crystallogr.*, 2010, **66**, 213–221.
- 8 T. O. Bricogne, G; Blanc, E; Brandl, M; Flensburg, C; Keller, P; Paciorek, W; Roversi, P; Sharff, A; Smart, O.S; Vonrhein, C; Womack, 2017.
- 9 G. Langer, S. X. Cohen, V. S. Lamzin and A. Perrakis, *Nat. Protoc.*, 2008, **3**, 1171–1179.

- 10 V. B. Chen, W. B. Arendall, J. J. Headd, D. A. Keedy, R. M. Immormino, G. J. Kapral, L. W. Murray, J. S. Richardson and D. C. Richardson, *Acta Crystallogr. Sect. D Biol. Crystallogr.*, 2010, **66**, 12–21.
- 11 F. Long, A. A. Vagin, P. Young and G. N. Murshudov, *Acta Crystallogr. Sect. D Biol. Crystallogr.*, 2007, **64**, 125–132.
- 12 A. A. Vagin, R. A. Steiner, A. A. Lebedev, L. Potterton, S. McNicholas, F. Long and G. N. Murshudov, *Acta Crystallogr. Sect. D Biol. Crystallogr.*, 2004, **60**, 2184–2195.
- 13 I. W. Davis, A. Leaver-Fay, V. B. Chen, J. N. Block, G. J. Kapral, X. Wang, L. W. Murray, W. B. Arendall, J. Snoeyink, J. S. Richardson and D. C. Richardson, *Nucleic Acids Res.*, 2007, **35**, 375–383.
- 14 P. Godden, E. Wilkes and D. Johnson, *Aust. J. Grape Wine Res.*, 2015, **21**, 741–753.

Chapter 4 Selection of candidates

All the work presented in this chapter is my own contribution unless stated otherwise. Dr. Louise Gourley and her team performed the crystallisation of *AheGH1* and *AacGH1* at the department of Life Sciences of the University of Milan (Italy).

4.1 Introduction

In this chapter, one β -GH family 1 from the halophilic organism *Halothermothrix orenii*, already described in the literature, was expressed, purified and fully characterised. After that, and based on their homology with *HorGH1* and also of their origin, three new candidates were selected: two β -glucosidases family 1 from the acidophiles *Alicyclobacillus herbarius* (*AheGH1*) and *Alicyclobacillus acidiphilus* (*AacGH1*), and one β -GH family 1 from the psychrophile *Paeniglutamicibacter antarcticus* (*PanGH1*). Their synthetic genes were ordered and cloned into an expression vector. A complete characterisation followed by activity and stability assays was performed with *AheGH1* and *AacGH1* and the results compared with *HorGH1*.

4.2 *Halothermothrix orenii*

The constructed vector (*HorGH1*-pET45b) was kindly provided to the Paradisi group by Prof. J. Siegel at UC Davis (California) among other 5 β -glucosidases from different extremophilic organisms. Previous work within the group on the characterisation of these 6 β -glucosidases, identified *HorGH1* as a very well expressing and stable enzyme. It was therefore chosen here as the most appropriate candidate to be tested in lab experiments simulating food industrial processes.

An initial characterisation of the enzyme was done to evaluate its suitability specifically in environments typical of wine processing.

HorGH1 was purified by immobilised metal affinity chromatography (IMAC) reaching final concentrations of 55 mg/mL.

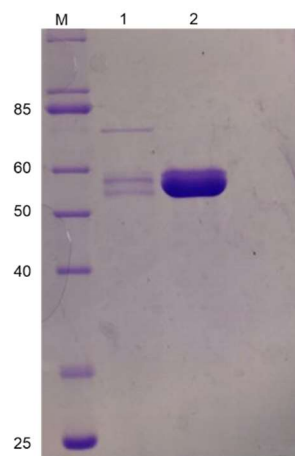


Figure 4.1. SDS-PAGE of the purification of *HorGH1*. (M) Molecular mass markers, (1) Flow-through, (2) Pure *HorGH1* eluted with 100% elution buffer.

Following purification, the enzyme was characterised to determine its kinetic parameters and to better understand its resistance to different conditions.

The compound *p*-nitrophenyl β D glucopyranoside was assessed as a synthetic substrate. Hydrolysis of this substrate is easily detectable using a UV-vis spectrophotometer since the product of the hydrolysis, *p*-nitrophenol (Fig. 4.2), has a maximum of absorbance at 420 nm, with an extinction coefficient of $8.64 \text{ mM}^{-1} \text{ cm}^{-1}$. The activity of *HorGH1* was calculated to be 10 U/mg of protein.

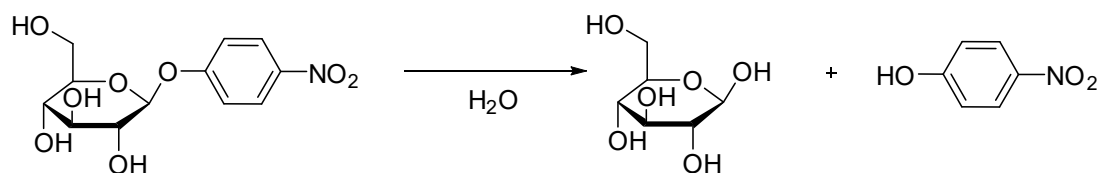


Figure 4.2. Hydrolysis reaction of *p*-nitrophenol- β -D-glucopyranoside

Firstly, kinetic characterisation of *HorGH1* was performed using a *p*NP-Glc concentration range from 0.1 mM and 20 mM. Data were obtained using a 96-well plate and then plotted with GraphPad Prism 8.4 to obtain the Michaelis-Menten curve. Estimated parameters are shown in Figure 4.3.

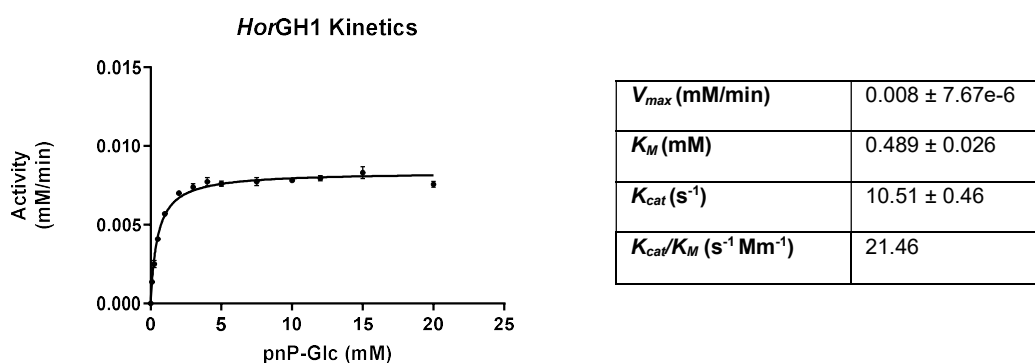


Figure 4.3. Kinetic parameters calculated for *HorGH1*. On the left, Michaelis-Menten fitting of the experimental data for *HorGH1*. Values correspond to the average of 3 replicates.

K_m is the Michaelis-Menten constant and it is defined as the concentration of substrate where the rate of the reaction is half of the V_{max} .

K_{cat} is dependent on the V_{max} but normalized by the concentration of enzyme used. K_{cat} is defined as the turnover number, indicating the number of molecules of substrate converted to product by one active site per unit of time. In this case, one active site equals one molecules of enzyme since *HorGH1* is present in the form of a monomer.

4.2.1 Activity assays

The suitability of *HorGH1* to deal with some of the main challenges that can be found in food industrial processes, such as the presence of sugar, ethanol, salt, etc. was tested. To do so, activity assays in the presence of two sugars (glucose and fructose), salt and ethanol were performed. All of these

experiments were done at 25 °C in buffer HEPES 100 mM, NaCl 500 mM pH 7.5.

The effect of glucose on *HorGH1* activity is reported in Fig. 4.4. Glucose inhibition is a common problem for several GH enzymes,¹ as the accumulation of the product of the hydrolytic process, naturally reduces the catalytic efficiency of the enzyme. Therefore, a broad range of glucose concentrations have been studied and it can be seen that the enzyme activity decreases with the increase in glucose concentration.

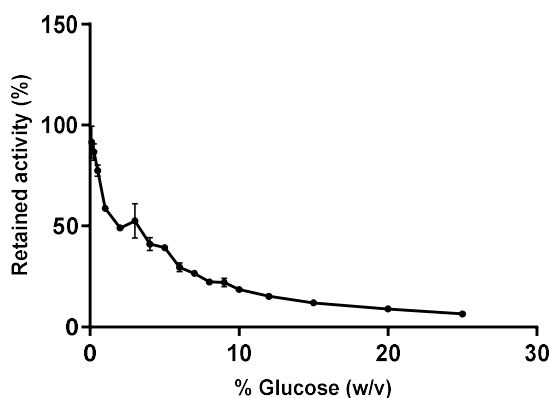


Figure 4.4. Glucose effect on *HorGH1* activity. The activity was tested using the standard activity assay.

As it can be appreciated in Fig. 4.5, fructose had a far lower inhibitory effect than glucose as fructose is not the enzyme natural substrate and thus, it does not show a tight binding to the active site. The retained activity varies between 99 % with 5 % of fructose and 72 % with 25 % (w/v) of fructose in the reaction mixture.

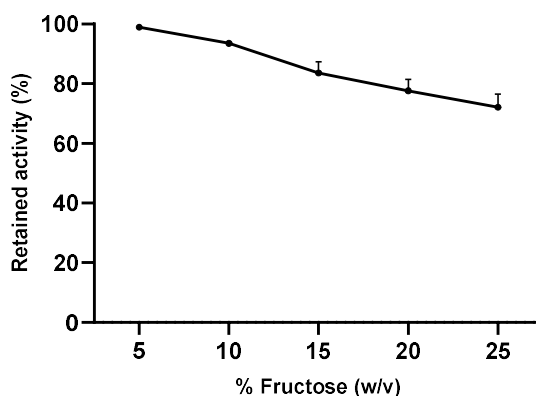


Figure 4.5. Fructose effect on *HorGH1* activity. The activity was tested using the standard activity assay.

Interestingly, the results of *HorGH1* activity in the presence of sodium chloride are quite impressive (Fig. 4.6). The relation between NaCl and enzyme activity is directly proportional; the higher the concentration of salt in the reaction, the higher the enzymatic activity. It has to be emphasized that with an 8 % (w/v) of NaCl in the reaction, the activity of *HorGH1* increases 2.5 times.

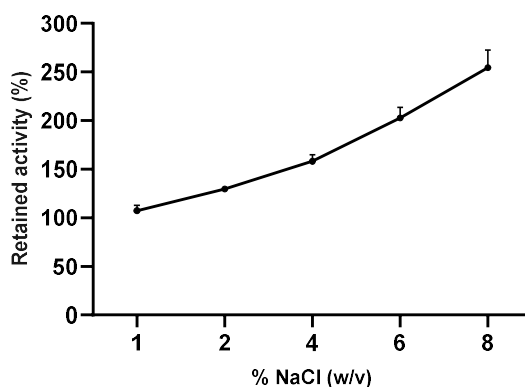


Figure 4.6. NaCl effect on *HorGH1* activity. The activity was tested using the standard activity assay

These results could be explained by making specific reference to the origin of this enzyme. As it was said before, *H. orenii* is a true halophilic and thermophilic anaerobic bacterium that was isolated from a Tunisian salt lake

and consequently, their enzymes (extremozymes) have the ability to perform optimally under significant salt concentrations.²

Among extremophiles, enzymes from halophilic microorganisms tolerate very high salinity, which normally leads to denaturation, aggregation, and precipitation of most other proteins. Genomic and structural analyses have established that halophilic enzymes have a higher pro-ratio of acidic amino acids versus hydrophobic ones and altered hydrophobicity compared to mesophilic enzymes, which enhance solubility and promote function in low water activity conditions.³ The ability of halostable enzymes to retain hydration shells has been already reported² and it is known that adaptation to solvents follows the same principle as adaptation to salt.⁴ For example, *HorGH1* α -amylases are stable over a wide range of salt concentrations which makes them ideal candidates as organic solvent tolerant enzymes.

This explanation could probably be also applied to *Hor* β -Glycosyl hydrolase.

The results of the effect of ethanol on the activity of *HorGH1* is reported in Fig. 4.7, and confirming literature findings, the enzyme tolerates exceptionally well the presence of ethanol in the reaction, with a retained activity over 100 % in all the ethanol concentrations tested.

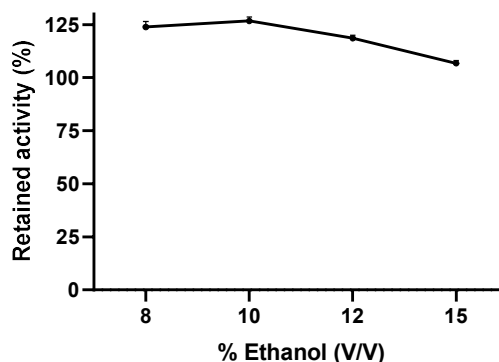


Figure 4.7. EtOH effect on *HorGH1* activity. The activity was tested using the standard activity assay

4.2.2 Stability assays

Enzyme long term stability is also a very valuable parameter. To assess the ability of the enzyme to withstand some of the main challenges found in food industrial processes for a certain amount of time, stability assays in the presence of two sugars (glucose and fructose), salt, ethanol and a different range of pHs were performed. All of these experiments were done at 25 °C in buffer HEPES 100 mM, NaCl 500 mM pH 7.5, with the exception of the pH stability assay that was done in Universal Buffer.

Results for the stability assay in the presence of glucose are reported in Fig. 4.8. The enzyme is very stable at all glucose ranges up to 2 weeks, always with a retained activity superior to 80 %. It can be appreciated that the retained activity increases during the first 24 h, following an important drop at 48h of incubation. After 1 week the activity rises again to decrease over the 2 weeks of incubation time.

No clear tendency can be observed in this assay, just an imitation of the behaviour of the enzyme incubated in favourable conditions (control positive),

suggesting *HorGH1* has a fairly stable behaviour over such time despite the presence of glucose in the media.

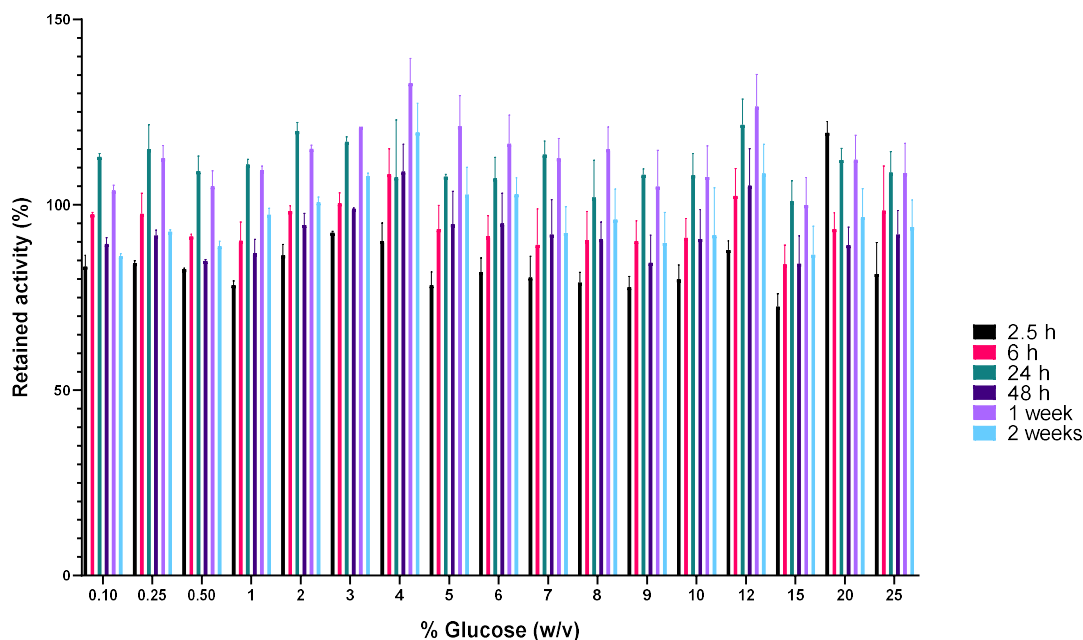


Figure 4.8. Glucose effect on *HorGH1* stability over 2 weeks. The activity was tested using the standard activity assay.

When incubated in the presence of fructose (Fig. 4.9), *HorGH1* follows exactly the same pattern than in the previous assay; the activity increases over the first 24 h, decreases at 48 h, increases at 1 week and decreases at 2 weeks of incubation. The only difference seems to be that the enzyme is more stable with 25 % (w/v) of fructose in the incubation mix.

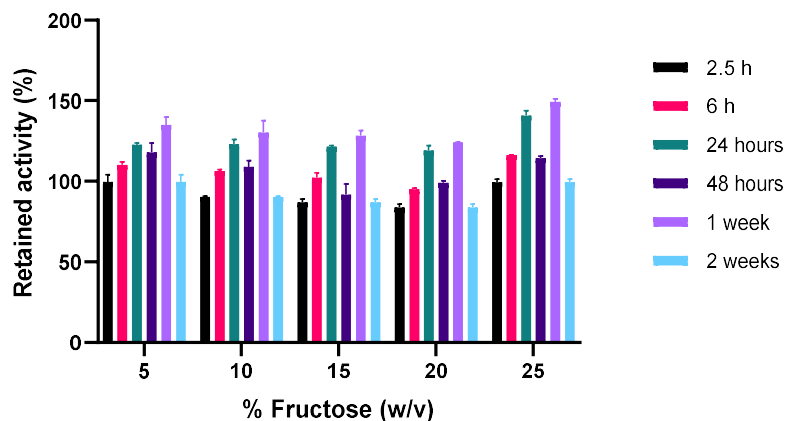


Figure 4.9. Fructose effect on *HorGH1* stability over 2 weeks. The activity was tested using the standard activity assay.

Regarding incubation with different sodium chloride concentrations (Fig. 4.10), the behaviour of the enzyme is completely stable over time; it has exactly the same performance with the presence of 20 %, 15 %, 10 % or 5 % (w/v) of NaCl in the incubation mixture for up to 2 weeks as easily explainable due to the halophilic nature of the microorganism.

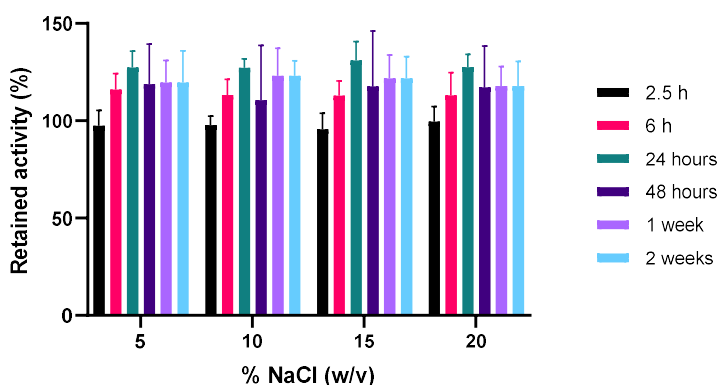


Figure 4.10. NaCl effect on *HorGH1* stability over 2 weeks. The activity was tested using the standard activity assay.

Very impressively, in the case of enzyme incubation at different ethanol concentrations (Fig. 4.11), with an ethanol content up to 15 % (v/v), the retained activity almost doubles after 1-week of incubation.

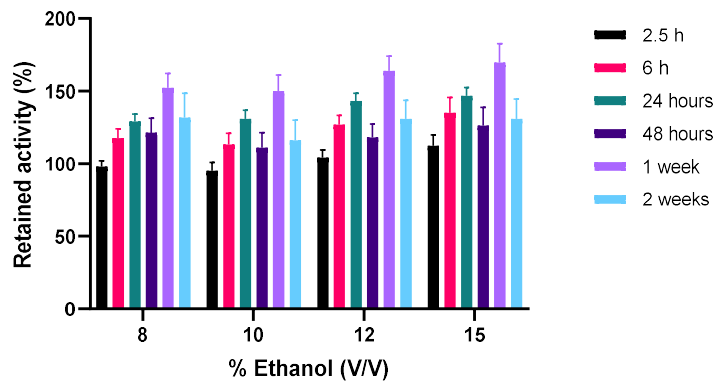


Figure 4.11. Ethanol effect on *HorGH1* stability over 2 weeks. The activity was tested using the standard activity assay.

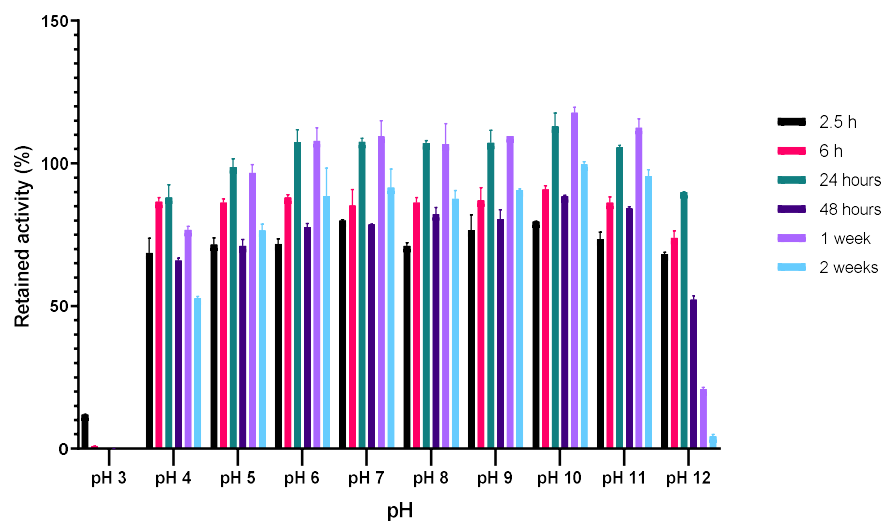


Figure 4.12. pH effect on *HorGH1* stability over 2 weeks. The activity was tested using the standard activity assay.

As a conclusion of all these experiments testing the activity and stability of *HorGH1* under different conditions, it can be said that the enzyme is an exceptional candidate for its use in the food industry. *HorGH1* retained much of its activity in the presence of fructose as well as moderate concentrations

of glucose, and its activity is enhanced by the presence of NaCl and ethanol. The enzyme was also very stable when incubated for 2 weeks in the presence of glucose, fructose, NaCl and ethanol. Regarding the incubation at a different range of pHs (Fig. 4.12), the enzyme retains all the activity in the range between 5 and 11, but the problem comes when the pH is below 4, when all the activity was lost after 6 hours.

4.3 Gene selection of new candidates

While *HorGH1* appears to be a very good candidate for possible industrial applications, its inactivation at very acidic pHs, triggered the search for new candidates. *HorGH1* amino acidic sequence was used as a template to probe genome databases.

Specifically, certain requirements were set to narrow the search field for new candidates: of particular importance for this project were the potential ability to be inherently stable at acidic pHs and/or low temperatures. These 2 “environments” are frequently found in the food industry; the wine industry works with a range of pH between 3 and 4, and some of the steps in the juice processing require temperatures below 20 °C. There is indeed limited availability of biocatalysts sufficiently stable under these conditions.

Therefore, a literature search on acidophilic and psychophilic organisms was performed. The selection criteria were that the species had to be able to tolerate acidic environments or cold temperatures, that they had at least one β -glucosidase coding sequence in their genome, and that, importantly, some other protein of the species had been successfully expressed before in *E. coli*. In fact, solubility issues are often encountered with the heterologous

expression of extremophilic proteins in mesophilic hosts, therefore this would mitigate that risk.

The genera *Alicyclobacillus* was selected as the most suitable acidophilic organism, as the species of this genera are able to live in pHs as acidic as 3.5 - 4.5.⁵

A BLAST search was performed with these genera against *HorGH1* (Table 4.1), using the BLAST software from NCBI and the EnsemblBacteria BLAST tool, to find proteins with β -glucosidase activity. The next table shows the most important parameters regarding the different species of the genus *Alicyclobacillus*, the gene coding for the β -glucosidase family 1, the query cover (percentage of aminoacidic sequence covered) and the percentage of identity of these proteins with *HorGH1*.

Table 4.1. Result of the BLAST between *HorGH1* and the genera *Alicyclobacillus*.

Name	Isolated	T ^a	pH	Accession	Query cover	Identity
<i>A. vulcanalis</i>	Coso Hot Springs, CA	36-65 °C (55 °C)	2.0-6.0 (4)	WP_076345037.1	97 %	58 %
<i>A. sendaiensis</i>	Soil Aoba-yama Park, Japan	40-65 °C (55 °C)	2.5-6.5 (5.5)	WP_062307411.1	97 %	57 %
<i>A. herbarius</i>	Herbal Tea	35-65 °C (55-60 °C)	3.5-6.0 (4.5-5)	WP_026963033.1	99 %	55 %
<i>A. shizuokensis</i>	Crop field in Shizuoka city, Japan	50 °C	4.0-4.5	WP_067929166.1	99 %	55 %
<i>A. hesperidum</i>	Solfataric soils of São Miguel in the Azores	35-60 °C (50-53 °C)	3.5-4.0	WP_006446764.1	97 %	55 %
<i>A. kakegawensis</i>	Soil in Kakegawa, Japan	50-55 °C	4.0-4.5	WP_067934019.1	99 %	54 %
<i>A. acidiphilus</i>	Acidic beverages	20-55 °C (50 °C)	2.5-5.5 (3)	WP_067621817.1	97 %	54 %
<i>A. acidoterrestris</i>	Soils and beverages (spoilage of fruit juices)	35-55 °C (42-53 °C)	2.5-5.8	WP_146824961.1	97 %	55 %
<i>A. contaminans</i>	Orange juice and soil in Fuji City, Japan	35-60 °C (50-55 °C)	3.0-6.0 (4-4.5)	WP_026973674.1	96 %	53 %
<i>A. pomorum</i>	Mixed fruit juice	30-60 °C (45-50 °C)	3.0-6.0 (4-4.5)	WP_026964753.1	99 %	54 %

Paeniglutamicibacter antarcticus, a microbe isolated in the Southern Ocean in Antarctica,⁶ was selected as the psychrophilic organism. Just for clarification,

the genera *Paeniglutamicibacter* and *Glutamicibacter* were previously known as *Arthrobacter*, and the species *Paeniglutamicibacter antarcticus* as *Arthrobacter antarcticus*.⁷ A BLAST search was also performed to make sure the species *P. Antarctica* had a β -glucosidase enzyme into its genome (Table 4.2).

Table 4.2. Result of the BLAST between *HorGH1* and the species *Paeniglutamicibacter antarcticus*.

Name	Isolated	T ^a	pH	Accession	Query cover	Identity
<i>Paeniglutamicibacter antarcticus</i>	Marine sediment in Antarctica	4-25 °C	7	WP_068737131.1	99 %	45 %

Following the BLAST search, the online software Clustal- ω was used to compare the sequences of aminoacids of the proposed β -glucosidases of the different species of *Alicyclobacillus* (Fig. 4.13) and the β -glucosidase from *P. antarcticus* (Fig. 4.14).

```

ACL70277.1 (Hor)      --MAKIIFFPEDFIWGAATSSYQIEGAFNEDGKGESIWDRFSHTPGKIENGDTGDIACDHY      58
WP_026964753.1      ----MAKFPEHFLFGAATAAYQVEGAAGEDGRGPSIWDVFSHTPGKVVNGETGDVACDHY      56
WP_076345037.1      ----MRKFPEGFIFWGTATASYQVEGATREGGRGRSIWDTFAHTPGKVAQHHGHDVACDHY      56
WP_062307411.1      ----MRRFPEGFVWGTATASYQVEGAAQEDGRGRSIWDVFSHTPGKVAHGHGTGDVACDHY      56
WP_006446764.1      -MSQNRSPFDDFIWGAATASYQIEGAAAEDGRGPSIWDTFSKTPGKVLHGHTGDIACDHY      59
WP_067621817.1      -MTGKRQFPDDFIWGAATASYQIEGAANEGGRGPSIWDTFSKTPGKVLLGHGTGDVACDHF      59
WP_026963033.1      MTRFESISFPQDFLFGTATASYQIEGAVHEDGRGESIWDRFSHTPGKVYQGHGTGDVACDHY      60
WP_067929166.1      MAREFIAFPFPGFLFGTATASYQIEGAVHEDGRGESIWDRFSHTPGKVYQGHGTGDVACDHY      60
WP_067934019.1      MIRAFIAFPFPGFLFGTATASYQIEGAVREDGRGESIWDRFSHTPGKVYQGHGTGDVACDHY      60
WP_146824961.1      ----MDFFSDFIWGTATAAYQIEGAVKEDGRGESIWDRFAHTPGCVFEGHTGDVACDHY      55
WP_026973674.1      MTRPFLDFPRDFVFGVATAAYQIEGAHDEGGRTPSIWDTFSHTPGKTKWGHGTGDVACDHY      60
          ** *::*::**::**::*** *_*:  ***** *::*** *_* **::****:

```

ACL70277.1 (Hor)	HLYREDIELMKEIGIRSYRFSSTSWPRILPEGKGRVNOQKGLDFYKRLVDNLLKANIREMIT	118
WP_026964753.1	HRHREDVALMKELGIHSYRFSIAWPRILFPHGTGALNEKGLDFYQRLVEELLKHDITPMAT	116
WP_076345037.1	HRYLDDIQLMKDLGISSYRFSIAWPRVMPPE-KGRVWVKGLDFYKRLIHALLEAGIRPAVT	115
WP_062307411.1	HRYQDDVRLMKELGISSYRFSIAWPRVMPPE-KGRVWVKGLDFYKRLATELLESIGIRPAAT	115
WP_006446764.1	HRYESDVKLMMAELGIRSYRFSIAWPRVMPPE-KGVVLDVSGDFYKRLLEQLHKHGITPAAT	118
WP_067621817.1	HRYESDVKLMADLGIRSYRFSIAWPRVMPPE-KGRYLESGDFYKRLIEQLHKHGITPAAT	118
WP_026963033.1	HRYREDVALMKELGIPAYRFSIAWPRIFPE-KGMKNEAGLDFYRRLLEALHEADIRSFVT	119
WP_067929166.1	HRYQEDVALMKELGIPAYRFSIAWPRISPE-KGVKNEAGLDFYRRLVEALQADIRPFAT	119
WP_067934019.1	HRYQEDVALMKELGIPAYRFSIAWPRIFPE-KGVKNERGLDFYRRLVEALRAADIRPFAT	119
WP_146824961.1	HRFQDDIQLMADLGI PAYRFSIAWPRIFPE-RGVYNQAGIDFYRKKVLETLHKHGIQPAVT	114
WP_026973674.1	HRYPKDIALMKELGIRAYRFSIAWPRVMPPE-RGVKNQQGIDFYKHLTLALHEAETPAVT	119
	* . _.: ** : ** : ** : ** : * * * * : * * * * : * * * * : * * * *	
ACL70277.1 (Hor)	LYHWDLPQALQDKGGWNRDTAKYFAEYARLMFEEFNGLVDLWVTHNEPWVAFEGHAFG	178
WP_026964753.1	LYHWDLPQALQDKGGWANRDTADAFAYADTVFRRLGDKIPMFITLNEPWCASAVLGHAVG	176
WP_076345037.1	IYHWDLPQWIEDDGGWNSRSTVSRFREYSEILFRELGLDLPVMWITHNEPWCASILGYGLG	175
WP_062307411.1	MYHWDLPQWMEDEGGWNNRSTVSRFLEYSEILFRELGLDLPVMWITHNEPWCASILGYGIG	175
WP_006446764.1	IYHWDLPQWIEDEGGWSNRRAVVDYYLEFAEKAFLRELGDQIPMWITHNEPWCASLLSYGIG	178
WP_067621817.1	IYHWDLPQWIEDEGGWSNRRAVVDYKFEAQFALGDDVPFVITHNEPWCASLLSYGIG	178
WP_026963033.1	LYHWDLPQWLQDRGGWANRDTAEYFAEYASLIYERLGDGIDAFITHNEPWCASAVLGHAVG	179
WP_067929166.1	LYHWDLPQWLQDKGGWNRDTAKYFAEYASLIYDQLGDGIASFITHNEPWCASAVLGHAVG	179
WP_067934019.1	LYHWDLPQWLQDKGGWANRDTAEYFAEYALLICDQLGDGIASFITHNEPWCASAVLGHAVG	179
WP_146824961.1	LYHWDLPQYLQDEGGWANRVTVDYFVEYAKKVFDELGDLPVPIFITHNEPWCASFLSYGLG	174
WP_026973674.1	LYHWDLPQWLDDLGGWLNDRDTEHFAEYAEVLVHRELGDLPVITHNEPWCASFLSYGLG	179
	: * * * * * : * * * * * . * * * * : * * * * : * * * * : * * * * : * * * *	
ACL70277.1 (Hor)	NHAPGTRKDFKTALQVAHHLLLSHGMAVDIFREEDLPEIGITLNLTPAYPAGDSEKDVKA	238
WP_026964753.1	VHAPGTDYQKALAAHHLLLSHGKAVQAFRQSGAVGVGLTNILSHIVPASDDPPDVAA	236
WP_076345037.1	AHAPGLCDWRRAYRAAHHLLLSHGHTVRLYRELGLKGEIGITLNLTPVYPASSRPEDVAA	235
WP_062307411.1	VHAPGLQDWRRAAYRAAHHLLLSHGHAVALYRALGLKGEIGITLNLTPVYAAATPLPEDLAA	235
WP_006446764.1	EHAPGLDWRRAAYRAAHHLLLSHGAEVVKLYRSLGLKGEIGITLNLTPAYSASDSDPDVAA	238
WP_067621817.1	EHAPGLKDWRRAYRAAHHLLLSHGAEVVKLYRELGLKGEIGITLNLTPAYPASDSDPDIAA	238
WP_026963033.1	VHAPGHTDWRFAAQAAHHILYSHGLAVQAHRASRSHKGEIGITLNLTPVYDAATDSATDQAA	239
WP_067929166.1	VHAPGHTDWRFAAQAAHHILYSHGLAVQAHRASRSHKGEIGITLNLTPVYDAATDSADKAA	239
WP_067934019.1	VHAPGHTDWRFAAQAAHHILYSHGLAVQAHRASRSHKGEIGITLNLTPVYDAATDSAADQAA	239
WP_146824961.1	HHAPGHRDWRFAAQAAHHILYSHGKAVEAYRAGGYQGEIGITLNLTPVYDAATDSADKAA	234
WP_026973674.1	VHAPGHTDWRFAAQAAHHILYSHGRAVQAYRAAGSGEVGIGITLNLTPVYDAATDSADKAA	239
	* * * * * : * * * * * . * * * * : * * * * : * * * * : * * * * : * * * *	
ACL70277.1 (Hor)	ASLLDDYINAWFLSPVFKGSYPEELHHIYEQNLGAFT-TQPGDMDIISRDIIDFLGINYYIS	297
WP_026964753.1	ASRMDALTNRWFLLPFQATYPTLRA-----LGVDQFTKDGDLALMSQPIDFLGVNYYF	291
WP_076345037.1	AHRQDMFQNRWFLDPLVFKGAYPEELLRRVDVAVGGFDVAVQPGDLEVISAPIDFLGVNYYIS	295
WP_062307411.1	AHRQDMFQNRWFLDPLVLRGEYPDELLRRVDQVVGDFDVAQPGDLDVVISAPIDFLGVNYYF	295
WP_006446764.1	AARQDCFSNRWFLDPLFKGEYPAEFMERVERFCGDLVVRAGDMEIATKMDFLGINFYT	298
WP_067621817.1	QQRQDAFNSRWFLDPLFKGEYPAEFMFRVERFCGDLNVIQPGDMETISVPQDFLGINFYT	298
WP_026963033.1	AEVSHAFNNRWFLDPLVAVGRGYPQEFQQLVEQRIGQDFVVRQGLDVAEPIIDFLGINFYT	299
WP_067929166.1	AEVSHAFNNRWFLDPLVGRGYPEAFQGMVEQVRGVPDFVIRSGDFDVISQIDFLGINFYT	299
WP_067934019.1	AEVSHAFNNRWFLDPLVCHGYPEAFQGMVEQVRGVPDFVIRSGDFDVISQIDFLGINFYT	299
WP_146824961.1	AKREDGFANRWFIIEPIAKGHYPQDMVAWVEGQLGAFDFIQPGDFEMISTPIDFLGINFYS	294
WP_026973674.1	AERVAGFNSNRWFIQPVFSGTYPTDVAALVESRFGAMDVFKAGDLVISTPVDLFLGVNYYT	299
	* * * * * : * * * * * . * * * * : * * * * : * * * * : * * * * : * * * *	
ACL70277.1 (Hor)	RMVVRHKPGDNLFNAAEVVKMEDRSTEMGWEIYPQGLYDILVRVNKEY-TDKPLYITENG	356
WP_026964753.1	EHRVKANPAD-PIIQATVLEPTGDLTAMGWGISPNGLRDVLLRIRRDY-GDIPMYVTENG	349
WP_076345037.1	RAVVADDPAD-PLLGVRHVPGEGPRTEMDEWEVYPEGLYDLSRLRRDY-GDVPIYITENG	353
WP_062307411.1	RALVADDPAD-PLLGVRHVPGDGPRTEMDEWEVYPDGLYDLSRLRRDY-GDIPYITENG	353
WP_006446764.1	RSLVADDPAD-PLLGVKHLKTDNPNVTDMGWEVYPDALYDLSRLRRDY-TDLPIYITENG	356
WP_067621817.1	RSVVKDDPADSLISVHGVPDNDNPNVTDMGWEIYPDALYDLSRLRRDY-TDLPIYITENG	357
WP_026963033.1	RSVVAANPDDALFGLRTEAPADNRTEMGWEIHPDSLYRLLTWVQ-SVTGQLPLYITENG	358
WP_067929166.1	RSVVAADPDDDFGVRTLEAPADNRTEMGWEIHPDSLYRLLTWVQ-SVTGELPLYITENG	358
WP_067934019.1	RSVVAADPDDAAFGIRTLEAPADNRTEMGWEIHPDSLYRLLTWVQ-SVTGELPLYITENG	358
WP_146824961.1	RNVFRAGTANAHQSEVVPANRVTDMGWEIHPESLYRLLTWVQ-SVTGELPLYITENG	354
WP_026973674.1	RNVVAHQPNQDQVLRHVAPPKEAQTGEMGWEIHPESLYRLLTWVQ-SVTGELPLYITENG	359
	. . . : * * * * * : * * * * : * * * * : * * * * : * * * *	

ACL70277.1 (<i>Hor</i>)	AAFDDKLTTEEGKIHDEKRINYLGDFHFKQAYKALKDGVPLRGGYVWVSLMDNFEWAYGYSKR	416
WP_026964753.1	AAFHDVV-EGDIVHDAPRISYLRRHLLAVREAMDAGVDVRRGYVWVSLMDNFEWHQGYAKR	408
WP_076345037.1	AAyddrv-EGGSVHDTNRIEYLAHFHFAAAHRFLAEGGNLRGYVWVSLMDNFEWAFGYTKR	412
WP_062307411.1	AAyddrv-EDGSVHDADRVTYLAGHFAAAHRFLAEGGNLRGYVWVSLMDNFEWAFGYTKR	412
WP_006446764.1	AASADVV-EDGNVHDADRIAYLHQHLEAARKFTISEGGNLRGYVWVSLMDNFEWAFGYTKR	415
WP_067621817.1	AANADAI-VNGEVEDTPRIDYVVRQHLDAHRFTIQEGGNLRGYVWVSLMDNFEWAFGYTKR	416
WP_026963033.1	AAFADep-VNGRVEDVRRIHYYIADHLEAAKRFVDAGGPKLGYFLWSFMDNFEWALGYSKR	417
WP_067929166.1	AAFADeL-VDGRVKDFRRVDYIADHLEAAKRFIDEggPLKGYFLWSFMDNFEWAMGYSKR	417
WP_067934019.1	AAFADep-VDGRVQDRRLDYIADHLEAAKRFIDEggPLKGYFLWSFMDNFEWAMGYSKR	417
WP_146824961.1	AAFQDEL-VEGAIHDEPRIHYVADHLEAAKRFIDEggPLKGYFLWSFMDNFEWAFGYSKR	413
WP_026973674.1	AAFDDAV-EDGAVHDVRRIDYVADHLEAAQRFTAEGGRKLGYYLWSLLDNYEWAFGYSKR	418
	** * . :.* *: *: * : . . : * :*:*:*:*:*:** **:*	
ACL70277.1 (<i>Hor</i>)	FGLIYVDYENGNRRFLKDSALWYREVIEKQVEAN-----	451
WP_026964753.1	FGLFYVDYPTQ-RRLWKDSARWYQNVTASeVQ-----	440
WP_076345037.1	FGIVYVDYETL-ARIPKDSYFWYQQVIRDRAIAPeATELAR-	452
WP_062307411.1	FGLVYVDYDTL-VRIPKDSYFWYQRVIREGGLVPEEAeTVR	453
WP_006446764.1	FGIIYVDYDTQ-ERIPKDSFEWYRQVIAANSLePETVQGTV--	454
WP_067621817.1	FGIIYVDYETQ-VRTPKASfHWYRQVIENNGLeTD-----	449
WP_026963033.1	FGMVYVDYEsQ-QRLVKDSGRWFSEQIAAHKQGVRA-----	452
WP_067929166.1	FGMVYVDYETQ-KRVVKDSGRWFSEQIAAHSSQVRA-----	452
WP_067934019.1	FGMVYVDYDTQ-KRIVKDSGRWFSEQIAAHRQARI-----	452
WP_146824961.1	FGMVYVDYATQ-VRTVKDSGKWYSGQIAHHRALSV-----	447
WP_026973674.1	FGIVHVDYETQ-ARTVKDSARWYSGQIAHQHAAPTAE-----	454
	:.:* . * * * *	

Figure 4.13. Homology between the β -glucosidases of the suggested species of the genera *Alicyclobacillus* and *HorGH1* using Clustal ω . (*) The aminoacids are identical, (:) The aminoacids have very similar configuration and properties, (.) The aminoacids are related, () The aminoacids are not related.

ACL70277.1 (<i>Hor</i>)	-----MAKIIFFPEDFIWGAATSSYQIEGAFNEDGKGESIWDRFShTPGKIENGDTGDIAC	55
WP_068737131.1	MNNQILQNFVWPNFLWGSATAAAQIEGAHSDGKEDSIWDAFARVPGAIAGGDHLETAV	60
	: :*:*:*:*:*:*:*: * : * * * * * : * * * * * * * : * * * * *	
ACL70277.1 (<i>Hor</i>)	DHYHLYREDIELMKEIGIRSYRfSTSWPRILPEgKGRVNQKGLDFYKRLVDNLLKANIRP	115
WP_068737131.1	DHYHRYAEDVSLMQIGLDSYRfSTSWARVVPgGR-TVNHKGLDFYRRLVDELLGAGILP	119
	* *	
ACL70277.1 (<i>Hor</i>)	MITLYHWDLPQALQDKGGWTRNDTAKYFAEYARLMFEeFNGLVDLWVTHNEPWWVAFEGH	175
WP_068737131.1	WLTLYHWDLPQALEERGgWANREtAYKfVEYAEAVYEkLgDRVShWTTfNEPLCSSLIGY	179
	: *	
ACL70277.1 (<i>Hor</i>)	AFGNHAPGTKDFKtALQVAHLLLSHGMAVDIFREEDLPGEIGITLNLTPAYPAGDS-EK	234
WP_068737131.1	AAGEHAPGRQEPRAALAAVHHQHlAHGMAASRLRSLG-AQELGITLNLtNAVpNDPTDPV	238
	* *	
ACL70277.1 (<i>Hor</i>)	DVKAASLLDDYINAWFLSPVfKGSYPeELHHIYEQNLGAFTTQPGDMDIISRDIDFLGIN	294
WP_068737131.1	DLEAARRIDALWNRMYLDPILLGSYPQDLLEDVKDYGLDELILEGDELINQPIDFLGVN	298
	* : *	
ACL70277.1 (<i>Hor</i>)	YYSRMVVRHK-----PGD-----NLfNAEV--VKMEDRPSTeMGWEIYPQGLYD	336
WP_068737131.1	HYHDDNVSGHELTkDEPEAEVPTeSPMSfFVGSEYVTFPSRNLPRtAMGWEVNPAGLRT	358
	: *	
ACL70277.1 (<i>Hor</i>)	ILVRVNKEYTDKP-LYITENGAAFDKLTTEEGKIHDEKRINYLGDFHFKQAYKALKDGVPL	395
WP_068737131.1	LLNRLKSDYPNLpALYITENGAAyEDSVESDGSVADtERTDYIMSHIAEvAAAVGDGVDI	418
	: *	
ACL70277.1 (<i>Hor</i>)	RGYVWVSLMDNFEWAYGYSKRfGLIYVDYENGNRRFLKDSALWYREVIEKQVEAN 451	
WP_068737131.1	RGYFVWVSLMDNFEWAWGyEKRFgIVRVDYETQERT-ikNSGLAYANLIEQSRtL-- 471	
	* *	

Figure 4.14. Homology between the β -glucosidase of the species *P. antarcticus* and *HorGH1* using Clustal ω . (*) The aminoacids are identical, (:) The aminoacids have very similar configuration and properties, (.) The aminoacids are related, () The aminoacids are not related.

As the species *P. antarcticus* (*Pan*) only presented one β -glucosidase, this was chosen for this project. In the case of *Alicyclobacillus*, the BLAST search

gave 10 different hits for β -glucosidases from different species. All of them displayed a good level of identity with *HorGH1* (between 53-57 %), and all the species grew at a similar range of pHs and temperatures. To select the enzymes, Clustal- ω was used again to assess the homology level between the proteins of the 10 candidates, in order to identify two sufficiently different genes and maximise diversity in the results. The results of this comparison can be seen in Table 4.3.

Table 4.3. Homology between β -glucosidases of different candidates.

Protein 1	Protein 2	Results
WP_076345037.1 (<i>A. vulcanalis</i>)	WP_062307411.1 (<i>A. sendaiensis</i>)	Length: 453 Identity:390/453 (86.1 %) Similarity:421/453 (92.9 %) Gaps: 1/453 (0.2 %) Score: 2182.0
WP_076345037.1 (<i>A. vulcanalis</i>)	WP_026963033.1 (<i>A. herbarius</i>)	Length: 464 Identity:252/464 (54.3 %) Similarity:320/464 (69.0 %) Gaps: 24/464 (5.2 %) Score: 1368.5
WP_076345037.1 (<i>A. vulcanalis</i>)	WP_067621817.1 (<i>A. acidiphilus</i>)	Length: 456 Identity:296/456 (64.9 %) Similarity:350/456 (76.8 %) Gaps: 11/456 (2.4 %) Score: 1693.0
WP_062307411.1 (<i>A. sendaiensis</i>)	WP_026963033.1 (<i>A. herbarius</i>)	Identity: 260/460 (56.5 %) Similarity:325/460 (70.7 %) Gaps: 15/460 (3.3 %) Score: 1402.0
WP_062307411.1 (<i>A. sendaiensis</i>)	WP_067621817.1 (<i>A. acidiphilus</i>)	Length: 457 Identity: 293/457 (64.1 %) Similarity:353/457 (77.2 %) Gaps: 12/457 (2.6 %) Score: 1688.0
WP_067621817.1 (<i>A. acidiphilus</i>)	WP_026963033.1 (<i>A. herbarius</i>)	Length: 454 Identity: 255/454 (56.2 %) Similarity: 319/454 (70.3 %) Gaps: 7/454 (1.5 %) Score: 1360.5

β glucosidases from *A. acidiphilus* (*AacGH1*) and *A. herbarius* (*AheGH1*) were chosen as the final candidates as a result.

All three putative β -GH1 sequences, *AheGH1*, *AacGH1* and *PanGH1*, were aligned with *HorGH1* (Fig. 4.15) to confirm the presence of the two conserved motifs characteristic of all GH1.

Pan	MNNQILQNFVWPNNFLWGSATAAAQIEGAAHSDGKEDSIWDAFARVPGAIAAGGDHLETAV	60
Hor	-----MAKIIIFPEDFIWGAATSSYQIEGAFNEDGKGESIWDRFSHTPGKIENGDTGDIAC	55
Ahe	---MTREFISFPQDFLFGTATASYQIEGAVHEDGRGESIWDRFSHTPGKVYQGTGDVAC	57
Aac	----MTGKRQFPDDFIWGAATASYQIEGAANEGGRGPSIWDTFSKTPGKVLLGHTGDVAC	56
	:*::*	
Pan	DHYHRYAEDVSLMQKIGLDSYRFSTSWARVVPGG-RTVNHKGLDFYSRLVDELGLGAILP	119
Hor	DHYHLYREDIELMKEIGIRSYRFSTSWPRILPEGKGRVNQKGLDFYKRLVDNLLKANIRP	115
Ahe	DHYHRYREDVALMKELGIPAYRFSIAWPRIPE-KGMKNEAGLDFYRRLLEALHEADIRS	116
Aac	DHFHRYESDVKLMADLGIKSYRFSLAWPRVPE-KGRYLESGFDFYKRLIEQLHKHGITP	115
	:* * .*: ** .*: :** :* *:. * . * :**** *:*: * . *	
Pan	WLTLYHWDLPQALEERGGWANRETAYKFVEYAEAVYEKLGDRVSHWTTFNELCSSLIGY	179
Hor	MITLYHWDLPQALQDKGGWTRNDTAKYFAEYARLMFEEFNGLVDLWVTHNEPWWVAFEGH	175
Ahe	FVTLYHWDLPQWLQDRGGWANRDTAEYFAEYASLIYERLGDGIDAFITHTNEPWCASFGLH	176
Aac	AATIYHWDLPQWIEDEGGWSNRAVVDYKFAEQAFKALGDDVPFWITHNEPWCASLLSY	175
	*:***** :*:***:* * .. :*: * : : : : * :*** : : : :	
Pan	AAGEHAPGRQEPRAALAAVHHQHHLAHSMAASRLRSLGA-QELGITLNLTNVNPNDPTDPV	238
Hor	AFGNHAPGTKDFKTALQVAHLLLSHGMAVDIFREEDLPEIGITLNLTPAYPAG-DSEK	234
Ahe	GFGVHAPGHTDWREAFQAAHHILYSHGLAVQAHRASSHKGQIGITLNLFTWVDAAT-DSAT	235
Aac	GIGEHAFLKDWRRAYRAAHHLLSHGEAVKLYRELGLKQIGITLNLTPAYPAS-DSPE	234
	. * ***** : : * ..** :** *.. * . :*****:* . . *	
Pan	DLEAARRIDALWNRMYLDPILLGSYPQDLLEDVKD-YGLDELILEGDLELINQPIDFLGV	297
Hor	DVKAASLLDDYINAWFLSPVFKGSYPEELHHIYEQNLGAFT-TQPGMDIISRDIIDFLGI	293
Ahe	DQAAAEEVSHAFNRRWFLEPVAGRGYPQEFQQLVEQRIGQDFVVRQGLAVIAEPIDFLGI	295
Aac	DIAAQRQDAFNSNRWFLDPIFKGEYPADFMPRVERFCGDLNVIQPGDMETISVPQDFLGI	294
	* * . * :*: * : * : : * : * : * : * : * : * : * : * : * : *	
Pan	NHYHDDNVSGHELTKEPEAEVPTESPMSSPFVSGSEYVTFPSRNLPRTAMGWEVNPAGLR	357
Hor	NYYSRMVVRHK-----PGDN-----L-FNA--EVVKMEDRPSTEMGWEIFPQGLY	335
Ahe	NFYTRSVVAAN-----PDDA-----L-FGL--RTLEAPADNRTEMGWEIHPDSLY	337
Aac	NFYTRSVVKDD-----PADD-----S-LIS--VHGVPTDNPVTDMGWEIYPDALY	336
	*. * * * . * * . * . * . * . * . * . * . * . * . * . * . * . * . *	
Pan	TLLNRLKSDYPNLPALYITENGAAYEDSVESDGSVADTERTDYIMSHIAEVAAVGDGVD	417
Hor	DILVRVNKEYTDKP-LYITENGAAFDDKLTTEGKIHDEKRINYLGDFKQAYKALKDGVP	394
Ahe	RLLTWVQSVTGQLP-LYITENGAFADEPV-NGRVEDVRRIHVIADHLEAAKRFVDAGGP	395
Aac	DLLHRLKNEYTDLP-IYITENGAANADAIV-NGEVEDTPRIDYVRQHLDAAHRFIQEGGN	394
	:* : : . : * :***** * : * : * * .*: .*: . : *	
Pan	IRGYFVWSLLDNFEWAWGYEKRFIVRVDYETQE-RTIKNSGLAYANLIEQSRTL---	471
Hor	LRGYVWWSLMDNFEWAYGYSKRFGLIYVDYENGRNFLKDSALWYREVIEKQGVAN-	451
Ahe	LKGYFLWSFMDNFEWALGYSKRFGMVYVDYESQQ-RLVKDSGRWFSEQIAAHKQVRA	452
Aac	LKGYLWWSLMDNFEWAFGYTKRFGIYVDYETQV-RTPKASFWHYRQVIENGLTD--	449
	:*****:***** * * *****: ***** * * * * : : *	

Figure 4.15. NEP and TENG motifs in *PanGH1*, *HorGH1*, *AheGH1* and *AacGH1*.

4.4 Characterisation of the new candidates: AacGH1, AheGH1 and PanGH1.

4.4.1 Cloning, expression, purification and kinetics

The synthetic genes coding for *AheGH1*, *AacGH1* and *PanGH1*, with *Bam*HI and *Hind*III flanking the sequences as restriction sites, were codon optimised for *E. coli* and then ordered from GenScript (Hong Kong).

The CloneJET PCR Cloning Kit from Thermo Scientific was used to clone the genes into pJET1.2, a commercial cloning vector. However, only *PanGH1* could be successfully cloned into it and subsequently subcloned into the expression vector pCH93b as the quality of the other two genes was insufficient. pCH93b is an ampicillin resistant cloning vector engineered in-house based on pET22a, where the TEV sequence has been inserted before the C-Term His-Tag and the periplasmic leading sequence has been skipped (Fig. 4.16). The vector was transformed into electro-competent XL10-Gold cells, and grown onto LB-Agar/amp plates.

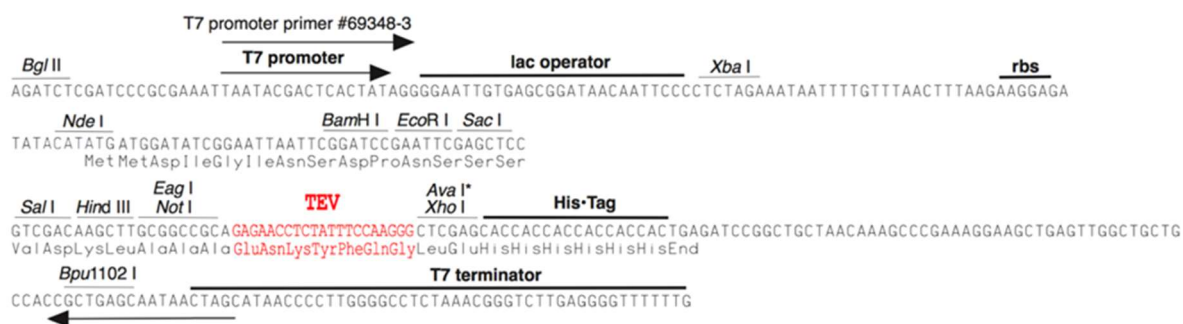


Figure 4.16. pCH93b cloning vector map.

The sequencing results of 6 isolated colonies identified a mistake in the synthetic gene which presented a deletion disrupting the gene frame. Site-

directed mutagenesis was performed using the QuickChange Lightning Multi Site-Directed Mutagenesis Kit from Agilent to repair the gene frame and the outcome was checked by sequencing.

AheGH1 and *AacGH1* genes were reordered from Thermo Fisher already into the commercial cloning vector pMA (Fig. 4.17).

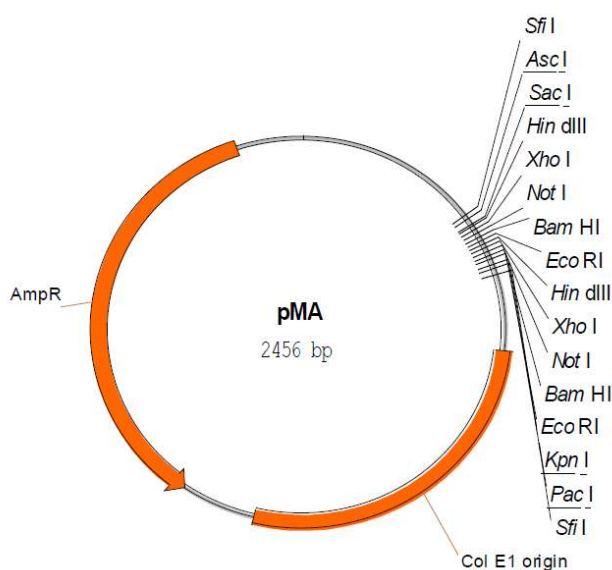


Figure 4.17. pMA cloning vector map

The genes were digested with BamHI and HindIII and ligated into the expression vector pCH93b, which includes a C-terminal poly-His tag for purification. The genes were sequenced and confirmed that the cloning was successful.

AheGH1 and *AacGH1* were expressed in LB media at 30 °C and purified using IMAC with an average yield of 75-100 mg/L of protein for *AheGH1* and 160-195 mg/L for *AacGH1* (Fig. 4.18). *AheGH1* has a theoretical molecular weight

of 52133.66 Da (\approx 52 KDa) and *AacGH1* of 54629 Da (\approx 55 KDa) estimated with the online tool ProtParam.⁸

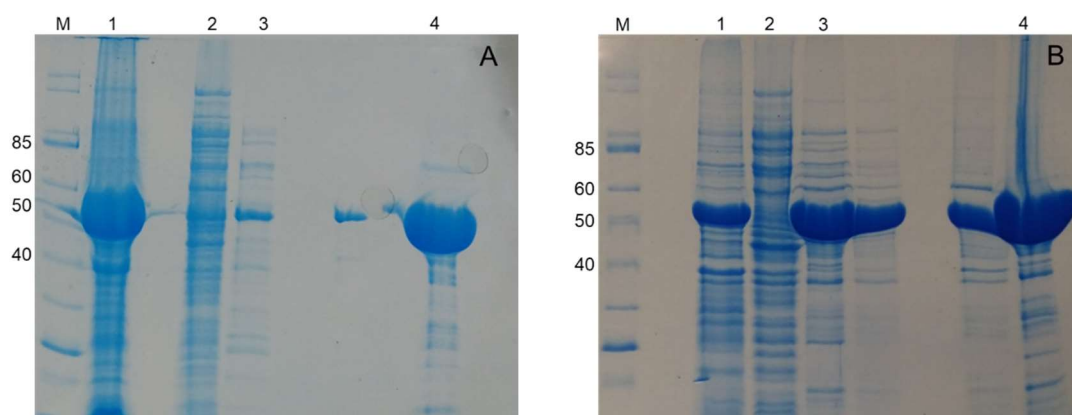


Figure 4.18. SDS-PAGE with the purification of *AheGH1* (A) and *AacGH1* (B). M: molecular weight markers, (1) Insoluble fraction after sonication, (2) Flow-through, (3) Fraction eluted with 10% elution buffer and (4) fraction eluted with 100% elution buffer.

The activity of *AheGH1* and *AacGH1* was calculated following the release of *p*-nitrophenol at 420 nm in a 96 well plate, and resulted to be 14 U/mg and 20 U/mg respectively.

The same expression strategy as for in the case of *AheGH1* and *AacGH1* was attempted with *PanGH1* but no protein was recovered from the soluble fraction, meaning that the protein was insoluble. Insolubility of the protein and formation of inclusion bodies are very common problems related with the expression of cold-adapted proteins.⁹

Different strategies varying the concentration of IPTG and the induction/expression temperatures were tried in order to achieve a more progressive expression of the enzyme and hence reducing the chances of insolubility. None of them worked and the enzyme was still produced with the insoluble fraction (Fig. 4.19).

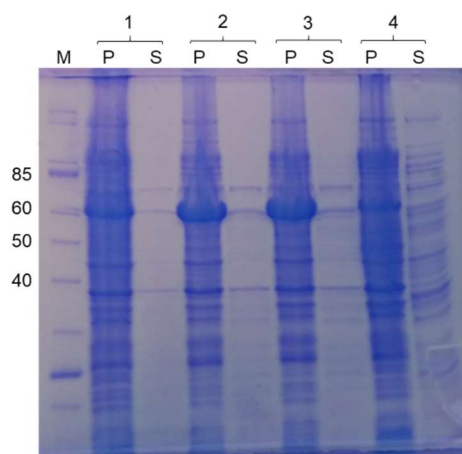


Figure 4.19. SDS-PAGE with different expression strategies attempted with *Pan*. (1) 1 mM IPTG, 4 h expression at 16 °C, (2) cold-shock, 1 mM IPTG, O/N expression at 16 °C, (3) 0.1 mM IPTG, O/N expression at 16 °C, (4) 0.01 mM IPTG, O/N expression at 16 °C. M: Molecular markers; P: Pellet; S: Supernatant.

Finally, the enzyme was expressed in autoinduction media at 16 °C. Purification followed using IMAC with a yield of 235 mg/L of protein (Fig. 4.20) *PanGH1* has a theoretical molecular weight of 55882.09 Da (\approx 56 KDa) estimated by ProtParam.⁸

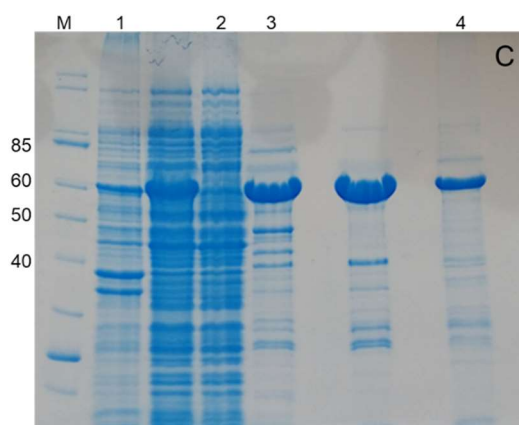


Figure 4.20. SDS-PAGE with the purification of *Pan*. M: molecular weight markers; (1) Insoluble fraction after sonication, (2) Flow-through, (3) Fraction eluted with 10% elution buffer and (4) fraction eluted with 100% elution buffer.

The activity of *PanGH1* was calculated following the release of *p*-nitrophenol at 420 nm in a cuvette, and resulted to be 5 U/mg.

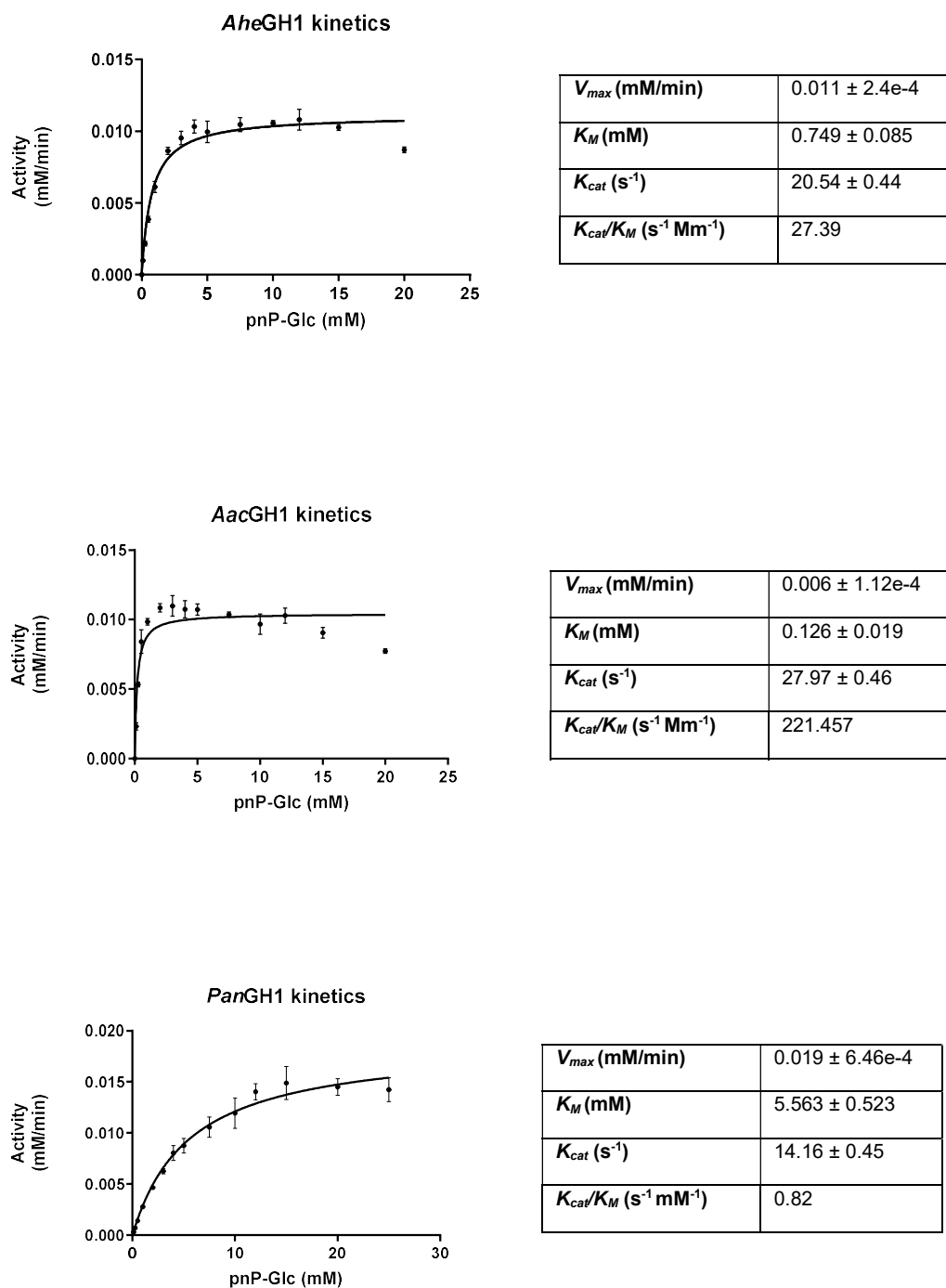


Figure 4.21. Kinetic parameters calculated for *AheGH1*, *AacGH1* and *Pan*. On the left, Michaelis-Menten fitting of the experimental data for the 3 of them. Values correspond to the average of 3 replicates.

The enzyme showing better affinity for the substrate was *AacGH1*, with a K_M six times lower than *AheGH1* and forty-four times lower than *PanGH1*. The catalytic efficiency (K_{cat}/K_M) measured for *AacGH1* was also eight times higher

than for *AheGH1* and almost 300-fold higher than for *PanGH1*. Taking into account all the data generated so far, together with the specific activity, it was concluded that *AacGH1* was the most efficient enzyme between the 3 new candidates, under the tested conditions. Also, it was more efficient in comparison with the model candidate *HorGH1*, which presented a K_M of 0.49 mM (four times higher than *AacGH1*) and a K_{cat}/K_M of 21.46 s⁻¹ mM⁻¹ (ten times lower than *AacGH1*).

4.4.2 Size-exclusion chromatography

At this point, it was decided not to continue with *PanGH1* for further characterisation as it was the less promising candidate following the results of the kinetics. Also, the difficult of handling and the variability in the expression and purification results make of *PanGH1* a problematic candidate to be escalated for its application in industry.

Size-exclusion chromatography was performed to determine the quaternary structure of *AheGH1* and *AacGH1*. A calibration curve was generated using protein standards.

Table 4.4. Calibration curve for size exclusion chromatography in the conditions referred. V_e makes reference to the elution volume expressed in minutes. MW is the molecular weight of each standard in kDa. V_e/V_o is the elution volume divided by the void volume of the column.

	V_e (min)	MW (kDa)	V_e/V_o	Log_{10} MW
Blue dextran	11	2000	1	3.30
B-amylase	16.5	200	1.5	2.30
Cytochrome C	24	12.4	2.1	1.09
Carbonic anhydrase	22	29	2	1.46
ADH	18	150	1.6	2.18
Albumin	19	66	1.7	1.82

AheGH1 and *AacGH1* were loaded into the column and their molecular mass was determined by direct comparison with the standards. For *AheGH1*, the results indicate a molecular weight of 99.7 kDa, and in the case of *AacGH1*,

119.9 kDa. These values (Fig. 4.22) indicate that both enzymes would be dimers, unlike *HorGH1* which is a monomer.¹⁰

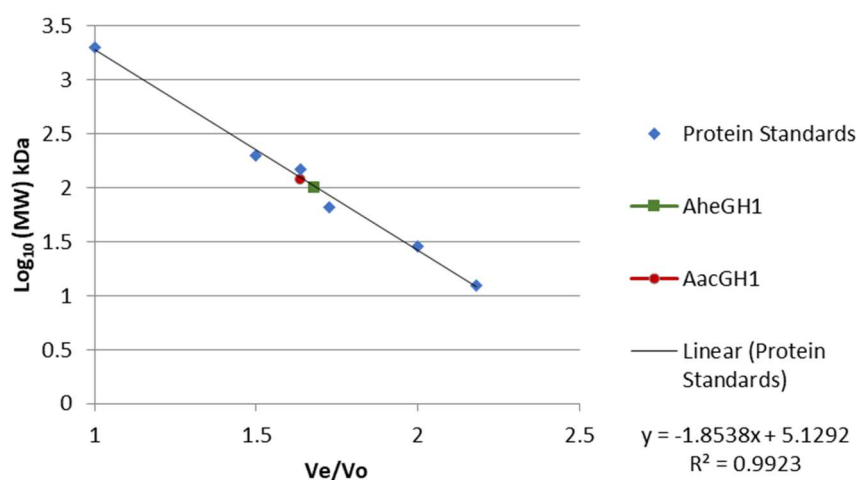


Figure 4.22. Graphic showing the correlation between the log₁₀ (MW) and the ratio V_e/V_o . The protein standards are represented in blue while *AheGH1* is represented in green and *AacGH1* in red.

4.4.3 Crystallisation

To further investigate the structure of both proteins, they were trialed for crystallisation. This was achieved in collaboration with Dr. Louise Gourlay (Department of Life Sciences of the University of Milan), who provided the following information for its inclusion in this chapter.

4.4.3.1 The 3D structure of *AheGH1*

Crystals of *AheGH1* enzyme belonging to the monoclinic space group P21 diffracted at 1.98 Å resolution. The asymmetric unit of *AheGH1* contains four independent molecules. The overall structure of the four *AheGH1* subunits is identical (RMSD values of 0.05 to 0.08 Å over 356 backbone C α atoms).

The final model was refined to R values of R_{work} 24.7% and R_{free} 29.8%. The presence of strong translational noncrystallographic symmetry (tNCS), as confirmed by a peak in the Patterson map, may justify the higher-than-

expected final R_{work} value, despite the high resolution of the structure (Table 3.3). Electron density map was overall of good quality, with electron density coverage across residues 2-450 (chain A), 2-451 (chain B), 3-447, (chain C) and 3-446 (chain D), except for a short stretch (P304-D322). Several ethylene glycol molecules derived from the crystallisation buffer were modelled into the electron density. In addition, two nickel cations were identified in the model, present during the affinity chromatography purification step. The metal cations are located at the dimer interfaces between chain A and the symmetry-related monomer C and between the B and D subunits and are coordinated in a tetrahedral arrangement by the side chains contributed from two histidine residues (H61) and two glutamate (E29) residues.

AheGH1 is arranged into a single $(\beta/\alpha)_8$ barrel fold, common to this family of glycosidases, with negligible main-chain displacements in peripheral loops and α -helices. Regions which show more significant changes in the secondary structure correspond to residues 272 to 281, folded into a gamma and two β -turns, and residues 409 to 416 that form two β -turns instead of the more common α -helices (Fig. 4.23).

A feature of the GH1 family is that despite low sequence identity (as low as 17%) they share high structure conservation. 3D structure-based comparisons performed with the DALI server (<http://ekhidna2.biocenter.helsinki.fi/dali/>)¹¹ revealed that the *AheGH1* protein has the highest structural similarity with a family 1 glucoside hydrolase from *Paenibacillus polymyxa* (*BglB*; PDB: 2O9P).¹² Despite average sequence identity (52%), superposition between the two proteins revealed a high degree of structural similarity (RMSD of 0.6 Å) over 441 aligned residues.

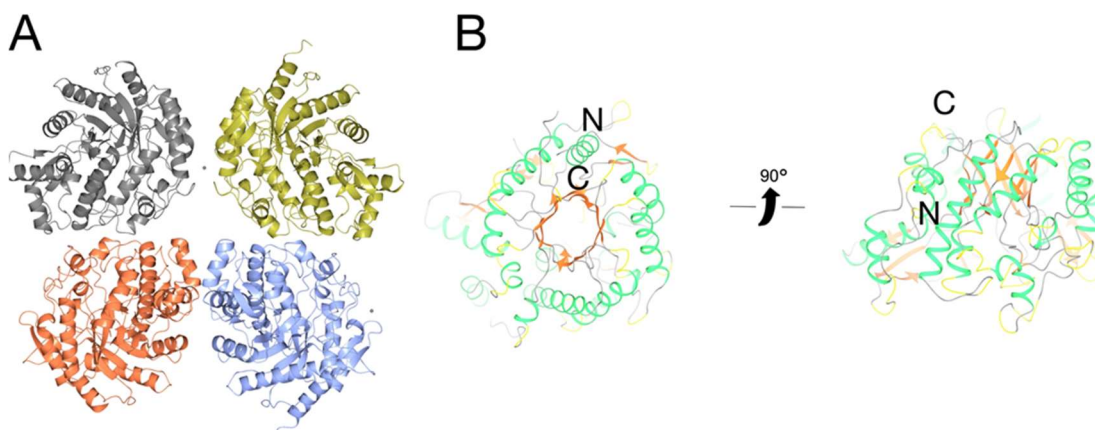


Figure 4.23. 3D structure of AheGH1. A) The AheGH1 tetramer present in the asymmetric unit; B) Top and side views of the AheGH1 monomer, with ribbons coloured according to secondary structure (β -strands in orange, α -helices in green, 3-, 4- and 5- turns in yellow, unstructured regions in grey). N- and C-terminal regions are labelled.

4.4.3.2 The AheGH1 active site

An enzyme template search of catalytic site templates made with the ProFunc server (<http://www.ebi.ac.uk/thornton-srv/databases/ProFunc>),¹³ identified the cyanogenic family 1 glycosyl hydrolase (CBG) from white clover (PDB:1CBG)¹⁴ as the top hit. AheGH1 and CBG share low (36.94%) overall sequence identity, yet high (73.47%) local sequence identity in their active sites over 49 equivalenced residues. At a structural level, they share high structural similarity (99.5% over 493 matched residues) and as for AheGH1, CBG is a homodimer in solution.¹⁴ In agreement with CBG and other GH1 members in general, the active site pocket contains several conserved polar and aromatic residues that are typically present in carbohydrate recognition sites that binds the nonreducing end of the substrate.¹ Based on comparisons with GH1 members, AheGH1 the main active site residues present are: R79, H122, E167, N166, N296, Y298, E356 and W402 (Fig. 4.24 & Fig. 4.25).

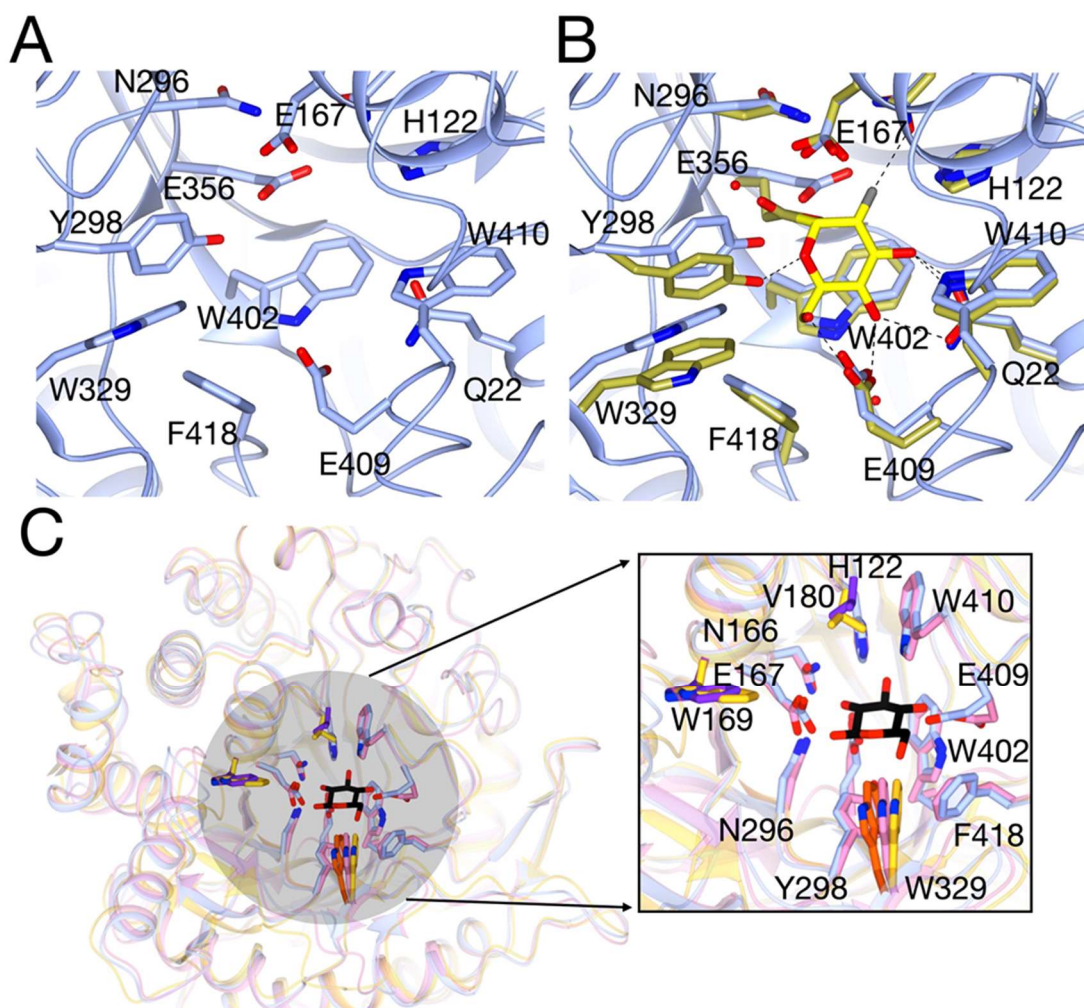


Figure 4.24. The *AheGH1* active site. A) Stereo-view of the *AheGH1* putative active site showing active site residues delineating the pocket (sticks). Proposed catalytic residues E356 and E167 are indicated; B) structural superposition of the active sites of *AheGH1* (blue) and the homologous protein *BglA* (gold, PDB: 1E4I) complexed with 2-deoxy-2-fluoro- α -D-glucopyranose catalytic intermediate (yellow sticks) and C) Superposition of *AheGH1* (ice blue) with *BglA* (yellow) and *BglB* (pink) in complex with glucose (PDB: 2O9T) and a detailed view of the glucose binding site. Glucose is shown as black sticks. *BglB* residues interacting with the glucose molecule, and corresponding *AheGH1* residues, are depicted as sticks and coloured accordingly. *AheGH1* residues conserved in *BglA* are coloured in purple. *AheGH1* W329, which is conserved in all the three homologues is coloured in orange. Residue numbering in all panels is for *AheGH1*. This figure was made with CCP4mg.¹⁵

The mechanism of catalysis generally described for this class of enzyme involves a double displacement reaction, requiring a proton donor and a nucleophile.¹⁴ Previous results are consistent with an ionized carboxylic acid group acting as a catalytic nucleophile and a histidine residue or carboxylic acid group (with a significantly elevated pKa) behaving as a general acid

catalyst. Based on comparisons made with GH1 members in general, E167 and E356 are likely to be the acid-base catalyst and nucleophile, respectively in the reaction (Fig. 4.24 & Fig. 4.25).

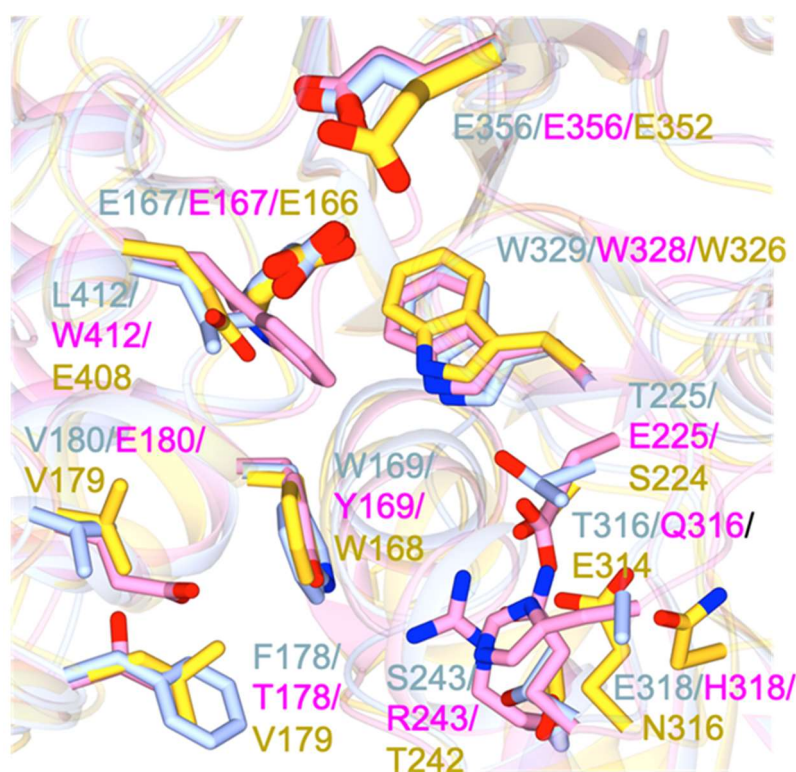


Figure 4.25. Structural superposition of the active sites of *AheGH1* (ice blue) and the homologous proteins *BglA* (yellow, pdb code 1E4I) and *BglB* (pink, pdb code 2O9P). The residues delineating the pocket are shown as sticks, labeled and colored accordingly. The catalytic glutamate residues are depicted with thicker sticks. The *AheGH1*-E318 side-chain is missing. This figure was generated using CCP4mg.

With regards to the active site architecture of GH1 enzymes in general, structural and thus functional differences are attributed to the loop regions that are present between the β/α motifs that shape the active site cavity. This may be appreciated by comparison of the overall sequence and structure conservation of *AheGH1* with all other enzymes of similar structure, using the ENDscript 2 server (<http://endscript.ibcp.fr/ESPrift/ENDscript/>).¹⁶ As expected, structure and sequence divergence occurs mainly in the loop regions connecting the β/α motifs (Fig. 4.26).

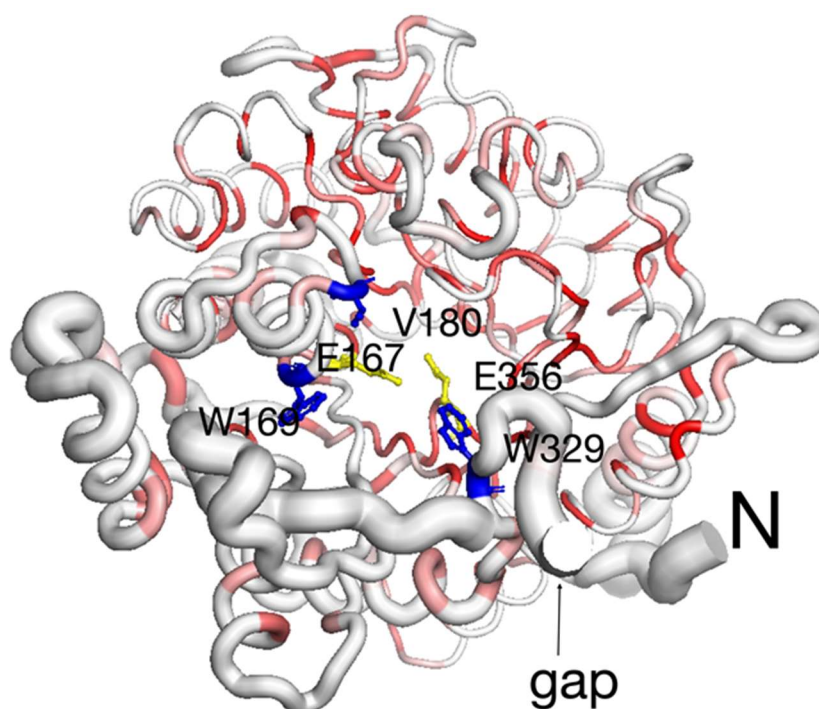


Figure 4.26. Overview of sequence and structure conservation of *AheGH1* with other glucosidases. Sausage representation indicating sequence and structure conservation of *AheGH1* with all other glycosyl hydrolases deposited in the Protein Data Bank was calculated using the ENDscript 2 server (<http://endscript.ibcp.fr/ESPrpt/ENDscript/>), using default parameters. Red shading indicates sequence conservation, with the darker colouring representing the highest sequence conservation. Structure conservation is indicated by sausage thickness with the least conserved regions indicated by increased thickness. The catalytic glutamate residues are indicated, as are the conserved residues shared in the loops of *BglA* and *BglB* that form the entrance to the active site tunnel. The gap in the *AheGH1*, due to lack of electron density is indicated.

In *BlgB*, nine active site residues are reported to delineate the entrance to the active site: Y169, T178, E180, R243, E225, Q316, H318, W328 and W412 (*BlgB* numeration)¹². These residues render the active site cavity narrower in comparison with its homolog *BglA* (PDB: 1E4Y).¹⁷ Except for W328, all remaining residues in *AheGH1* are not conserved (Fig. 4.26). Higher similarity, in terms of sequence identity, was on the other hand detected between *AheGH1* and the *BglA* active site, defined by residues W168, L177, V179, S224, T242, E314, N316, W326 and E408. Three out of the nine residues (i.e., W168, V179 and W326; Fig. 4.26) are conserved between the two proteins. In addition, according to the nature and steric hindrance of the side-chains of the

residues defining the active site, the *AheGH1* cavity is more similar to that of *BglA*.

4.4.3.3 The 3D structure of *AacGH1*

AacGH1 was crystallised in the P1 spacegroup (eight molecules in the asymmetric unit) and the structure solved and refined to 1.55Å resolution (Table 3.4). Electron density was well-defined from N-terminal residues 3-6 to C-terminal residues 448-449, depending on the *AacGH1* chain present in the crystal asymmetric unit. Electron density was absent for the initial N-terminal and last C-terminal residues, some loop regions and some solvent accessible side chains, which were flexible and lost to the solvent. As calculated using secondary structure matching of 443 main chain residues using the SUPERPOSE program, all eight *AacGH1* chains were highly similar (RMSD = 0.26 Å). Chains C and F were more complete, with regards to modelled residues, therefore all subsequent analyses were carried out on chain C.

AacGH1 presents the canonical glycoside hydrolase family 1-fold, consisting of a central TIM barrel motif, comprised of alternating α -helices and β -strands (α/β)₈ (Fig. 4.27). As observed for other members of this family, *AacGH1* contains several additional secondary structure elements, including a few short α -helices and a two-stranded and a three-stranded anti-parallel β -sheet that are peripheral to the TIM barrel.

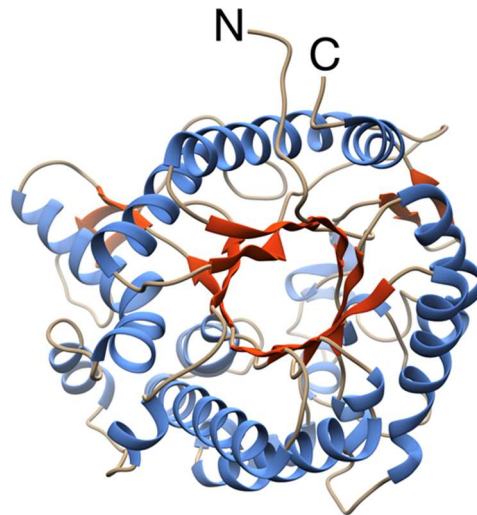


Figure 4.27. AacGH1 structure. Ribbon secondary structure representation of chain C of the AacGH1 monomer, illustrating the central TIM barrel, typical of glycoside hydrolase members. The N- and C- termini are labelled. This figure was generated using Chimera¹⁶.

The sequence- and structure-based conservation of AacGH1 was assessed using the ENDscript 2.0 server (<http://endscript.ibcp.fr/ESPript/cgi-bin/ENDscript.cgi>) and reveals, as expected, that the TIM barrel is the most highly conserved region with respect to both sequence and structure¹⁶ (Fig. 4.28).

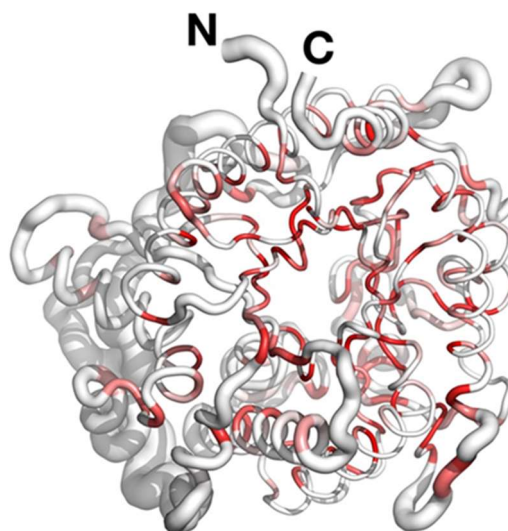


Figure 4.28. Sequence and structure-based conservation of the AacGH1 monomer with other structure homologs, analysed by the ENDscript 2.0 server (<http://endscript.ibcp.fr/ESPript/cgi-bin/ENDscript.cgi>). The darker the red colour, the higher the sequence conservation and the thicker the sausage, the least structural conservation is present. This figure was generated using Pymol 2.0.6.

The highest structural homology is shared (50% sequence identity) with a metagenomic β -glycosidase (PDB entry 5XGZ) (RMSD of 1.4 Å over 434/445 aligned residues), as deduced using the DALI 3D structure comparison server (<http://ekhidna2.biocenter.helsinki.fi/dali/>). Only flexible loops displayed structural divergence.¹¹

A 3D functional template search carried out using ProFunc (<http://www.ebi.ac.uk/thornton-srv/databases/ProFunc/>)¹³ revealed that AacGH1 has an active site architecture that is most similar (E-value 1.36E-18) to a cyanogenic β -glucosidase from white clover (*Trifolium repens*; PDB entry 1CBG).¹⁴ The two proteins share 40.0% sequence identity and 99.5% structural identity, and at the active site, they have 31 and 10 identical and similar residues, respectively.

4.4.3.4 The AacGH1 active site

The active site represents the principal surface cavity of the enzyme, and electron density corresponding to Bis-Tris Propane, present as the buffer in the crystallisation condition, was observed here for each AacGH1 chain (Fig. 4.29).

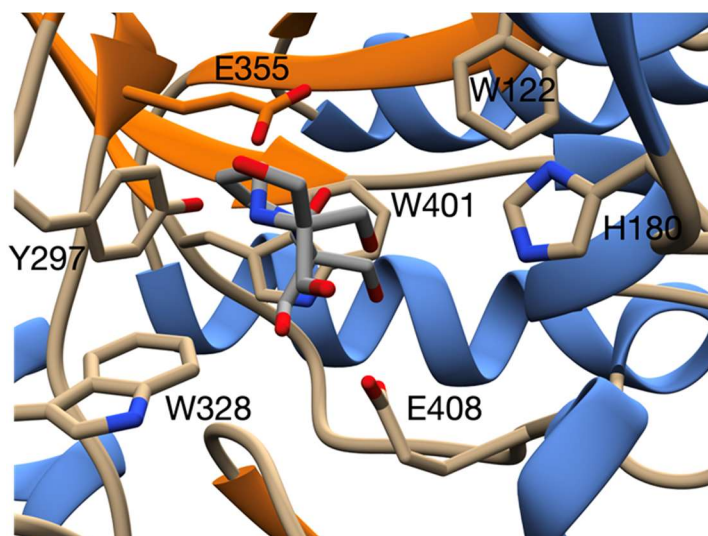


Figure 4.29. Detailed view of the active site of the AacGH1 monomer. Active site residues are indicated as sticks. The catalytic glutamate residue is highlighted in orange, whereas the Bis Tris Propane ligand is shown as grey sticks. This figure was generated using Chimera.

Based on comparisons made with the white clover β -glucosidase, AacGH1 contains the active site residue E355 (E397 in β -glucosidase) housed in the conserved I(V)TENG motif, typical of glycosyl hydrolase family 1 members. In other members, E355 has been shown to be responsible for the nucleophilic attack on the substrate. A salt bridge formed with R78 and hydrogen bonds with Y297 and a conserved active site water molecule, ensure it is deprotonated (Fig. 4.29). A second glutamate residue, E166 (E183 in β -glucosidase), is known to be the proton donor in the reaction. E166 is also

housed in a conserved motif, although instead of the canonical LNEP motif, in *AacGH1* we find HNEP.

4.4.4 Activity assays

A thorough characterisation of the new proteins was carried out, to test a range of different conditions for both activity and stability in the presence of sugars, solvents, different pHs and different temperatures. The aim of this was to be able to correlate the inherited catalytic characteristics of the newly identified GH1s with potential applications in industrial food processes.

HorGH1 was included for comparison in all tests to ensure consistency as the composition of the activity buffer was changed with regard to the initial characterisation (from buffer HEPES (100 mM), sodium chloride (500 mM) pH 7.4 to buffer HEPES (50 Mm) Ph 7.4) and this can affect the behaviour of the enzyme.

A potential application of interest in this project was the production of wines. The sugar content in fresh grapes is 15-25 % (w/w), from which ≈ 7 -12 % (w/v) correspond to glucose and ≈ 7 -12 % (w/v) to fructose. During the fermentation process, glucose, fructose and, in some wines, additional sucrose are converted progressively into ethanol to finally produce wines with a residual glucose content of ≈ 0.05 % (w/v) in dry wines, ≈ 3 % (w/v) in sweet wines, and up to ≈ 12 % (w/v) in very sweet wines as Sauternes.¹⁹

As mentioned before, glucose inhibition is a common problem among β -GH1 enzymes^{1,20} and specifically among fungal β -GH1s,²¹ origin of most of the enzymes in the wine industry, which restricts their application. Remarkably, some β -glucosidases of the GH 1 family are tolerant to or even activated by

glucose.²² One example is the novel β -glucosidase (Bgl6) characterised by Cao *et al.* which has a half maximal inhibitory glucose concentration glucose of 3.5 M.²³ The effect of glucose on *HorGH1*, *AheGH1* and *AacGH1* is reported in Figure 4.30.

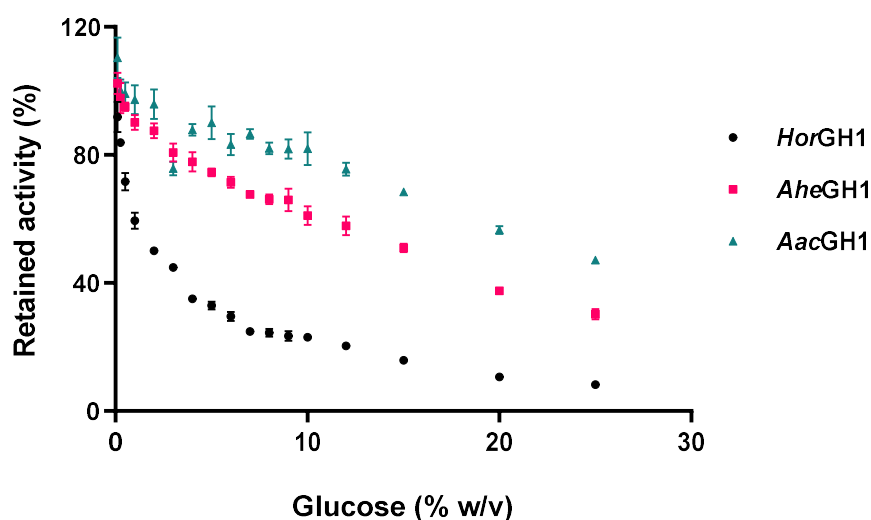


Figure 4.30. *HorGH1*, *AheGH1* and *AacGH1* retained activity (%) at different glucose concentrations. The activity was tested using the standard activity assay.

In all cases, enzymatic activity decreases as the concentration of glucose increases. However, both *AheGH1* and *AacGH1* have a significantly enhanced tolerance to glucose in comparison with *HorGH1*. It is quite remarkable that with 25 % of glucose in the reaction, the retained activity for *AacGH1* is almost 50 %. It has been reported that glucose tolerance is related to the active-site accessibility, the narrower and deeper the channel is, the more tolerant the enzyme will be.²⁴

Fructose has, in general, a lower inhibitory effect than glucose (Fig. 4.31). The retained activity of *HorGH1* and *AheGH1* in all the concentrations tested is very similar, in all cases between 60-90 %.

Interestingly, fructose seems to positively affect the activity of *AacGH1*, with a 50 % enhancement when 25 % of fructose is added in to the reaction.

In the case of their future testing in wine, the results suggest that fructose during wine fermentation will not be a handicap for *HorGH1* and *AheGH1*, and in fact it can be beneficial for *AacGH1*.

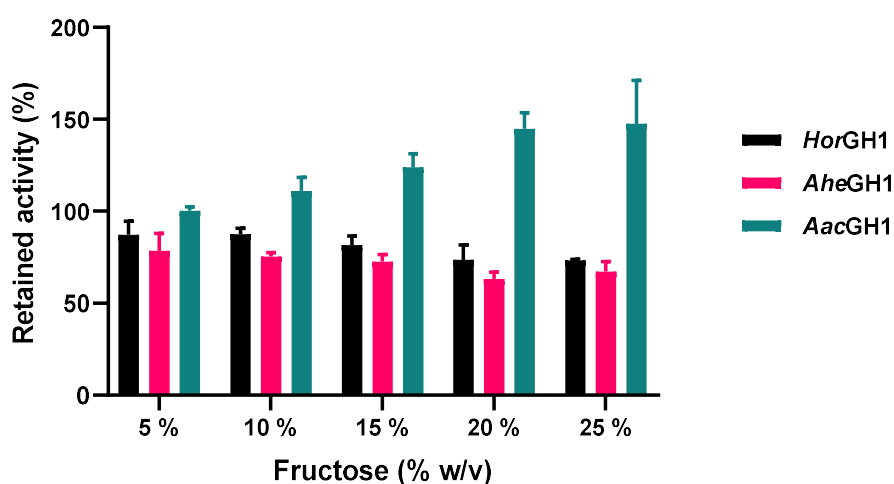


Figure 4.31. *HorGH1*, *AheGH1* and *AacGH1* retained activity (%) at different fructose concentrations. The activity was tested using the standard activity assay.

Most enzymes from mesophilic organisms have a significant loss of activity in the presence of organic solvents. This could be attributed to the loss of crucial water molecules that maintain the protein conformation, affecting the K_M and V_{max} values, and, in the most dramatic cases the overall protein folding. Retained activity in the presence of organic solvents is possible only when the surface and the active site remain well hydrated. The ability of halostable enzymes to retain hydration shells has been already reported.² This explanation is applied to *HorGH1*, which retained between 40 and 110 % of the activity in all cases.

The astonishing example in this experiment is *AheGH1*, which presents an impressive co-solvent tolerance in practically all cases. With 10 and 20 % of ethanol in the reaction, *AheGH1* is 50 % more active than without ethanol at all.

AacGH1 also performs very well with ethanol and poorly with ACN, and it suffers in several cases when the concentration of the co-solvent reaches 20 % (methanol, DMSO and THF).

The most interesting co-solvent in this work is ethanol as it is the most common solvent used in the food industry. In all the industrial applications of interest for this project, the concentration of ethanol is not going to be superior to 20 % (v/v), and consequently, all 3 enzymes look like very good candidates as they retained good activity even at such concentrations (Fig. 4.32).

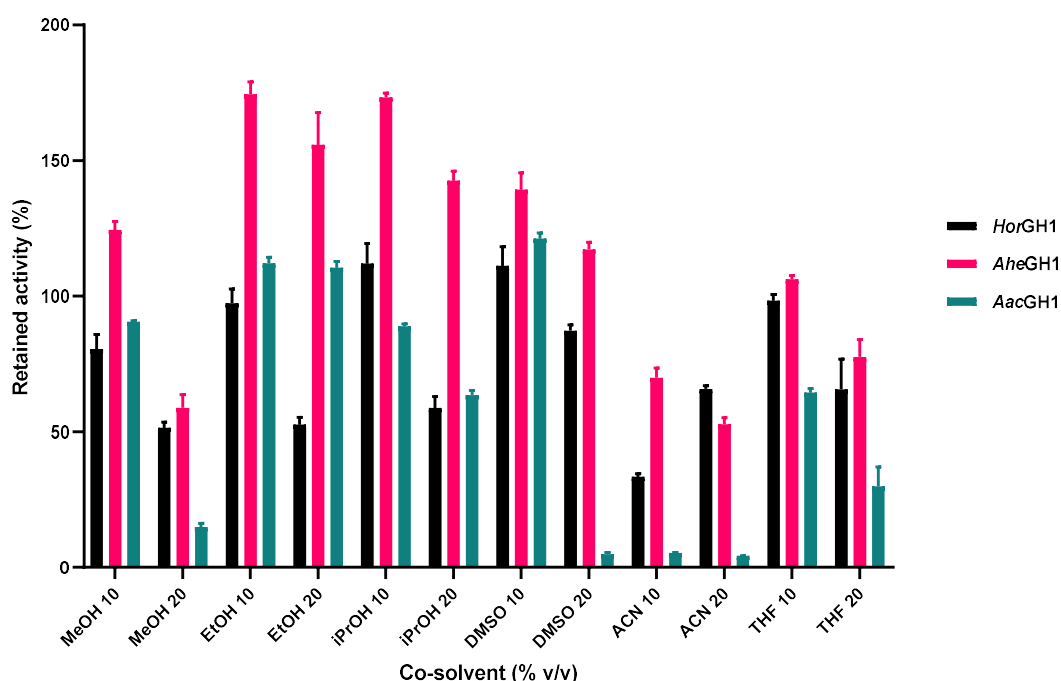


Figure 4.32. *HorGH1*, *AheGH1* and *AacGH1* retained activity (%) at different co-solvents concentrations. The activity was tested using the standard activity assay.

In this instance, the performance of the enzymes in the presence of NaCl was not assessed as no industrial process requiring the presence of NaCl will be tested.

4.4.5 Stability assays

From the previous characterisation of *HorGH1* and the results of the activity assay of the 3 enzymes in the presence of glucose and fructose, it is expected that the stability of the enzymes will not be affected after a period of incubation with glucose and fructose and, thus, the stability test in the presence of glucose and fructose was not performed.

The stability of the enzyme in the presence of solvents is also very relevant (see section 1.2.3). *HorGH1* was the most stable of the three (Fig. 4.33), retaining over 60 % activity after 5 days incubation at all 12 conditions. *AheGH1* (Fig. 4.34) had a very similar behaviour, though not as sustained (activity was severely affected after 5 days). *AacGH1* (Fig. 4.35) increased its activity to 100-120 % after 48 hours of incubation in methanol, ethanol, isopropanol (10 %) and DMSO, which suggests a really high tolerance, even an improvement on its activity in the presence of some co-solvents. However, the retained activity of *AacGH1* following 30 min incubation with ACN (20 %) or THF was virtually zero. The retained activity collapses, in all cases, after 5 days of incubation.

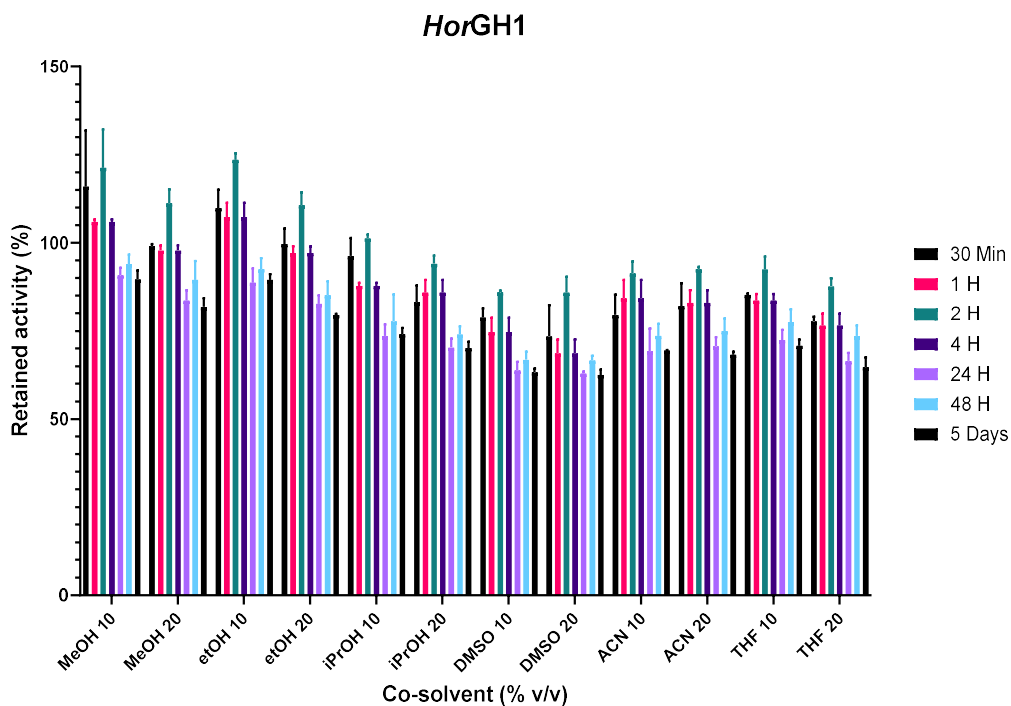


Figure 4.33. *HorGH1* retained activity (%) after incubation with different co-solvents. The activity was tested using the standard activity assay.

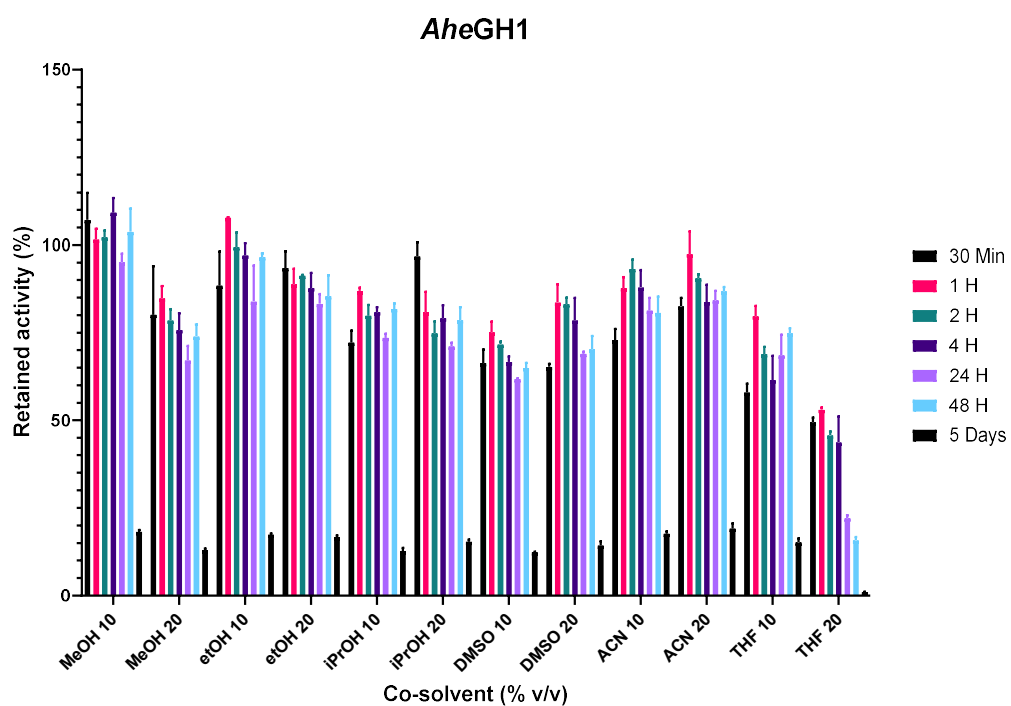


Figure 4.34. *AheGH1* retained activity (%) after incubation with different co-solvents. The activity was tested using the standard activity assay.

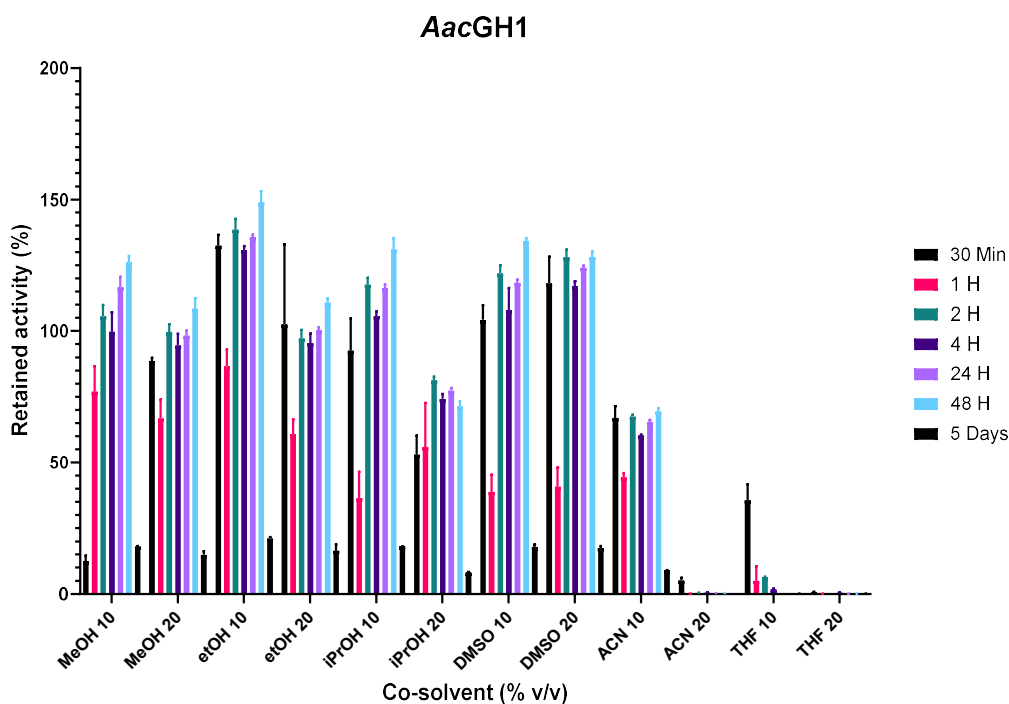


Figure 4.35. *AacGH1* retained activity (%) after incubation with different co-solvents. The activity was tested using the standard activity assay.

Once again, in the temperature stability assay, *HorGH1* (Fig. 4.36) was the most stable of the three enzymes. Its retained activity was above 50 % at all temperatures for over 5 days confirming literature findings.² It was only fully deactivated after 5 days incubation at 65 °C. *AheGH1* (Fig. 4.37) appears to retain above 40 % activity up to 55 °C. In the case of *AacGH1* (Fig. 4.38), the enzyme is quite stable up to 45 °C, maintaining 60% of its activity, but above 55 °C the enzyme loses the activity after 24 hours of incubation time.

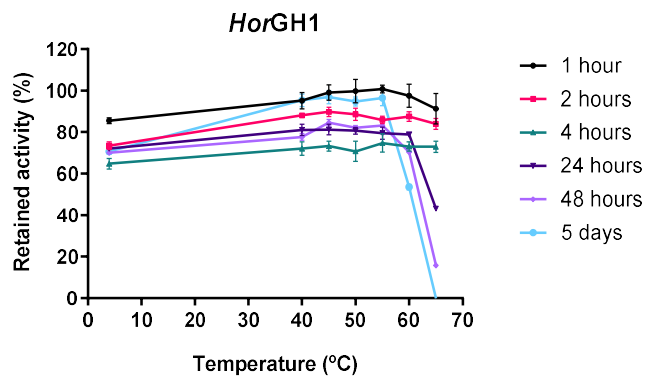


Figure 4.36. *HorGH1* retained activity after incubation at different temperatures. The activity was tested using the standard activity assay.

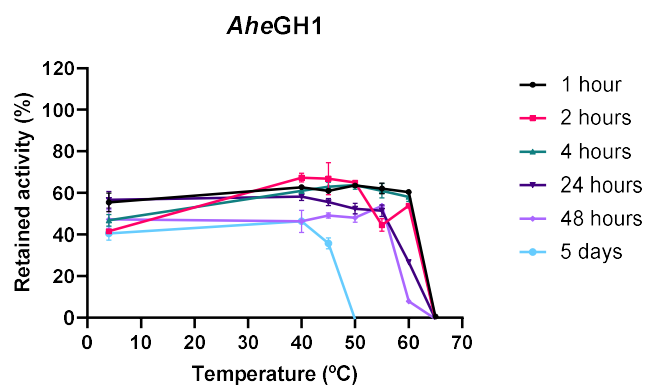


Figure 4.37. *AheGH1* retained activity after incubation at different temperatures. The activity was tested using the standard activity assay.

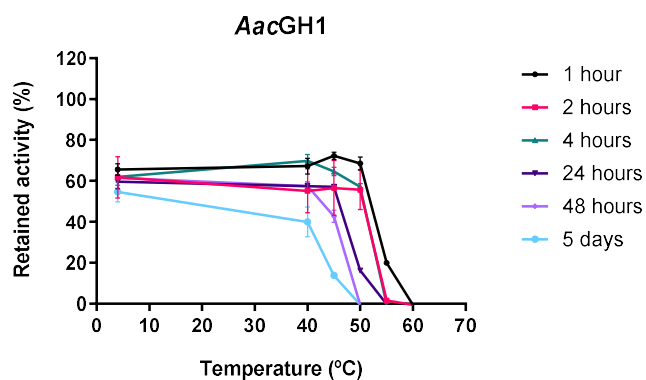


Figure 4.38. *AacGH1* retained activity after incubation at different temperatures. The activity was tested using the standard activity assay.

The results obtained for the enzymatic stability at a different pHs were quite surprising. Both, *AheGH1* and *AacGH1* were selected from thermo-acidophilic organisms in comparison with *HorGH1* which is from a thermo-halophilic organism. This selection was geared towards the application of the new candidates in the wine industry. Apart from other physicochemical characteristics, a distinctive parameter of the process of making wine is its acidic pH, around 3 and 4.

Despite their backgrounds, *HorGH1* (Fig. 4.39) seemed to be more stable than *AheGH1* (Fig. 4.40) and *AacGH1* (Fig. 4.41), retaining around 60 % of activity at all pHs, with exception of pH 3 where it was completely inactivated after 24 h. This same pattern was followed by *AheGH1*, but in its case the retained activity at pH 3 was insignificant, and dropped dramatically after 24 h of incubation at pH 4 and 12. The case of *AacGH1* was quite interesting because after 48 h its retained activity between pH 5 and 10 was over 100 %, reaching in some cases 140 %, which suggested that *AacGH1* could be highly suitable to industrial processes involving a neutral-basic range of pH, due to its remarkable stability under a very broad pH range. However, when tested at pH 3 the retained activity was negligible, and at pH 4 it dropped to 20 % after 4 h and then to 0.

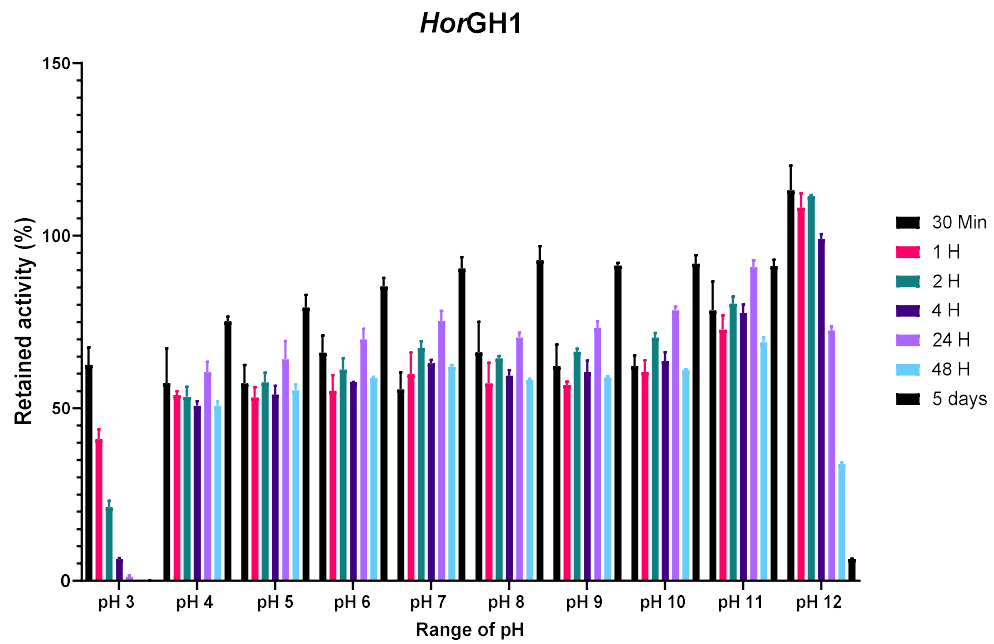


Figure 4.39. *HorGH1* retained activity after incubation at a different range of pHs. The activity was tested using the standard activity assay.

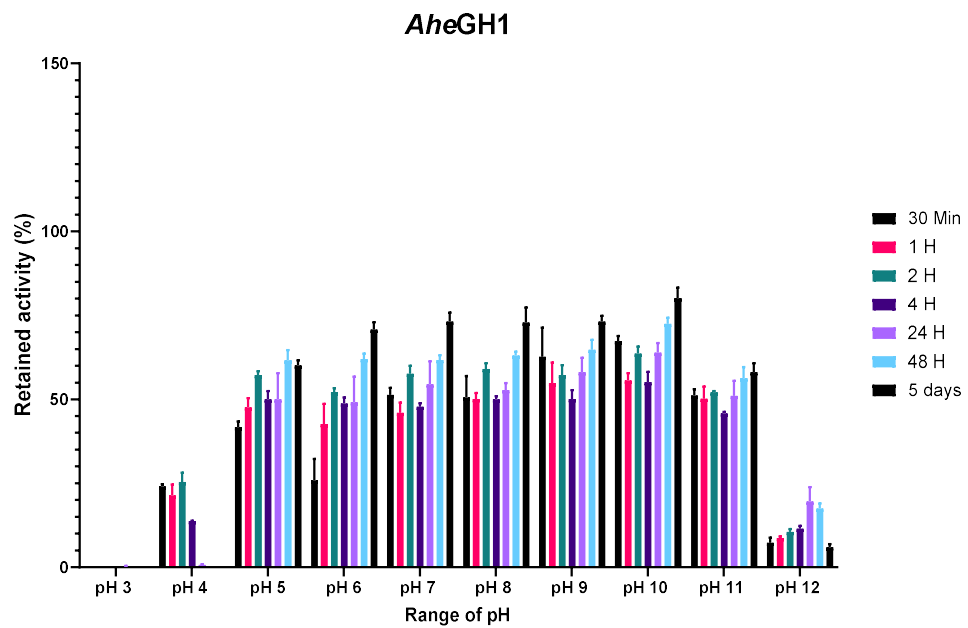


Figure 4.40. *AheGH1* retained activity after incubation at a different range of pHs. The activity was tested using the standard activity assay.

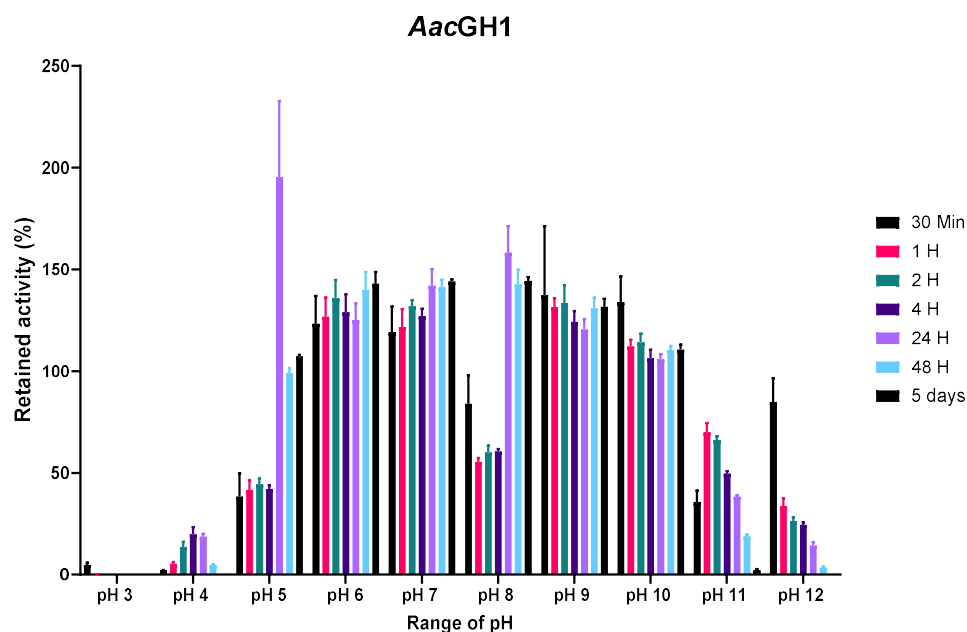


Figure 4.41. AacGH1 retained activity after incubation at a different range of pHs. The activity was tested using the standard activity assay.

Indeed, those were not the results hoped for from two acidophilic enzymes, however, the ability of the microorganism in dealing with acidic pH does not always translate to the isolated catalyst. Most adaptation mechanisms developed by acidophiles to survive at low pHs involve very efficient homeostasis which prevents the ingress of protons to the cytoplasm.²⁵ Consequently, the cytoplasmatic enzymes of those organisms do not necessarily deal with acidic conditions and hence are not adapted to it.

In conclusion to the characterisation of the 3 enzymes, it can be said that the kinetic characterisation of *AheGH1* and *AacGH1* showed that both enzymes have a higher affinity for the tested substrate and that they are more active than *HorGH1*. Regarding the activity assays, *AacGH1* had an impressive tolerance for glucose and fructose which suggests it may be a very good candidate for the food industry. *AheGH1*, on the other hand, saw its activity

incremented in the presence of organic co-solvents, also a very attractive feature for the alcoholic beverages industry.

On the stability assays, where the activity of the enzymes at a different pHs, temperatures and co-solvents was tested over 5 days, *HorGH1* still the one performing better, with a more stable behaviour over the length of the experiment.

4.5 Bibliography

- 1 C. S. Chan, L. L. Sin, K.-G. Chan, M. S. Shamsir, F. A. Manan, R. K. Sani and K. M. Goh, *Biotechnol. Biofuels*, 2016, **9**, 174.
- 2 A. Bhattacharya and B. I. Pletschke, *Enzyme Microb. Technol.*, 2014, **55**, 159–169.
- 3 S. DasSarma and P. DasSarma, *Curr. Opin. Microbiol.*, 2015, **25**, 120–126.
- 4 D. Alsafadi and F. Paradisi, *Extremophiles*, 2013, **17**, 115–122.
- 5 A. Gordon, *Case study: Addressing the problem of Alicyclobacillus in tropical beverages*, Elsevier Inc., 2017, vol. 2.
- 6 P. K. Pindi, R. Manorama, Z. Begum and S. Shivaji, *Int. J. Syst. Evol. Microbiol.*, 2010, **60**, 2263–2266.
- 7 H. J. Busse, *Int. J. Syst. Evol. Microbiol.*, 2016, **66**, 9–37.
- 8 B. A. Gasteiger E., Hoogland C., Gattiker A., Duvaud S., Wilkins M.R., Appel R.D., in *The Proteomics Protocols Handbook*, ed. J. M. Walker, Humana Press, 2005, pp. 571–607.
- 9 G. E. K. Bjerga, R. Lale and A. K. Williamson, *Bioengineered*, 2016, **7**, 33–38.
- 10 L. D. Kori, A. Hofmann and B. K. C. Patel, *Acta Crystallogr. Sect. F Struct. Biol. Cryst. Commun.*, 2011, **67**, 111–113.
- 11 L. Holm, *Bioinformatics*, 2019, **35**, 5326-5327.
- 12 P. Isorna, J. Polaina, L. Latorre-García, F. J. Cañada, B. González and

- J. Sanz-Aparicio, *J. Mol. Biol.*, 2007, **371**, 1204–1218.
- 13 R. A. Laskowski, J. D. Watson and J. M. Thornton, *Nucleic Acids Res.*, 2005, **33**, 89–93.
- 14 T. Barrett, C. G. Suresh, S. P. Tolley, E. J. Dodson and M. A. Hughes, *Structure*, 1995, **3**, 951–960.
- 15 S. McNicholas, E. Potterton, K. S. Wilson and M. E. M. Noble, *Acta Crystallogr. Sect. D Biol. Crystallogr.*, 2011, **67**, 386–394.
- 16 X. Robert and P. Gouet, *Nucleic Acids Res.*, 2014, **42**, 320–324.
- 17 J. Sanz-Aparicio, J. A. Hermoso, M. Martínez-Ripoll, B. González, C. López-Camacho and J. Polaina, *Proteins Struct. Funct. Genet.*, 1998, **33**, 567–576.
- 18 E. F. Pettersen, T. D. Goddard, C. C. Huang, G. S. Couch, D. M. Greenblatt, E. C. Meng and T. E. Ferrin, *J. Comput. Chem.*, 2004, **25**, 1605–1612.
- 19 J. Bakker and R. J. Clarke, *Wine Flavour Chemistry*, 2nd edition, Wiley-Blackwell, 2012.
- 20 P. Pang, L. chuang Cao, Y. huan Liu, W. Xie and Z. Wang, *J. Struct. Biol.*, 2017, **198**, 154–162.
- 21 A. Sørensen, M. Lübeck, P. S. Lübeck and B. K. Ahring, *Biomolecules*, 2013, **3**, 612–631.
- 22 Y. Yang, X. Zhang, Q. Yin, W. Fang, Z. Fang, X. Wang, X. Zhang and Y. Xiao, *Sci. Rep.*, 2015, **5**, 17296.

- 23 L. Cao, Z. Wang, G. Ren, W. Kong, L. Li, W. Xie and Y. Liu, *Biotechnol. Biofuels*, 2015, **8**, 202.
- 24 P. O. De Giuseppe, T. D. A. C. B. Souza, F. H. M. Souza, L. M. Zanphorlin, C. B. Machado, R. J. Ward, J. A. Jorge, R. D. P. M. Furriel and M. T. Murakami, *Acta Crystallogr. Sect. D Biol. Crystallogr.*, 2014, **70**, 1631–1639.
- 25 H. Stan-Lotter and S. Fendrihan, *Adapt. Microb. Life to Environ. Extrem. Nov. Res. Results Appl. Second Ed.*, 2017, 1–342.

Chapter 5 Hydrolytic capacity of *HorGH1*, *AheGH1* and *AacGH1* towards two wine glucosides

The work presented in this chapter was performed at the Australian Wine Research Institute, Adelaide, Australia. It is my exclusive contribution unless otherwise stated and it has been included in a publication: L. Delgado, M. Parker, I. Fisk, F. Paradisi “Performance of the extremophilic enzyme *BglA* in the hydrolysis of two aroma glucosides in a range of model and real wines and grape juices” submitted to Food Chemistry 2020.

5.1 Introduction

Aroma is considered a key aspect of wine quality. Despite the identification of over 800 aroma compounds¹ only a small number of them contribute substantially to the aroma of wine.^{2,3} Among the volatiles that are important to the aroma of wine there are fruity and floral monoterpenes (geraniol, linalool and α -terpineol) and volatile phenols (guaiacol and cresols), which, depending on their concentration and wine style, could affect differently the overall flavour and aroma.

Monoterpenes, formed in grapes during ripening, are crucial components of the varietal wine bouquet of Muscat and floral varieties⁴ but a major fraction is entrapped as flavourless, odourless, non-volatile glycosides, constituting an important reservoir of aroma.⁵ Monoterpenes can be liberated from their glycosides by acid or enzymatic hydrolysis; but as acid hydrolysis is a slower process^{6,7} and can cause rearrangements of the released aglycones, enzymes represent a useful alternative and can be added to maximize the aromatic potential of wines.^{8,9}

Phenolic glycosides are also formed when berries are exposed to smoke from bush fires and prescribed forest burns as the grapevines can uptake smoke constituents like guaiacols, cresols and syringols, and accumulate them in the form of glycoconjugates. However in this case, their hydrolysis leads to the release of volatile phenols (VP) giving the wine a “smoky” or “ashy” aroma/flavour.^{10–12} In addition, breakdown of glycosides of volatile phenols in the mouth, mediated by enzymes of the oral microflora can also contribute to smoky and ashy aftertaste.¹³ In this case, if enzymatic hydrolysis can be

performed effectively during the wine processing, phenolic glycosides can be reduced, and the release of VPs can then be minimised using different techniques,¹⁴ improving the overall flavour.

The aglycone moiety in terpenyl and phenol glycosides can be linked to a β -D-glucopyranose unit or to a disaccharide.¹⁵ While β -glucosidases are capable of cleaving the glycosidic bond between the carbohydrate moiety and the aglycone,¹⁶ the release of the aglycone from disaccharide glycosides would normally require the action of other glycosyl hydrolases.

Endogenous glycosidases from the grape and the winery environment have been extensively studied for this purpose; however, they do not tolerate well the harsh physical and chemical conditions that usually characterize wine processing such as low pH, high glucose and fructose, and sulphite content. Grape and yeast glycosidases present low activity under fermentation conditions,¹⁷ therefore commercial preparations are mainly obtained from fungi and have primarily pectinase activity, with secondary glycosidase activity. Fungal glycosidases have a weak catalytic specificity which could lead to the hydrolysis of pigment glycosides, and consequent spoiling of colours and flavours.¹⁸ In addition, glucose inhibition is a common problem among fungal β -glucosidases.^{19–21} Hence, the search for new enzymatic alternatives, more adapted to the wine conditions is highly relevant.

The hydrolytic performance of the 3 β -glucosidases *HorGH1*, *AheGH1* and *AacGH1* with two glucosides relevant to floral wine aroma and smoke-taint affected wines was evaluated and compared with a commercial preparation called Rapidase® Revelation Aroma.

5.2 Enzyme expression, purification and lyophilisation

HorGH1, *AheGH1* and *AacGH1* were successfully expressed and purified by metal affinity chromatography with an average yield of 55, 75 and 170 mg protein/L of culture respectively. Commercial preparation Rapidase® Revelation Aroma is described as “a micro granulated pectolytic enzyme preparation with the four essential α and β -glycosidases activities”, therefore it is a mix of proteins with different enzymatic activities. Rapidase® was used directly from the commercial packaging, with no further treatment, as the purification of the protein/proteins having β -glucosidase activity was unfeasible. An SDS-PAGE was done to assess the enzymatic purity of the 3 enzymes and the composition of the commercial preparation (Fig. 5.1).

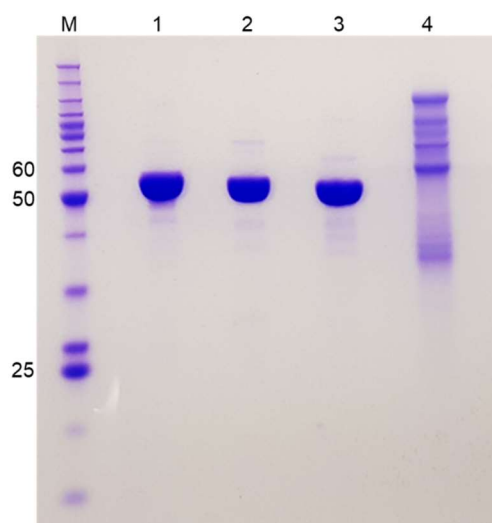


Figure 5.1. SDS-PAGE gel of *HorGH1*, *AheGH1*, *AacGH1* and Rapidase®. (M) Molecular mass marker, (1) Purified Hor, (2) Purified Ahe, (3) Purified Aac, (4) Rapidase preparation. Protein loading: 7.5 μ g. Protein concentration: 1 mg/mL.

Following dialysis, *HorGH1*, *AheGH1* and *AacGH1* were lyophilized and stored at 4 °C until needed. An activity assay under standard conditions was performed before and after lyophilisation confirming enzymatic stability with a

specific activity of 5.5 U/mg of protein for *HorGH1*, 9.3 U/mg for *AheGH1* and 20 U/mg for *AacGH1*. As it can be observed in Fig. 5.1, the commercial preparation is a mix of different unknown proteins. Based on its molecular weight, estimation by quantification analysis using Li-cor Odyssey Fc scanner and software Image Studio version 4.0 suggests that 10 % of the commercial preparation would correspond to β -glucosidases. The specific β -glucosidase activity of the commercial preparation was calculated as 0.16 U/mg of protein.

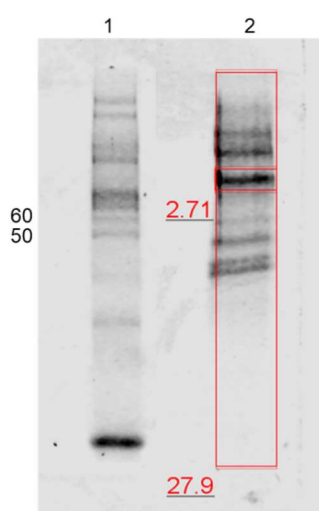


Figure 5.2. Quantification of the band corresponding to the β -glucosidase in the Rapidase® preparation are indicated in red (Li-cor Odyssey Fc scanner and software Image Studio version 4.0). (1) Protein ladder, (2) β -glucosidase in Rapidase®.

5.3 Assessment of the enzymatic performance in model wines and juices

5.3.1 Composition of the matrices

Three model systems were chosen as matrices to start the trials with. Model systems are less complex media and they are therefore intermediates between the buffer systems of the initial characterization and the real wines and juices.

Two different model wines were selected in representation of a completely sugar dry wine and a table wine with sugar concentrations typical for Australian commercial wines.²² Model wine 1 (MW1) consisted of saturated potassium hydrogen tartrate with 10 % (v/v) ethanol and pH 3.5. Model wine 2 (MW2) consisted of saturated potassium hydrogen tartrate with 10 % (v/v) ethanol, 6 g/L glucose, 6 g/L fructose and pH 3.5.

Model juice (MJ) was prepared using water, 100 g/L glucose, 100 g/L fructose, 0.2 g/L citric acid, 3 g/L malic acid, 2.5 g/L tartaric acid and pH 3.7. pH was adjusted with tartaric acid 1M in all cases.

Table 5.1. Summary of the composition of MW1, MW2 and MJ.

Matrix	EtOH content	Sugar content	pH
Model wine 1 (MW1)	10 %	0	3.5
Model wine 2 (MW2)	10 %	12 g/L glc + fru	3.5
Model juice (MJ)	0	200 g/L glc + fru	3.7

5.3.2 *Enzymatic stability*

Stability assays of *HorGH1*, *AheGH1*, *AacGH1* and Rapidase® were carried out in the two model wine systems (MW1 and MW2) and in the model juice (MJ), mimicking operational conditions. The appropriate amount of lyophilised enzyme was dissolved in the different systems and incubated for varying periods of time at 22 °C. An activity test was performed at suitable intervals (1 h, 3 h, 24 h, and 120 h) to assess how the chemical conditions of the matrix (pH, ethanol and sugars) affected the stability of the enzymes. Unfortunately, and in line with the preliminary results obtained in the initial characterisation at a different range of pHs (see Chapter 4), *AheGH1* and *AacGH1* showed a complete loss of stability after 1 h of incubation in all the matrices, and hence,

only the results corresponding to *HorGH1* and Rapidase® are shown in Figure 5.3.

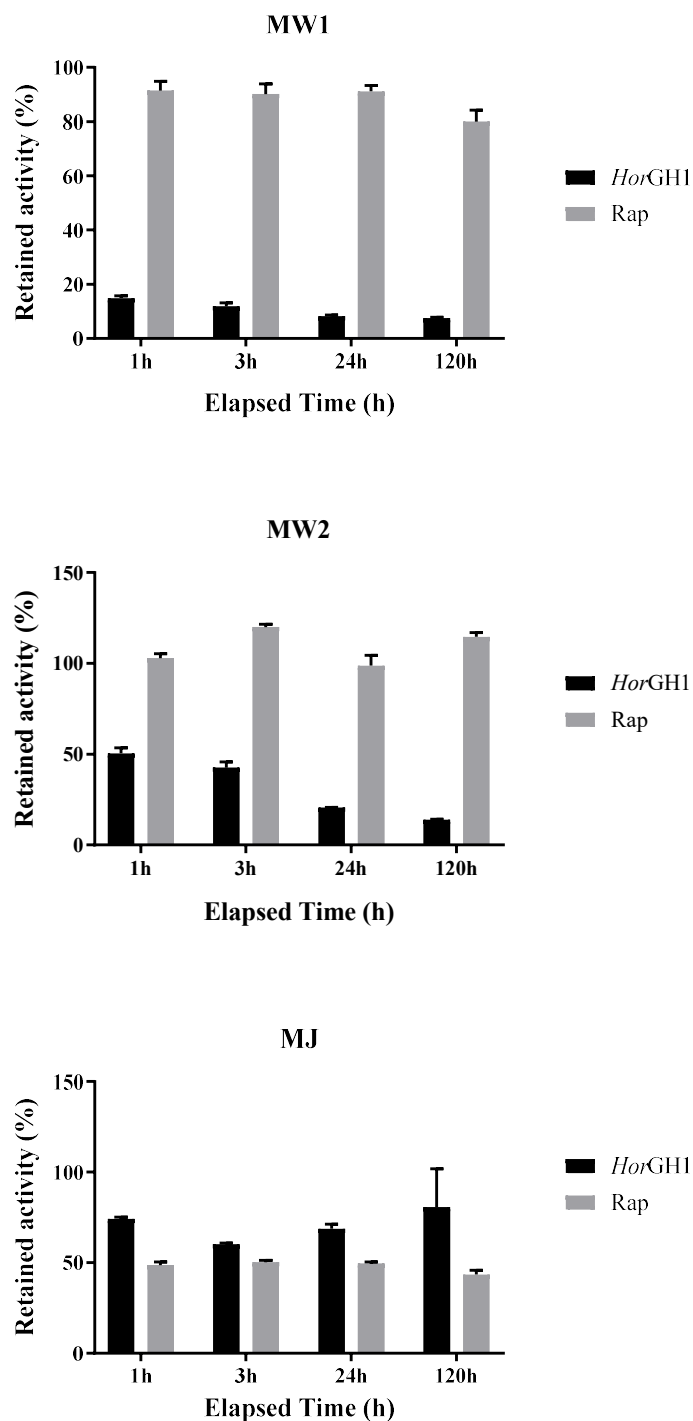


Figure 5.3. *HorGH1* and Rapidase® stability assays in Model wine 1 (MW1), Model wine 2 (MW2) and Model juice (MJ) incubated at 22 °C during 1 h, 3 h, 24 h and 120 h. Each data point is an average of 3 measurements.

Commercial Rapidase® shows a better stability in the case of MW1 (10 % ethanol, no sugar, pH 3.5) and MW2 (10 % ethanol, 12 g/L glu+fru, pH 3.5) retaining over 80 % activity after 5 days of incubation. Hor retains 7 % of its activity after 5 days incubation in MW1 and 14 % in the case of MW2. That means a two-fold increase with respect to MW1. As the sugar content is the only difference between these two model matrices, it appears that fructose and glucose have a protective effect towards *HorGH1* stability.

This is further confirmed from the results observed in MJ (no ethanol, 200 g/L of glu+fruc, pH 3.7) where *HorGH1* is considerably more stable, retaining around 80 % of activity after 120 h incubation. In the same matrix, Rapidase® stability (43 %) suffers in comparison with its performance in model wines, where the pH and the sugar content are significantly lower, and it compares poorly with *HorGH1*.

5.3.3 Release of volatiles from glucosides in model systems

The hydrolytic capacity of *HorGH1*, *AheGH1* and *AacGH1* in comparison with Rapidase® was evaluated with geranyl and guaiacyl glucoside (Fig. 5.4) by measuring the release of the free volatiles in the gas phase with SPME-GC-MS.

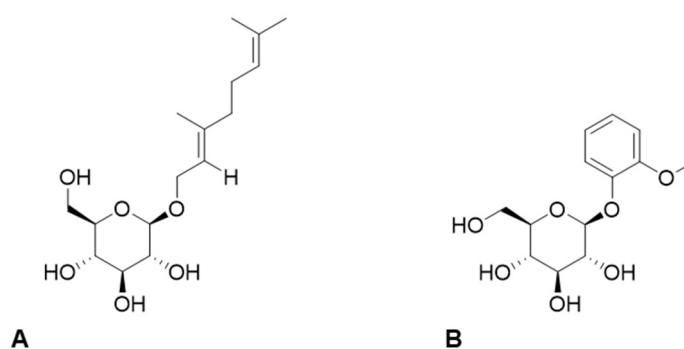


Figure 5.4. (A) Geranyl glucoside, (B) Guaiacyl glucoside.

Different concentrations of protein (1, 0.03, 0.01 and 0.001 mg/mL) were preliminary tested to have a first impression of the performance of the different enzymes on the matrices. But, taking into account the recommended dosage of Rapidase® for white wines, 1 mg of lyophilised powder per hectolitre of wine, and for red wines, 2 mg/hl, the final concentration to carry on all the experiments was accorded to be 1 mg/mL of matrix. However, *HorGH1*, *AheGH1* and *AacGH1* have been used as purified preparations in all the assays to better assess their performance. To have consistency among all systems, the effective enzyme quantity has been determined by Bradford Protein Assay using bovine serum albumin as standard,²³ and the powders weighed to achieve 0.01 mg of protein per mL of matrix in all tests.

In separate 20 mL SPME vials, 3 mL of MW1, MW2 and MJ were spiked with 5 µg of geranyl glucoside and 5 µg of guaiacyl glucoside. The amount of enzyme added to each sample was 0.01 mg/mL. The samples were left shaking at 22 °C for different incubation periods to allow enzymatic hydrolysis. The reaction was stopped by adding 2 mL of saturated CaCl₂. Internal standards, d7-geraniol and d3-guaiacol, were added (2 µg) and the liberated aglycones were analysed using SPME-GCMS. All experiments were carried out in triplicate.

Geraniol and guaiacol calibration curves with a linear range between 0.02-5 µg were determined (Fig. 5.5).

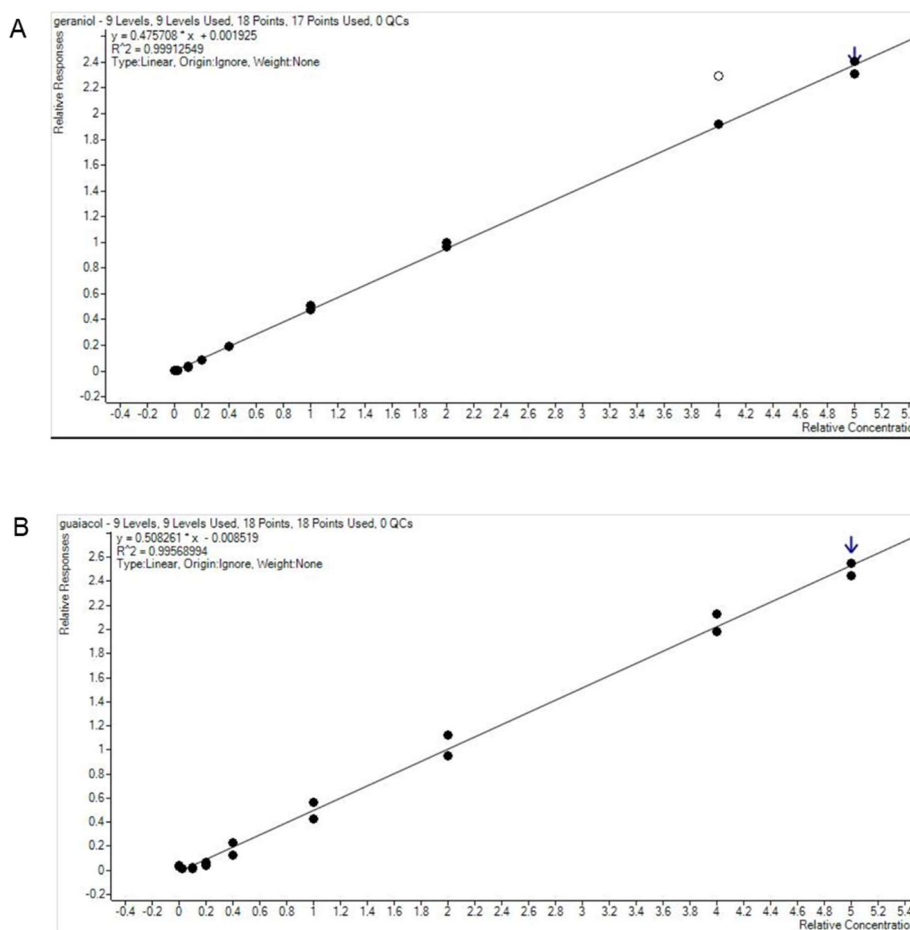


Figure 5.5. Calibration curves for geraniol and guaiacol, with the equation and the R-squared value. (A) Geraniol, (B) Guaiacol.

Interestingly, despite a lower stability observed for *HorGH1* (Fig 5.3), the catalytic efficiency of this enzyme in MW1 equals that of Rapidase® in the release of geraniol with no significant differences (Table 5.2). The release of guaiacol by *HorGH1* is, on the other hand, considerably better after 5 days (97 %) in comparison with Rapidase® (75 %). The observed drop in the hydrolysed substrate after 8 days incubation is a known artefact due to the rearrangement of the terpenes under acidic conditions.^{24,25}

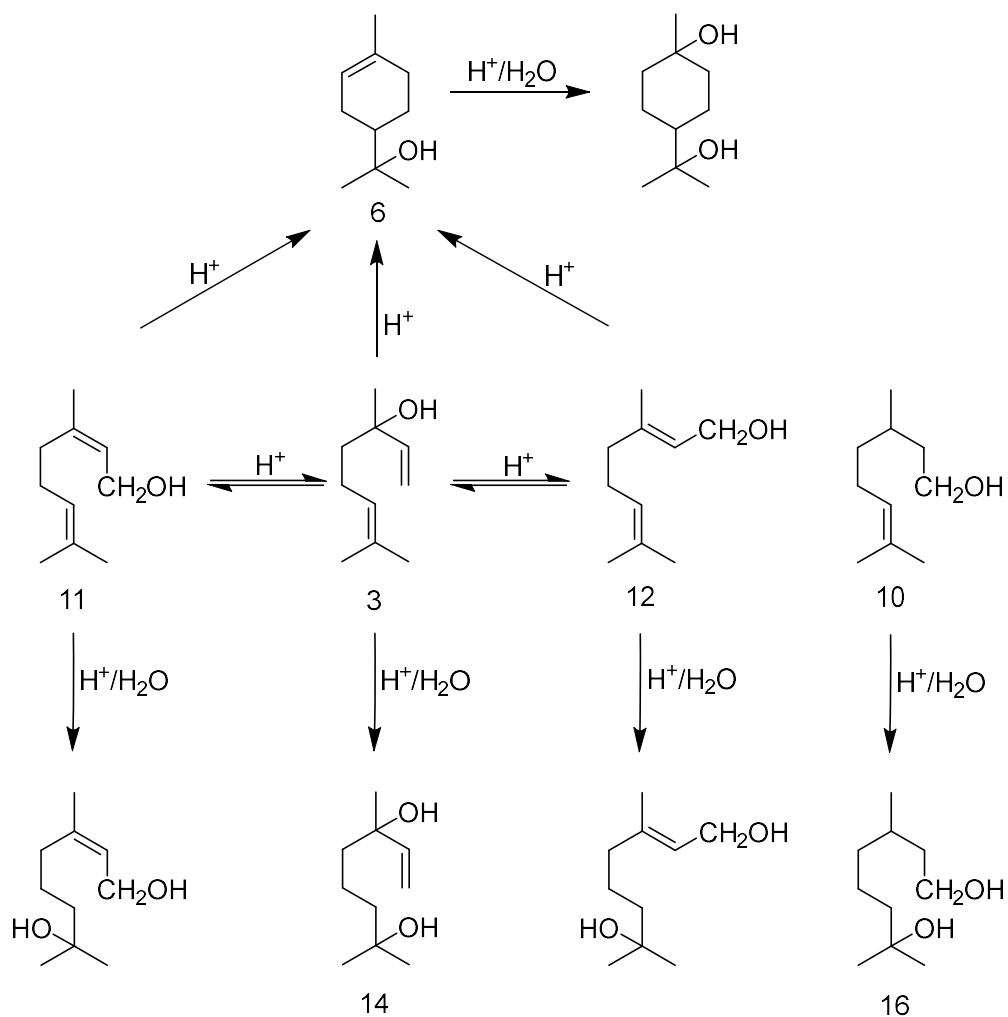


Figure 5.6. Acid catalysed rearrangements of monoterpenes.²¹

The hydrolytic capacity of *AheGH1* towards geraniol glucoside halves the values achieved by *HorGH1*, and when referring to guaiacol glucoside accounts for a 5-fold reduction in comparison with *HorGH1*.

AacGH1 achieves values of less than 1 % in both cases.

Table 5.2. *HorGH1*, *AheGH1*, *AacGH1* and *Rapidase*® release of geraniol and guaiacol over 24 h, 5 d and 8 d in Model wine 1.

MW1	Substrate	Enzyme	Time	Geraniol released (μg)	% Hydrolysis
Geranyl glucoside	<i>HorGH1</i>		24h	2.33 ± 0.09	96
			5d	2.51 ± 0.11	≥ 99
			8d	2.19 ± 0.05	90
	<i>AheGH1</i>		24h	0.96 ± 0.04	39
			5d	1.06 ± 0.01	43
			8d	–	–
	<i>AacGH1</i>		24h	0.01 ± 0.00	0.5
			5d	0.01 ± 0.00	≤ 0.5
			8d	–	–
	<i>Rapidase</i> ®		24h	2.42 ± 0.03	99
			5d	2.65 ± 0.15	≥ 99
			8d	2.52 ± 0.11	≥ 99
<hr/>					
	Substrate	Enzyme	Time	Guaiacol released (μg)	% Hydrolysis
Guaiacyl glucoside	<i>HorGH1</i>		24h	1.57 ± 0.07	72
			5d	2.12 ± 0.01	97
			8d	1.20 ± 0.27	55
	<i>AheGH1</i>		24h	0.16 ± 0.06	7
			5d	0.27 ± 0.10	10
			8d	–	–
	<i>AacGH1</i>		24h	0.01 ± 0.01	0.5
			5d	0.05 ± 0.01	≤ 0.5
			8d	–	–
	<i>Rapidase</i> ®		24h	0.64 ± 0.04	29
			5d	1.64 ± 0.12	75
			8d	1.39 ± 0.07	64

When the catalytic performance was assessed in MW2 (Table 5.3), *Rapidase*® hydrolytic capacity was diminished in comparison with MW1. The formation of geraniol was complete after 24 h incubation in samples containing *HorGH1*, however in the case of *Rapidase*® 5 days are required to reach complete hydrolysis, compared with 24 h required in MW1. *AheGH1* only reaches a 12 % hydrolysis after 5 days and *AacGH1* less than 0.5 %.

The guaiacol yielded in samples treated with *HorGH1* is 62 % after 5 d incubation while with *Rapidase*®, *AheGH1* and *AacGH1* the release of guaiacol after the same incubation period is 6 times lower (10 %), 12 times

lower (5 %) and 120 times lower (0.5 %) respectively. The difference between MW1 and MW2 is once again the sugar content. It is known that glucose is a common inhibitor for many β -glucosidases²⁶ and a content of 6 g/L seems to affect the activity of the commercial preparation, but also of *AheGH1* and *AacGH1*. Probably glucose is causing inhibition of the enzymes. The results are also in line with those obtained in the stability assays. Unusually, *HorGH1* tolerates very well high sugar contents.

Following an analysing of the results obtained in the stability assays and in the release of volatiles, it can be concluded that neither *AheGH1* nor *AacGH1* are good candidates to be used in the wine industry, where the chemical conditions of most wines (pH lower than 4 and variable sugar content) seem to be too harsh for their catalytic performance. As the model juice has a similar pH and higher sugar content than the model wines, and real matrices are even more complex than model ones, *AheGH1* and *AacGH1* are not progressed further. The results obtained with these two enzymes are not comparable with those obtained by *HorGH1* or the commercial preparation Rapidase®. From here onwards, only the performance of *HorGH1* and Rapidase® will be discussed.

Table 5.3. *HorGH1*, *AheGH1*, *AacGH1* and Rapidase® release of geraniol and guaiacol over 24 h and 5 d in Model wine 2.

MW2	Substrate	Enzyme	Time	Geraniol released (μg)	% Hydrolysis		
	Geranyl glucoside	<i>HorGH1</i>	24h	2.49 ± 0.08	≥ 99		
			5d	2.79 ± 0.07	≥ 99		
		<i>AheGH1</i>	24h	0.24 ± 0.00	10		
			5d	0.28 ± 0.01	12		
		<i>AacGH1</i>	24h	0.00	≤ 0.5		
			5d	0.00	≤ 0.5		
		Rapidase®	24h	1.33 ± 0.10	55		
			5d	2.70 ± 0.10	≥ 99		
			Substrate	Enzyme	Time	Guaiacol released (μg)	% Hydrolysis
			Guaiacyl glucoside	<i>HorGH1</i>	24h	0.77 ± 0.04	35
5d	1.36 ± 0.03				62		
<i>AheGH1</i>	24h			0.04 ± 0.03	2		
	5d			0.10 ± 0.09	5		
<i>AacGH1</i>	24h			0.00	≤ 0.5		
	5d			0.01 ± 0.00	0.5		
Rapidase®	24h			0.04 ± 0.00	2		
	5d			0.23 ± 0.02	10		

Results in MJ (Table 5.4) highlight an outstanding performance of *HorGH1* in comparison with the commercial preparation. While Rapidase® hydrolysis capacity is below 6 % for both compounds, the percentage of glycosides hydrolysed by *HorGH1* is over 60 % for geraniol and over 25 % for guaiacol after 5 days incubation, reaching 45 % after 8 days. Those results highlight once more the very low threshold of Rapidase® for sugars.

Table 5.4. *HorGH1* and Rapidase® release of geraniol and guaiacol over 24 h, 5 d and 8 d in Model juice.

MJ	Substrate	Enzyme *****	Time ***a	Geraniol released (µg)	% Hydrolysis
	Geranyl glucoside	<i>HorGH1</i>	24h	0.94 ± 0.04	39
			5d	1.54 ± 0.04	63
			8d	1.15 ± 0.21	47
		Rapidase®	24h	0.03 ± 0.01	1
			5d	0.07 ± 0.02	3
			8d	0.08 ± 0.02	3
Substrate	Enzyme *****b	Time *****b	Guaiacol released (µg)	% Hydrolysis	
Guaiacyl glucoside	<i>HorGH1</i>	24h	0.00	0	
		5d	0.55 ± 0.11	25	
		8d	0.98 ± 0.01	45	
	Rapidase®	24h	0.00	0	
		5d	0.04 ± 0.00	2	
		8d	0.12 ± 0.04	5	

5.4 Assessment of the enzymatic performance in real wines and juices

5.4.1 Composition of the matrices

Two commercially available wines, a white (WW) and a red (RW), and a Chardonnay grape juice (WJ) produced in-house were used. The WW was a 2017 Chardonnay from Riverina, Australia with an alcohol content of 12.2 % (v/v), 4.9 g/L glucose and fructose, titratable acid 6.4 g/L and pH 3.35, the RW a 2016 Shiraz from South Eastern Australia with an alcohol content of 13.9 % (v/v), 5.8 g/L glucose and fructose, titratable acid 6.2 g/L and pH 3.66, while the Chardonnay juice had total soluble solids 22.6 °Brix (~20% total sugar content), 52 mg/L SO₂ and pH 3.5 (Table 5.5). Chardonnay and Shiraz grape varieties were chosen due to their low monoterpene content.

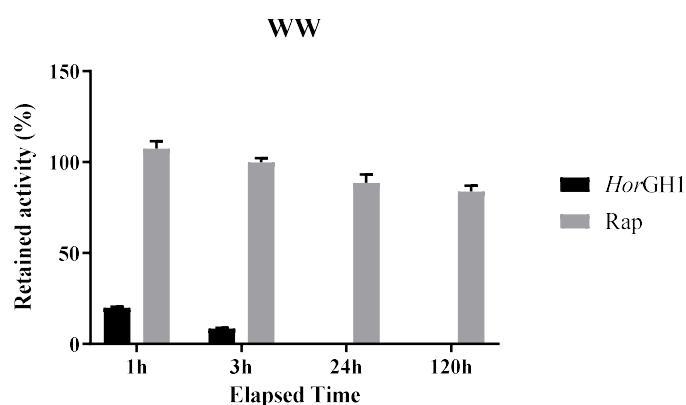
Table 5.5. Summary of the composition of White wine (WW), Red wine (RW) and White grape juice (WJ).

Matrix	EtOH content	Sugar content	pH
White wine (WW)	12.2 %	4.9 g/L glc + fru	3.35
Red wine (RW)	13.9 %	5.8 g/L glc + fru	3.66
White grape juice (WJ)	0	22.6 ° Brix	3.5

5.4.2 Enzymatic stability

Following the same procedure as in section 5.3.2, the stability of *HorGH1* and Rapidase® was assessed in both real wines and juice. Real wines and juices are more complex matrices than model systems and the enzymes can lose stability more easily due to multiple factors encompassing both physical and chemical characteristics of wine/juice.

In WW, *HorGH1* does not retain any activity after 24 h incubation. However, its stability improves when incubated in RW, retaining 15 % of activity, which is likely due to the difference in pH between the two systems; 3.35 for WW (white) and 3.66 for RW (red). In addition, the alcohol content (1.7 % more in RW) seems to not affect the stability of *HorGH1*. On the contrary, Rapidase® shows the opposite behaviour with a 15 % drop in activity when incubated for 5 days in RW in comparison with WW and again this is consistent with the higher glucose and fructose content in the red wine (5.8 g/L for the red wine and 4.9 g/L for the white wine) which negatively impacts the stability of the commercial preparation. In WJ, Rapidase® outperforms *HorGH1*, the white juice has less sugar content as well as a more acidic pH than the model juice which clearly impacts *HorGH1* stability.



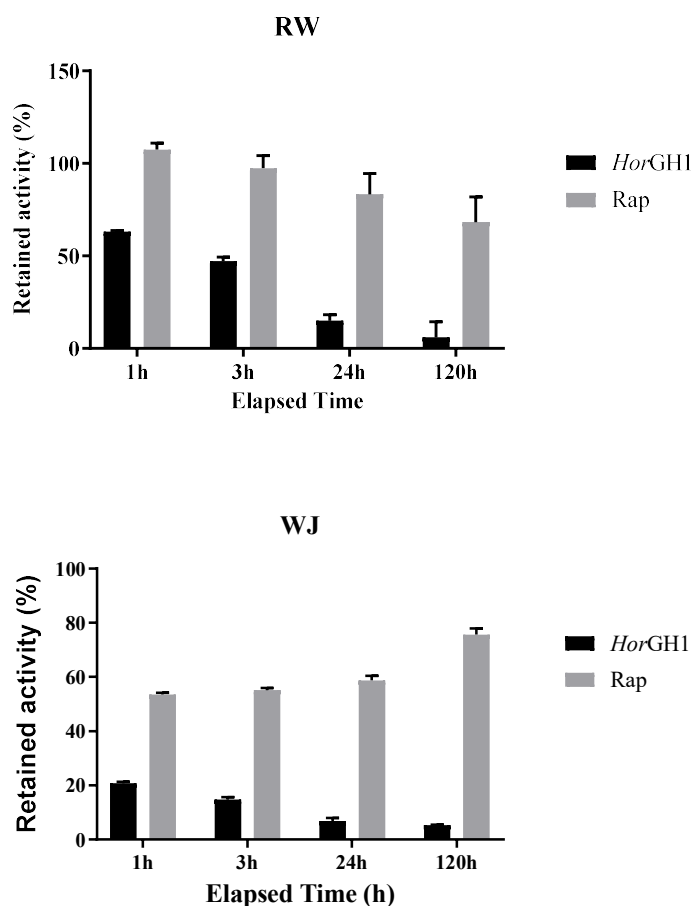


Figure 5.7. Hor and Rapidase® stability assays in White wine (WW), Red wine (RW) and White grape juice (WJ) incubated at 22 °C during 1 h, 3 h, 24 h and 120 h. Each data point is an average of 3 measurements.

5.4.3 Release of volatiles from glucosides in real wines and juice

The exact protocol and calibration curves used for the release of volatiles in model systems was also followed for the release of volatiles in real matrices (See section 5.3.3). As it has been explained before, only the performance of *HorGH1* in comparison with Rapidase® has been tested in this set of experiments.

The complexity of real wines makes it challenging to underpin the specific element(s) which either inhibits or destabilises an enzyme. Potentially, any physical and chemical characteristic of wine is at play: interactions with other molecules, inhibition by sulphur dioxide, rearrangements between

components, low pH, sugar content, phenolic glycosides, etc.²⁷ In all cases, hydrolysis was slower and that is reflected in the results.

Rapidase® showed improved activity in WW (Table 5.6), while the hydrolytic capacity of *HorGH1* is very limited. On the other hand, after 5 days incubation in RW (Table 5.7), *HorGH1* releases over 30 % geraniol and over 3 % guaiacol. This improvement of the performance of *HorGH1* in red wine is probably related to a 0.31 pH units difference and 0.9 g/L sugars between white wine and red wine.

Table 5.6. *HorGH1* and Rapidase® release of geraniol and guaiacol over 5 d in White Wine (WW).

WW	Substrate	Enzyme *****	Time	Geraniol released (µg)	% Hydrolysis
	Geranyl glucoside	<i>HorGH1</i>	5d	0.01 ± 0.01	0
		Rapidase®	5d	1.94 ± 0.02	80
	Substrate	Enzyme ***b	Time	Guaiacol released (µg)	% Hydrolysis
	Guaiacyl glucoside	<i>HorGH1</i>	5d	0.00	0
		Rapidase®	5d	0.24 ± 0.00	11

Table 5.7. *HorGH1* and Rapidase® release of geraniol and guaiacol over 5 d in Red Wine (RW).

RW	Substrate	Enzyme ***a	Time	Geraniol released (µg)	% Hydrolysis
	Geranyl glucoside	<i>HorGH1</i>	5d	0.75 ± 0.06	31
		Rapidase®	5d	2.00 ± 0.07	82
	Substrate	Enzyme *b	Time	Guaiacol released (µg)	% Hydrolysis
	Guaiacyl glucoside	<i>HorGH1</i>	5d	0.07 ± 0.00	3
		Rapidase®	5d	0.23 ± 0.03	11

In the case of grape juice (WJ) (Table 5.8), after 5 days incubation *HorGH1* continues to show significantly better hydrolysis percentage for geraniol: 10 % against 6 % of Rapidase®. The amount of guaiacol liberated by *HorGH1* is also slightly higher (2 %) than the one released by Rapidase® (1 %).

Table 5.8. *HorGH1* and Rapidase® release of geraniol and guaiacol over 5 d in real White juice (WJ).

WJ	Substrate	Enzyme **	Time	Geraniol released (µg)	% Hydrolysis
	Geranyl glucoside	<i>HorGH1</i>	5d	0.26 ± 0.01	10
	Rapidase®	5d	0.14 ± 0.01	6	
	Substrate	Enzyme	Time	Guaiacol released (µg)	% Hydrolysis
	Guaiacyl glucoside	<i>HorGH1</i>	5d	0.03 ± 0.01	2
		Rapidase®	5d	0.02 ± 0.01	1

5.5 Detailed pH stability assay in MW1, MW2 and MJ

The previous results show that *HorGH1* loses stability between pH 3 and 4. To further narrow the pH fork causing it, a more accurate stability assay of *HorGH1* and Rapidase® was carried out with 0.2 pH intervals between pH 3 and 4 in MW1, MW2 and MJ at 22 °C (Fig. 5.8). Retained activity was measured after 1 h, 3 h, 24 h and 120 h, same intervals as in the enzyme stability experiment in different matrices summarised in Figure 5.3. Unfortunately, measures after 120h incubation were no longer reliable, probably due to sample concentration by water loss. Those results are not shown.

HorGH1 loses virtually all activity within 24h of incubation in MW1 and MW2 at a pH lower than 3.6. However, in MJ at pH 3.2, the enzyme still retains 20 % of its activity after the same incubation time. The experiment clearly shows that the more sugar the matrix contains, the higher activity *HorGH1* retains, at all pHs. Rapidase® is clearly independent on pH and the preparation is equally stable between 3 and 4, however, the sugar content present in MJ reduces its activity by almost 50 % very rapidly. These results confirm once again the suitability of *HorGH1* for matrices with high content of sugars, for example

during the maceration or other early stages of the winemaking, previous to the fermentation. Certainly, *HorGH1* displays great potential for its application in juices. In this work only grape juice has been tested but the results in model juice suggest that any other fruit juice would be a suitable matrix for *HorGH1*, especially those having a pH over 3.5, like some apple, orange or lemon juices.²⁸

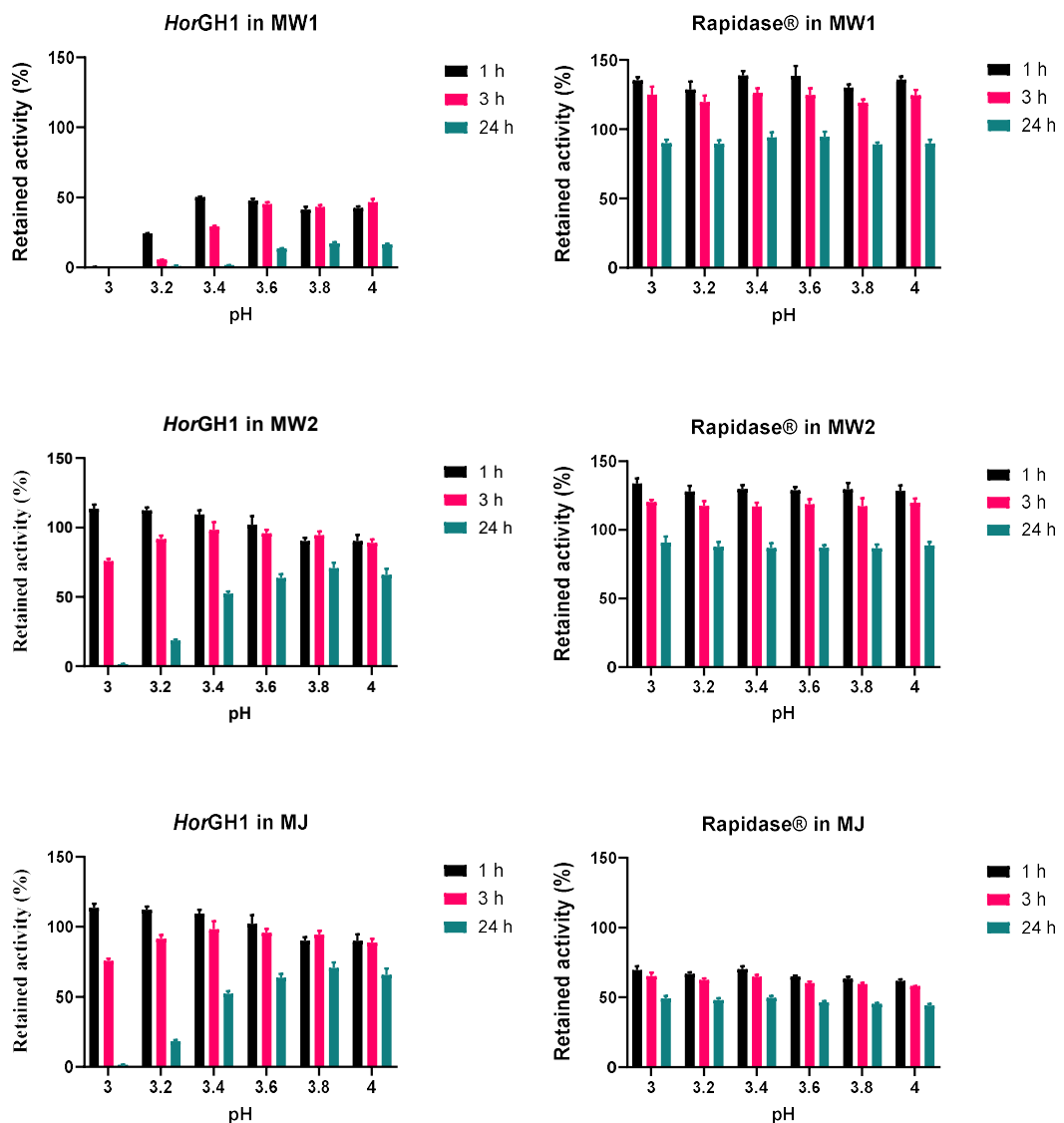


Figure 5.8. *HorGH1* and Rapidase® detailed pH stability assays in Model wine 1 (MW1), Model wine 2 (MW2) and Model juice (MJ) incubated at 22 °C during 1 h, 3 h and 24 h. Each data set is an average of 3 measurements.

5.6 Conclusions

As final conclusion of the all range of experiments in this chapter, it can be stated that the hydrolytic capacity of *HorGH1* for geraniol glucoside and guaiacol glucoside was significantly better than the commercial preparation in all the tested matrices containing high sugar content, where the performance of Rapidase® decreases considerably. *HorGH1* is also stable and active in the presence of ethanol as it can be observed from the results in model wines. On the other hand, the activity of *HorGH1* is very pH dependent and in matrices with a pH below 3.5, like real white wine, the enzyme is not able of hydrolysing glycosides.

Great tolerance to sugar content along with improved performance over a broad pH range makes of *HorGH1* an excellent candidate for aroma amelioration and mitigation of smoke taint in grape juices and wines, especially during the early stages of the winemaking process when the sugar content and the pH range is higher than in fermented wines.

5.7 Bibliography

- 1 A. Rapp, *Fresenius J Anal Chem*, 1990, **337**, 777-785.
- 2 I. L. Francis and J. L. Newton, *Aust. J. Grape Wine Res.*, 2005, **11**, 114–126.
- 3 N. Loscos, P. Hernández-Orte, J. Cacho and V. Ferreira, *J. Agric. Food Chem.*, 2009, **57**, 2468–2480.
- 4 E. Sánchez Palomo, M. S. Pérez-Coello, M. C. Díaz-Maroto, M. A. González Viñas and M. D. Cabezudo, *Food Chem.*, 2006, **95**, 279–289.
- 5 G. K. Skouroumounis, R. Massy-Westropp, M. A. Sefton and P. J. Williams, *J. Agric. Food Chem.*, 1995, **43**, 974–980.
- 6 K. D. Mojsov, D. Andronikov, A. Janevski, S. Jordeva and S. Zezova, *Adv. Technol.*, 2015, **4**, 94–100.
- 7 A. Wilkowska and E. Pogorzelski, *Food Chem.*, 2017, **237**, 282–289.
- 8 P. González-Pombo, L. Fariña, F. Carrau, F. Batista-Viera and B. M. Brena, *Food Chem.*, 2014, **143**, 185–191.
- 9 C. B. Z. Günata, I. Dugelay, J.C. Sapis, R. Baumes, in *Progress in Flavour Precursor Studies*, ed. P. W. P. Schreier, 1993, pp. 219–234.
- 10 Y. Hayasaka, K. A. Dungey, G. A. Baldock, K. R. Kennison and K. L. Wilkinson, *Anal. Chim. Acta*, 2010, **660**, 143–148.
- 11 C. M. Mayr, M. Parker, G. A. Baldock, C. A. Black, K. H. Pardon, P. O. Williamson, M. J. Herderich and I. L. Francis, *J. Agric. Food Chem.*,

- 2014, **62**, 2327–2336.
- 12 D. P. Singh, H. H. Chong, K. M. Pitt, M. Cleary, N. K. Dokoozlian and M. O. Downey, *Aust. J. Grape Wine Res.*, 2011, **17**, 13–21.
- 13 M. Parker, P. Osidacz, G. A. Baldock, Y. Hayasaka, C. A. Black, K. H. Pardon, D. W. Jeffery, J. P. Geue, M. J. Herderich and I. L. Francis, *J. Agric. Food Chem.*, 2012, **60**, 2629–2637.
- 14 L. van der Hulst, P. Munguia, J. A. Culbert, C. M. Ford, R. A. Burton and K. L. Wilkinson, *Planta*, 2019, **249**, 941–952.
- 15 A. K. Hjelmeland and S. E. Ebeler, *Am. J. Enol. Vitic.*, 2015, **66**, 1–11.
- 16 G. Singh, A. K. Verma and V. Kumar, *3 Biotech*, 2016, **6**, 1–14.
- 17 E. Sánchez Palomo, M. C. Díaz-Maroto Hidalgo, M. Á. González-Viñas and M. S. Pérez-Coello, *Food Chem.*, 2005, **92**, 627–635.
- 18 K. Hu, Y. Qin, Y. S. Tao, X. L. Zhu, C. T. Peng and N. Ullah, *J. Food Sci.*, 2016, **81**, M935–M943.
- 19 C. S. Chan, L. L. Sin, K.-G. Chan, M. S. Shamsir, F. A. Manan, R. K. Sani and K. M. Goh, *Biotechnol. Biofuels*, 2016, **9**, 174.
- 20 A. Sabel, S. Martens, A. Petri, H. König and H. Claus, *Ann. Microbiol.*, 2014, **64**, 483–491.
- 21 S. Maicas and J. J. Mateo, *Appl. Microbiol. Biotechnol.*, 2005, **67**, 322–335.
- 22 P. Godden, E. Wilkes and D. Johnson, *Aust. J. Grape Wine Res.*, 2015, **21**, 741–753.

- 23 M. M. Bradford, *Anal. Biochem.*, 1976, **72**, 248–254.
- 24 D. Hampel, A. L. Robinson, A. J. Johnson and S. E. Ebeler, *Aust. J. Grape Wine Res.*, 2014, **20**, 361–377.
- 25 G. K. Skouroumounis and M. A. Sefton, *J. Agric. Food Chem.*, 2000, **48**, 2033–2039.
- 26 P. O. De Giuseppe, T. D. A. C. B. Souza, F. H. M. Souza, L. M. Zanphorlin, C. B. Machado, R. J. Ward, J. A. Jorge, R. D. P. M. Furriel and M. T. Murakami, *Acta Crystallogr. Sect. D Biol. Crystallogr.*, 2014, **70**, 1631–1639.
- 27 P. F. H. Plank and J. B. Zent, in *Beer and Wine Production*, Ed. B. H. Gump, 1993, pp. 181–196.
- 28 Z. Yan, X. Zhang, C. Bao, H. Tang, Q. Zhao, L. Hu and J. You, *Sensors Actuators, B Chem.*, 2018, **262**, 869–875.

Chapter 6 Hydrolytic capacity of *HorGH1*, *AheGH1* and *AacGH1* towards glucovanillin and soybean isoflavones

The work presented in this chapter is my exclusive contribution unless otherwise stated. Christian M. Heckman helped to complete the green vanilla experiments and some of the isoflavones' calibration curves.

This work has been included in two publications: "Release of soybean isoflavones using a β -Glucosidase from *Alicyclobacillus herbarius*" published in ChemBioChem in 2020 and "Producing natural vanilla extract from green vanilla beans using a β -glucosidase from *Alicyclobacillus acidiphilus*" published in Journal of Biotechnology in 2021.

6.1 Introduction

As well as in wine production, β -glucosidases can be applied in other food processing strategies, such as vanilla and flavonoids extractions.

Current methods for production of natural vanilla extract are long and tedious,¹ and the efficiency of vanillin extraction is usually conditioned by different factors during the traditional curing process (temperatures and weather conditions).² As an important fraction of vanillin is present in the form of glucovanillin (Fig. 6.1) in green beans, endogenous β -glucosidases contribute to its hydrolysis; however, these enzymes lose efficiency steadily during the curing process which lasts up to 180 days.³

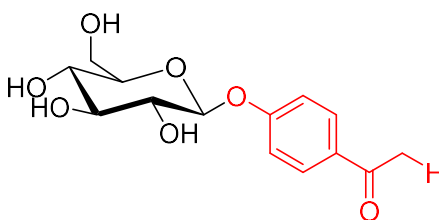
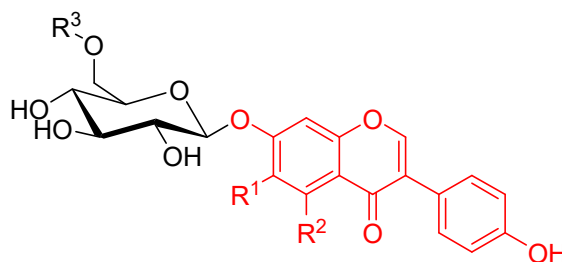


Figure 6.1. Structure of glucovanillin

More complex than vanillin, the isolation of isoflavones from plants is in demand. Consumption of soybean has become more and more popular in recent years because it is an excellent protein source for the human diet. In addition, soybean contains several compounds considered important food supplements due to their health properties, especially isoflavones. Soybeans contain mainly three types of isoflavones (daidzein, genistein, and glycitein), which may be found in four different forms (Fig. 6.2): as aglycons, 7-O- β -D-glucosides, 7-O-(6''-O-acetyl)glucosides, or 7-O-(6''-O-malonyl) glucosides.⁴ Recently, commercial preparations of isoflavones have become very popular

as some health benefits have been reported.⁵ However, when the biological activities of these compounds are considered, the bioavailability of the aglycone has been suggested to be higher than that of the glycoside; however, it is a minor constituent of unfermented soy products.⁶



glycitin: $R^1 = \text{OMe}$, $R^2 = \text{H}$

genistin: $R^1 = \text{H}$, $R^2 = \text{OH}$

daidzin: $R^1 = R^2 = \text{H}$

$R^3 = \text{H}$, acetyl, or malonyl

Figure 6.2: Structure of the main isoflavone glucosides (glycitin, genistin, and daidzin) found in soybean. The isoflavone moiety (glycitein, genistein, and daidzein) is highlighted in red. The sugar may be further acetylated or malonylated.

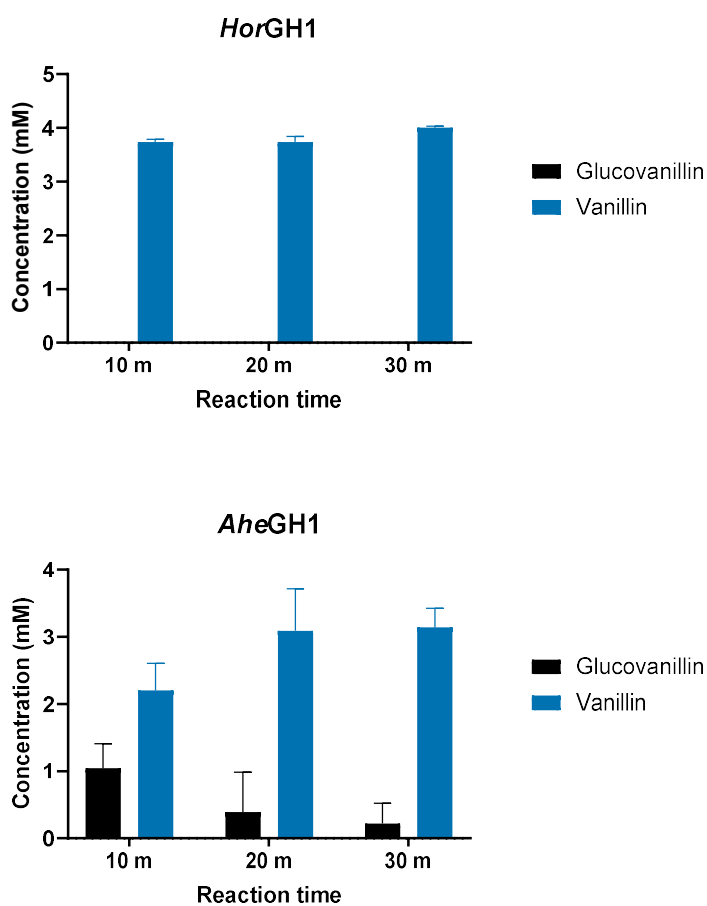
β -glucosidases can be used in both processes to hydrolyse glucosides to their aglycons. The industrial processing for extracting isoflavones and glucovanillin includes the use of organic solvents (mostly ethanol) to solubilise them.^{7,8} Accordingly, resistance to organic solvents would be one of the essential features that a β -glucosidase intended for these processes will have to present. The use of an extremophilic organism as a source of an appropriate exogenous enzyme can offer a valid alternative.

In this chapter the hydrolytic performance of the 3 β -glucosidases *HorGH1*, *AheGH1* and *AacGH1* in ethanol-water extracts of green vanilla pods and soybean flour has been evaluated.

6.2 Assessment of the enzymatic performance towards glucovanillin

6.2.1 Enzymatic hydrolysis over synthetic vanillin

Prior to the testing of the enzyme in the real matrix, the hydrolytic activities of *HorGH1*, *AheGH1* and *AacGH1* (0.01mg/mL) towards synthetic vanillin 4-O- β -d-Glucoside (4.5 mM) were assessed (Fig. 6.3).



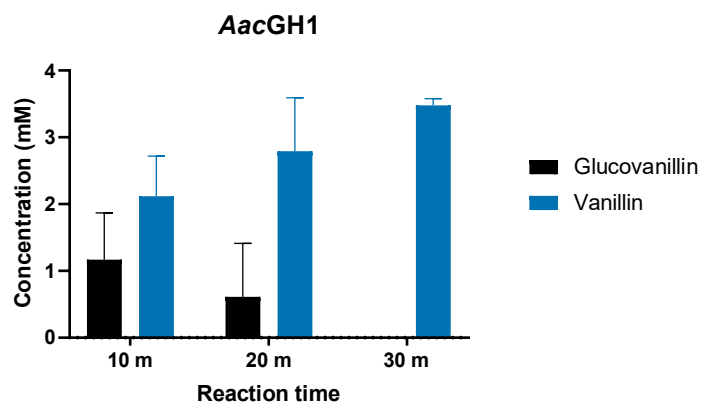


Figure 6.3. Enzymatic hydrolysis rate of glucovanillin to vanillin over 30 min in water. Glucovanillin concentration: 4.5 mM, enzyme concentration: 0.01 mg/mL. Error bars represent standard deviations (n = 3).

The progression of the hydrolysis was checked after 10, 20 and 30 min. While *HorGH1* achieved a complete conversion of the glucoside to the aglycon after 10 min *AacGH1* needed 30 min to complete it. In the case of *AheGH1*, the complete hydrolysis was not observed and after 30 min there was still a 7% of glucovanillin in the reaction.

6.2.2 Enzymatic hydrolysis over real vanilla extract

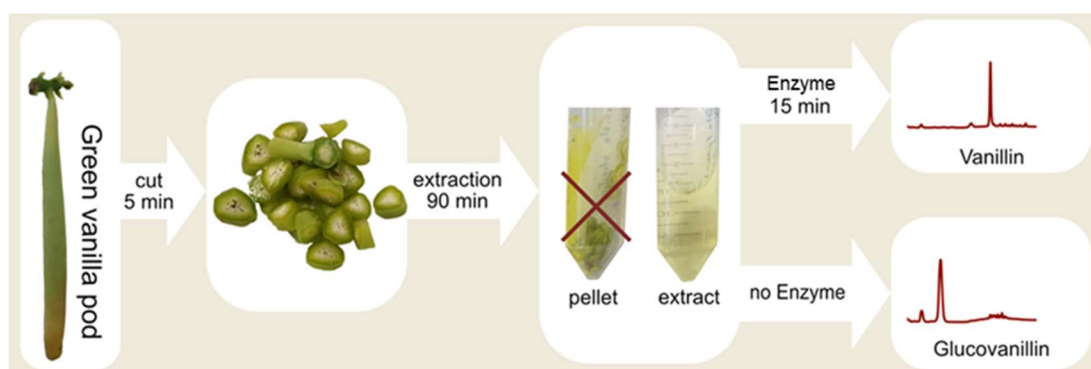
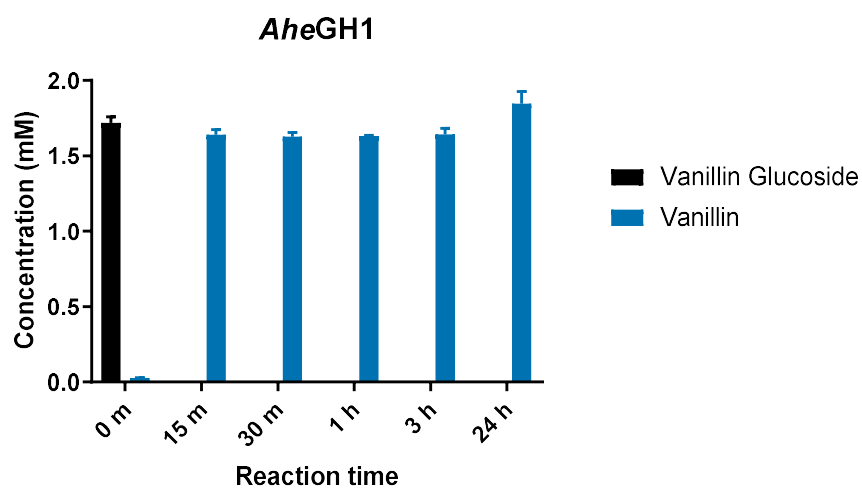
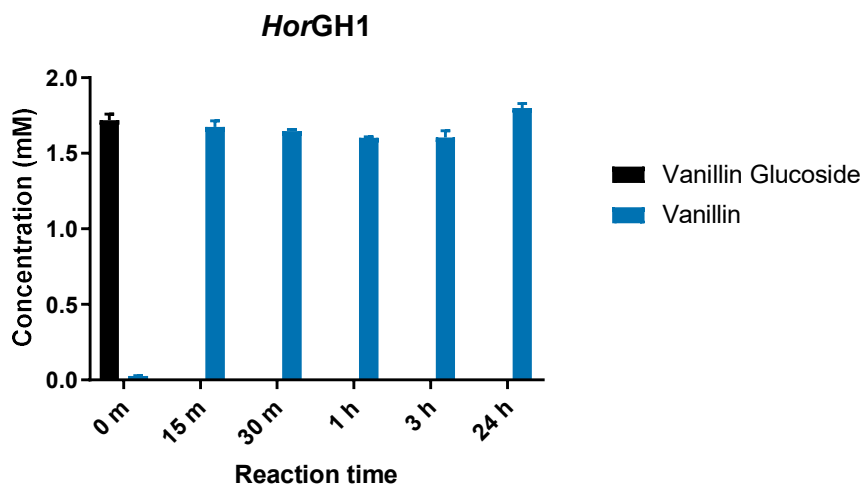


Figure 6.4. Process to produce vanilla extract from green vanilla.

Following the process in Figure 6.4, vanillin glucoside (1.7 mM) and, as expected, virtually no free vanillin were extracted from a green vanilla pod sample. The green vanilla pod extract was aliquoted, treated with the three different enzymes (0.5 mg/mL), and the reaction monitored for 24 h (15 min, 30 min, 1 h, 3 h, and 24 h) by HPLC.



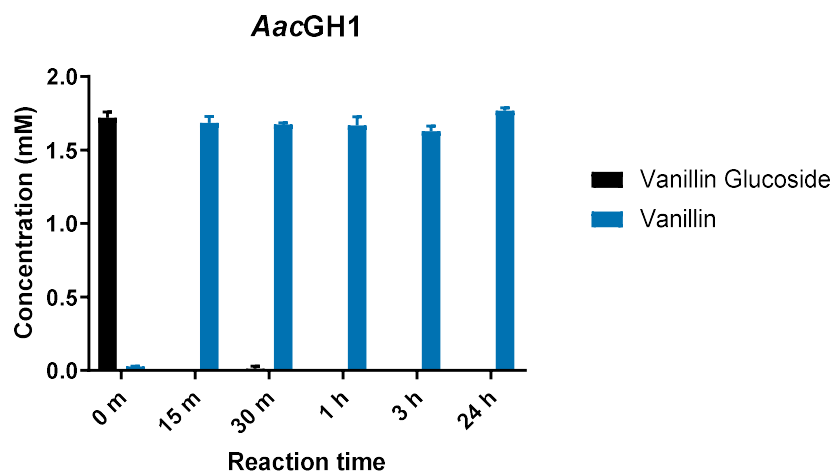


Figure 6.5. Hydrolysis reaction of the green vanilla extract at 0 min, 15 min, 30 min, 1 h, 3 h and 24 h at 30 °C. Enzyme loading 0.5 mg/mL. Error bars represent standard deviations (n = 3).

Results show that within 15 min incubation time the 3 hydrolases convert the whole amount of glucoside to the aglycon (Fig. 6.5), while no spontaneous conversion takes place in the absence of the biocatalyst in the same time span. In addition, several additional peaks have been identified (and quantified) in the treated extract which are absent in the untreated one, therefore attributable to enzymatic hydrolysis. To illustrate this, in Fig. 6.6 it can be observed an example of the chromatogram of the sample treated with *AacGH1*, this is representative also of the chromatograms obtained with the other two enzymes which gave virtually identical traces: vanillic acid (0.07 mM), 4-hydroxybenzoic acid (0.08 mM), and 4-hydroxybenzaldehyde (0.17 mM). These structural analogues of vanillin are known to be present in glycosylated form in green vanilla, and contribute significantly to the complex aroma of cured vanilla.⁹ The formation of additional compounds in low concentration was also observed, but they could not be clearly identified.

Indeed, the smell of the treated extract more closely resembled that of vanilla than simply pure vanillin.

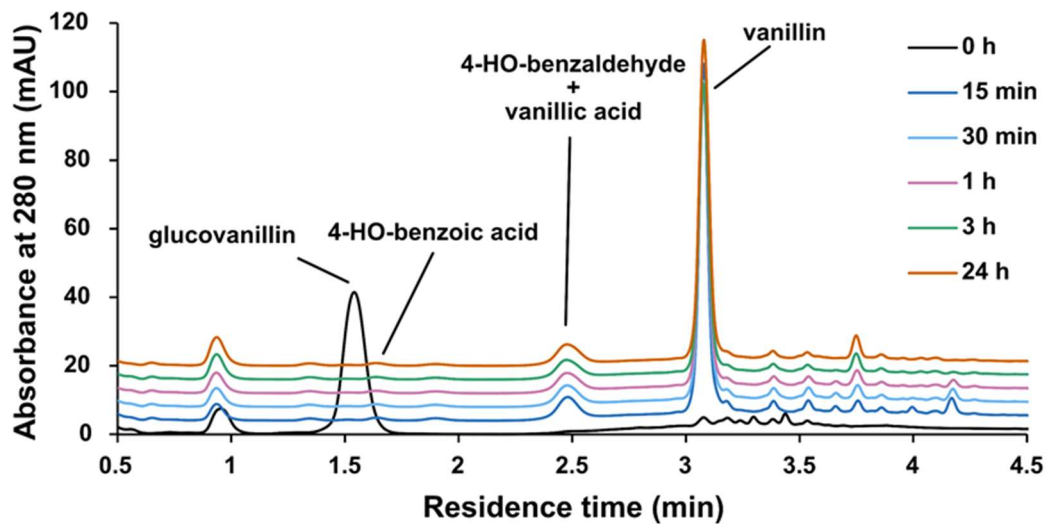
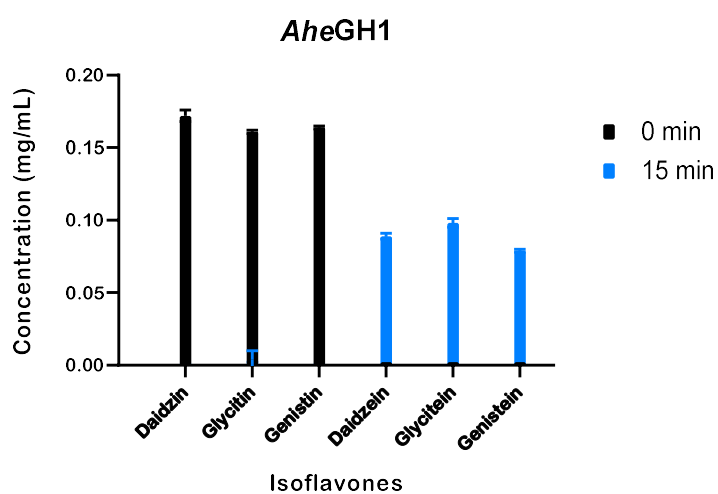
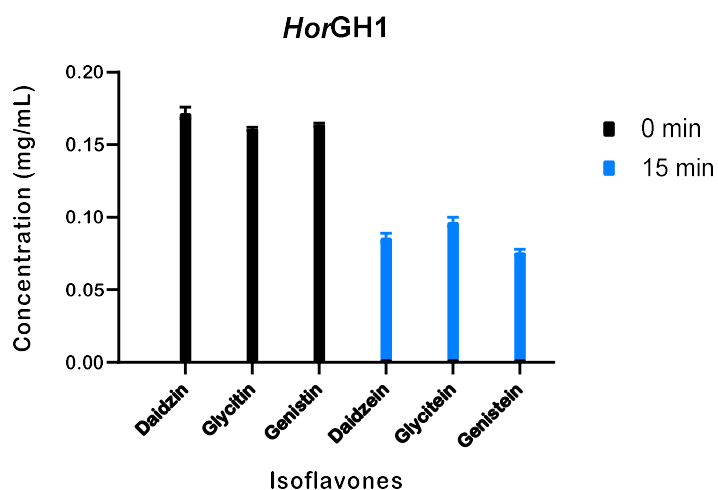


Figure 6.6. Overlaid chromatograms (280 nm) of a green vanilla extract over the course of treatment with *AacGH1*. Signals offset by 4 mAU for clarity.

6.3 Assessment of the enzymatic performance towards synthetic isoflavone glucosides

Similarly to the vanillin approach, prior to the testing of the enzymes in the real matrix, the hydrolytic activity of *HorGH1*, *AheGH1* and *AacGH1* towards 3 isoflavones glucosides (daidzin, glycitin, genistin) was assessed over 15 min incubation at 30 °C (Fig. 6.7).



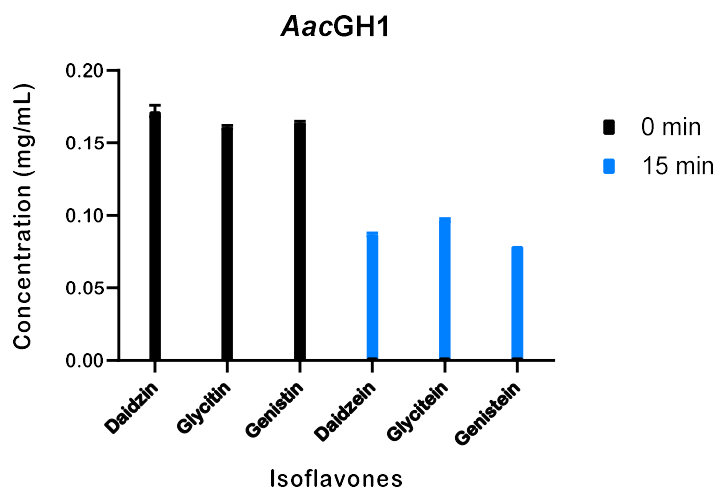


Figure 6.7. Enzymatic hydrolysis of 3 glucosides: daidzin, glycitin and genistin at time 0 and after 15 min reaction at 30 °C. Reactions were performed in 55% water, 30% DMSO and 15% ethanol.

In the control reaction, where no enzyme was added, no hydrolysis occurred, and the 3 isoflavone glucosides remained intact. When *HorGH1*, *AheGH1* or *AacGH1* were added to the reaction, 100% conversion to the correspondent aglycons, daidzein, glycitein and genistein was consistently achieved. It is important to highlight that this hydrolysis occurs in the presence of 30% DMSO in addition to 15% ethanol present in the reaction, as both solvents have been used to solubilise the isoflavone glucosides in their stock solutions. These results are in line with the findings from the activity and stability assays in the presence of different co-solvents explained previously in sections 4.4.4 and 4.4.5 of this thesis.

6.4 Enzymatic performance over soybean flour

Following the initial testing of the 3 enzymes with the synthetic isoflavone glucosides, their performance was then tested with a real isoflavone mixture extracted from soybean flour. An analysis of the crude extract, before any enzymatic treatment, showed that the content of 7-*O*- β -D-glucosides, daidzin

and genistin are in similar amounts (~ 0.02 mg/mL), while the content of glycitin is 6 times lower. The 2 malonyl-glucosides are 3 times more abundant than the 7-O- β -D-glucosides, reaching 0.06 mg/mL. As expected, free aglycons daidzein, glycitein and genistein are almost non-existent in the extraction mixture. The composition of this mixture is detailed in Fig. 6.8.

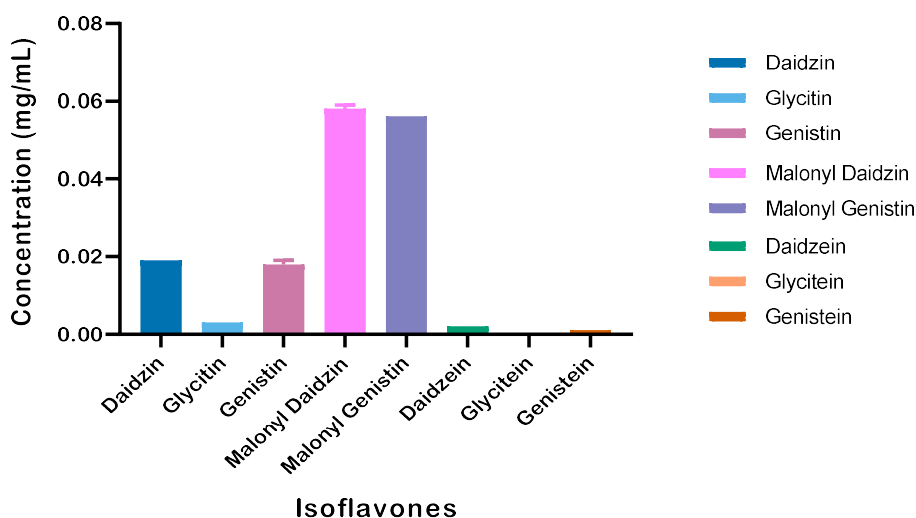
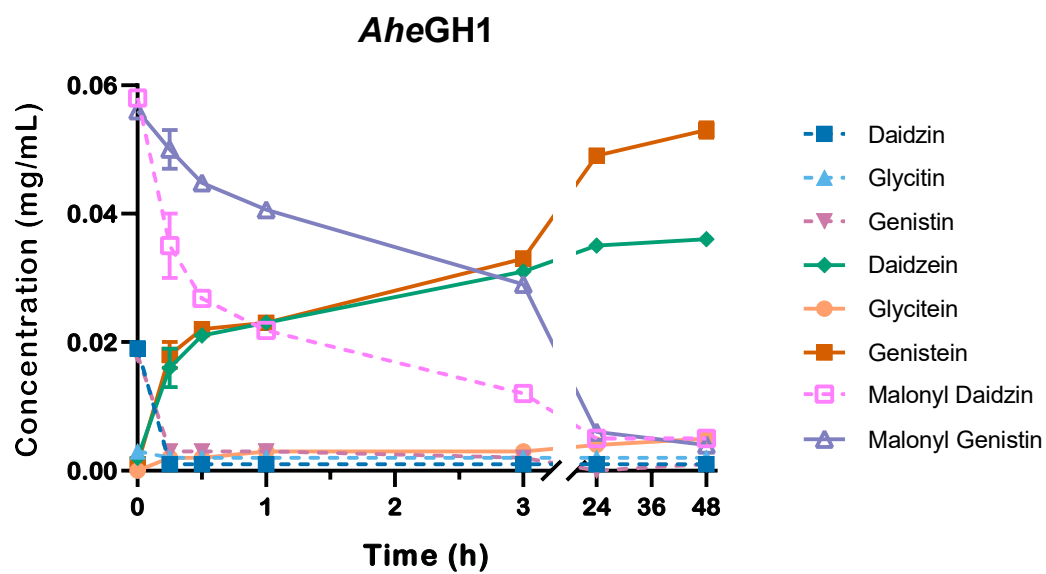
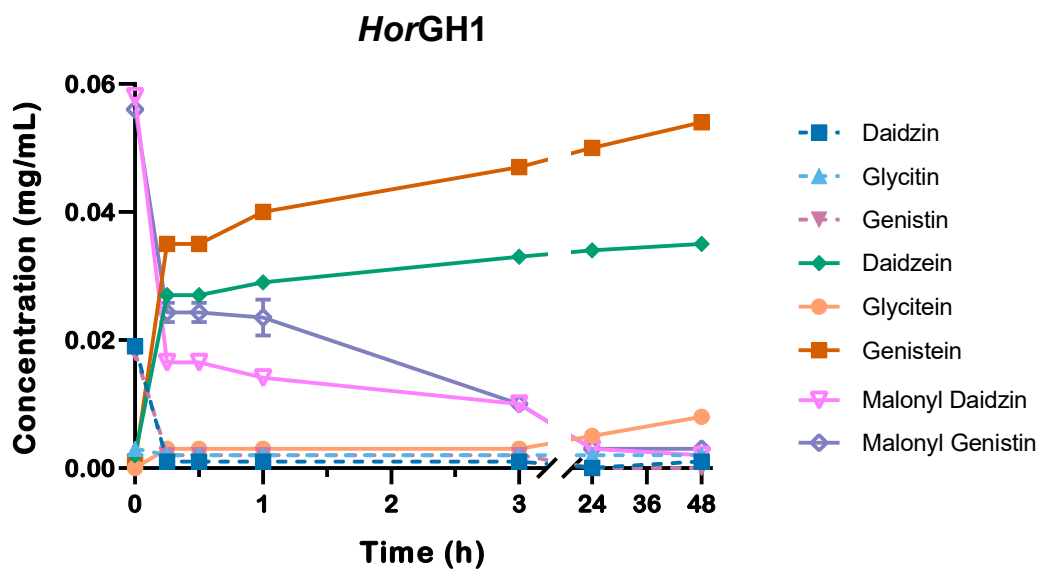


Figure 6.8. Composition of the isoflavone mixture determined by HPLC following extraction from soybean flour.

The soybean flour extract was incubated with the different GHs. In this case, each reaction was followed over time to monitor the hydrolysis of the isoflavone glucosides and aliquots were taken from the biotransformation at time 0 and after 15 min, 30 min, 1 h, 3 h, 24 h and 48 h. The evolution in the hydrolysis rate achieved by the 3 enzymes is represented in Fig. 6.9.



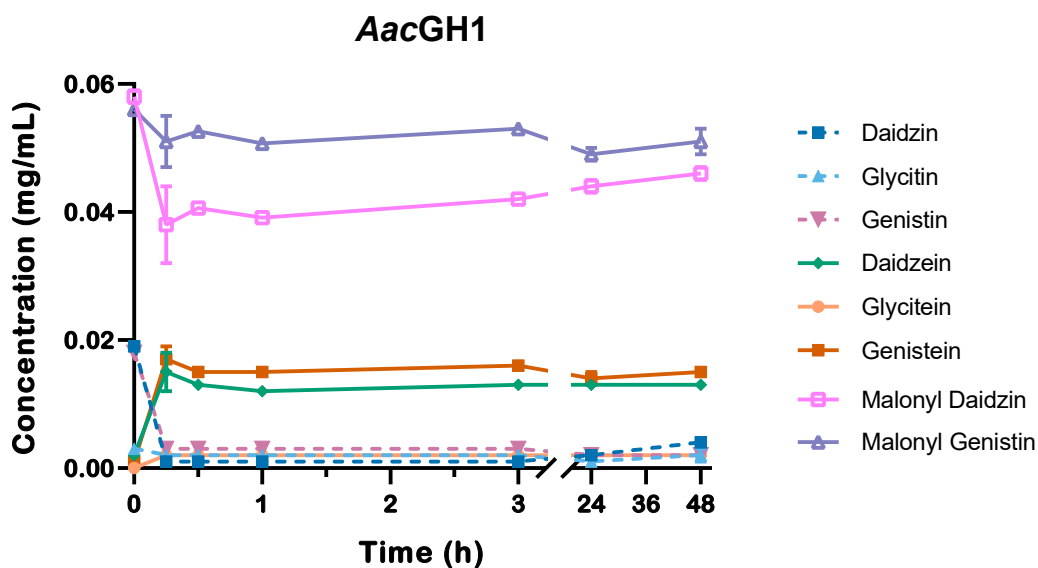


Figure 6.9. Hydrolysis reaction over soybean isoflavones glucosides at time 0, after 15 m, 30 m, 1 h, 3 h, 24 h and 48 h at 30 °C when *HorGH1*, *AheGH1* or *AacGH1* are present in the reaction.

Within 15 min of incubation, almost no isoflavone glucosides remained in the mixtures treated with *AheGH1*, *AacGH1* and *HorGH1*, matching what had been observed with the standards. However, the amount of aglycons in the sample treated with *HorGH1* and *AheGH1* continued to increase as the incubation time progresses. Concurrently, a decrease of the two additional malonyl daidzin and malonyl genistin peaks was also observed (Example of *AheGH1* chromatogram in Fig. 6.10).

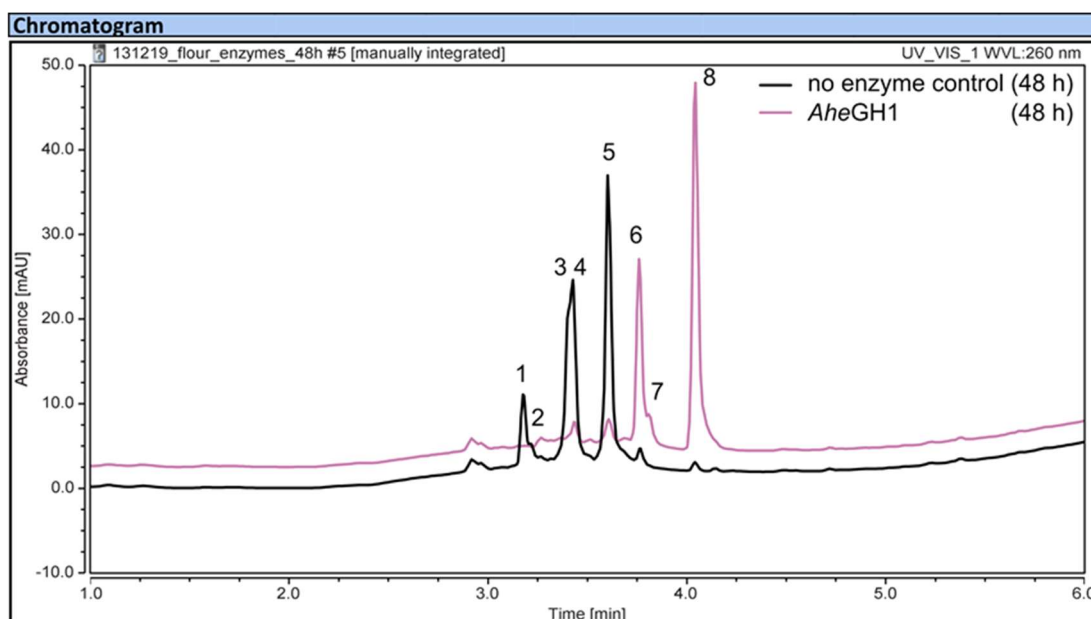


Figure 6.10. Chromatogram of soy flour extract with and without enzymatic treatment (48 h), 260 nm. 1: daidzin, 2: glycitin, 3: genistin, 4: malonyl-daidzin, 5: malonyl-genistin, 6: daidzein, 7: glycitein, 8: genistein.

The hydrolytic capacity of the enzymes had initially only been evaluated towards the 7-O- β -D-glucosides daidzin, glycitin and genistin. After quantification, the increase in aglycons closely matched the decrease observed for the malonyl-glucosides (Fig. 6.9), confirming that *HorGH1* and *AheGH1* were also capable of hydrolysing this bulkier form. Interestingly, the hydrolysis rate of the malonyl-glucosides for *HorGH1* is remarkably higher than for *AheGH1*. While *AheGH1* needs 3 h to achieve 65% conversion, *HorGH1* only needs 15 min to achieve the same rate.

On the other hand, *AacGH1* seemed not able to hydrolyse the malonyl-glucosides, accepting only the 7-O- β -D-glucosides.

To sum up, the evaluation of the hydrolytic capacity of *HorGH1*, *AheGH1* and *AacGH1* towards vanillin glucoside, in its synthetic and natural form, and towards the most common isoflavones found in soybeans, concluded that all 3 enzymes can efficiently hydrolyse the glucosides to their aglycons (in some

cases also transforming malonyl-glucosides), hence, they are promising candidates to be applied in both fields. In the case of the profitable vanilla industry, the use of the enzymes allows natural complex vanilla flavour to be obtained without the need of a lengthy curing process (2 hours in comparison to half a year), which might be of particular interest for the processing of substandard harvests (such as damaged crops) where the traditional curing process would be economically unfeasible. When referring to the soybean industry, enzymes constitute a promising alternative for the production of soybean isoflavones.

6.5 Bibliography

- 1 K. Anuradha, B. N. Shyamala and M. M. Naidu, *Crit. Rev. Food Sci. Nutr.*, 2013, **53**, 1250–1276.
- 2 V. T. Pardío, A. Flores, K. M. López, D. I. Martínez, O. Márquez and K. N. Waliszewski, *J. Food Sci. Technol.*, 2018, **55**, 2059–2067.
- 3 M. J. W. Dignum, J. Kerler and R. Verpoorte, *Food Rev. Int.*, 2001, **17**, 119–120.
- 4 S. Kudou, Y. Fleury, D. Welti, D. Magnolato, T. Uchida, K. Kitamura and K. Okubo, *Agric. Biol. Chem.*, 1991, **55**, 2227–2233.
- 5 C. Cui, R. L. Birru, B. E. Snitz, M. Ihara, C. Kakuta, B. J. Lopresti, H. J. Aizenstein, O. L. Lopez, C. A. Mathis, Y. Miyamoto, L. H. Kuller and A. Sekikawa, *Nutr. Rev.*, 2020, **78**, 134–144.
- 6 D. C. Vitale, C. Piazza, B. Melilli, F. Drago and S. Salomone, *Eur. J. Drug Metab. Pharmacokinet.*, 2013, **38**, 15–25.
- 7 P. A. Murphy, K. Barua and C. C. Hauck, *J. Chromatogr. B Anal. Technol. Biomed. Life Sci.*, 2002, **777**, 129–138.
- 8 K. N. Waliszewski, S. L. Ovando and V. T. Pardo, *J. Food Eng.*, 2007, **78**, 1267–1273.
- 9 D. Klimes, I Lamparsky, *Int Flavours Food Addit.*, 1976, **7**, 272–291.

Chapter 7 Conclusions and final remarks

The results obtained during the course of this research project showcase that extremozymes could be an excellent alternative to overcome some of the handicaps that mesophilic enzymes present when applied in industrial food processes. This is mainly lack of stability due to the harsh conditions that some industrial processes involve, for instance, high sugar concentrations when involving fruit processing, presence of organic solvents to allow the solubilisation of some food ingredients, or extreme temperatures and pHs depending on the applied treatment.

In Chapter 4, and based on the good performance of the halophilic β glucosidase *HorGH1* previously characterised by the Paradisi group, 3 novel enzymes were selected based on their homology with *HorGH1*; the acidophilic *AheGH1* and *AaaGH1*, and the psychrophilic *PanGH1*. After their heterologous expression in *E.coli*, the crystal structure of *AheGH1* and *AacGH1* was fully solved. Kinetic parameters were also assessed, showing the best results for *AacGH1*, with a K_M of 0.126 mM and a K_{cat} of 27.97 s⁻¹. At this point, *PanGH1* was discarded due to expression and purification issues, the rest were subjected to characterisation, including activity and stability assays in the presence of glucose, fructose, organic solvents and a broad range of pH and temperatures. Glucose inhibition being a common problem for β glucosidases, the results suggested very good glucose tolerance for *AheGH1* and *AacGH1*, maintaining more than 50% activity with 15% glucose in the reaction. *AacGH1* was the most active GH1 in the presence of sugars of the 3, showing even an enhancement of its activity when 25% fructose was added to the reaction. Regarding organic solvents, the activity of *AacGH1* was not affected by 10-20% ethanol, which is the most used solvent

in the food industry, and the activity of *AacGH1* was enhanced 0.5-fold by it. In terms of temperature stability, *HorGH1* showed the best stability of the 3, retaining 50% of its activity after 5 days of incubation at 60 °C. With regard to pH stability, *HorGH1* was once again the most stable, retaining some activity after 24h incubation at pH3 and 5 days incubation at pH 12. As a conclusion, the 3 enzymes appeared to be excellent candidates for further assessment of their behaviour and performance in food processing.

In Chapter 5, the hydrolytic capacity of *HorGH1*, *AheGH1* and *AacGH1* in comparison with the commercial preparation Rapidase®, was assessed towards 2 wine glucosides (geranyl glucoside and guaiacyl glucoside) added to different matrices. Results showed that *AheGH1* and *AacGH1* were unable to deal with the low pH of the model and the real wine, and for hence were not a real competitor of the commercial preparation. However, *HorGH1* was significantly better than Rapidase® in all the tested matrices containing high sugar content, revealing a great tolerance to sugars. On the other hand, *HorGH1* was very pH dependent and in matrices with a pH below 3.5, the enzyme is not able to hydrolyse glucosides. All the results make *HorGH1* an excellent candidate to be applied in early stages of the winemaking process, when the sugar content and the pH is more elevated than in fermented wines.

Finally, in Chapter 6, the performance of *HorGH1*, *AheGH1* and *AacGH1* was tested on the hydrolysis of glucovanillin and soybean isoflavones. The uniqueness of both of these processes is the use of ethanol to solubilise the compounds, and thus, the need of enzymes able to deal with the solvent. As

a conclusion, all 3 enzymes are able to hydrolyse glucovanillin, in its synthetic and natural form, and also soybean glucosides to their aglycons. Hence, they are promising candidates to be used in both fields.

Acknowledgments

Without any doubt, the first person who I need to thank is my supervisor Francesca Paradisi. Thanks for the very first day we talked, when I came to your office telling you I wanted to do the PhD in your group but I wasn't sure if I could cope with all the chemistry that biocatalysis implies. Immediately you calmed me down and offered me an awesome project regarding the use of enzymes in the food industry. Thanks for that, it was the best decision I could ever take. Thanks for your dedication, your time, your unwavering support, your scientific lessons and your personal warmth towards me. I very much appreciate it.

Thanks to my second supervisor Ian Fisk, for your willingness to help me at every chance you had, your scientific and personal advices and thanks for Australia, the best experience of my PhD.

Thanks to my lab colleagues (my friends), especially to Dr. David Roura and Dr. Maria Romero for helping me out with scientific issues but mostly for all the laugh we have had. To Dr. Martina Contente, Dr. Eimear Hegarty, Dr. Ana I. Benítez-Mateos, Nourah Almulhim, Valentina Marchini, Chris Heckman and Stefania Gianolio for making me proud of being part of the Paradisi Rese@rch group.

Special thanks to my family: my parents and my husband. You always believed in me even when I didn't believe in myself anymore. Thanks for being there every time I needed to cheer up, to complain, to celebrate, to discuss, to take a decision. To sum up, thanks for supporting me ALWAYS through these 4 years of PhD and in my whole life, you are the light of my

pathway. Thanks to the love of my life, baby Mario, for being such a lovely little boy and letting me to prepare this thesis, inside and outside the bump.

Thanks to the CDT in Sustainable Chemistry management board, Pete License, Chris Moody and Perislava Williams. You chose me to be part of this wonderful program and you have been there all this time helping me to take the best of it. Thanks also to the CDT Cohort 3, specially to Vera Salgado. Thanks to the EPSRC for the funding.

And lastly, I would like to thank all the people who make my time in Nottingham more enjoyable, like my beloved people from "Gazpacheros in Nottingham" and my beautiful cats Kendy and Uva.